ARL/AERO-PROP-R-163

AR-003-010

DEPARTMENT OF DEFENCE

DEFENCE SCIENCE AND TECHNOLOGY ORGANISATION

AERONAUTICAL RESEARCH LABORATORIES

MELBOURNE, VICTORIA

AERO PROPULSION REPORT 163

APPLICATIONS OF VIBRATION ANALYSIS TO THE CONDITION MONITORING OF ROLLING ELEMENT BEARINGS

by

N. S. SWANSSON and S. C. FAVALORO

COPY No

JANUARY 1984

AR-003-010

DEPARTMENT OF DEFENCE
DEFENCE SCIENCE AND TECHNOLOGY ORGANISATION
AERONAUTICAL RESEARCH LABORATORIES

AERO PROPULSION REPORT 163

APPLICATIONS OF VIBRATION ANALYSIS TO THE CONDITION MONITORING OF ROLLING ELEMENT BEARINGS

by

N. S. SWANSSON and S. C. FAVALORO

SUMMARY

Condition monitoring methods for rolling element bearings, which utilize the high frequency vibrations generated by bearing damage, have been investigated and compared experimentally. Kurtosis values, spectra of vibration signal envelopes and pulse measurement methods provided effective detection of early damage, but kurtosis in particular was not effective in evaluating extensive damage, where a combination of methods is required.

Comparison of different accelerometer types used as vibration sensors gave very similar results, but an acoustic emission transducer provided indications of incipient damage significantly earlier than the accelerometers.

Tests were conducted under reasonably favourable conditions of measurement so further testing under less favourable conditions is proposed and the effect of such conditions is briefly considered.

POSTAL ADDRESS: Director, Aeronautical Research Laboratories,
Box 4331, P.O., Melbourne, Victoria, 3001, Australia

REPRODUCTION QUALITY NOTICE

This document is the best quality available. The copy furnished to DTIC contained pages that may have the following quality problems:

- Pages smaller or larger than normal.
- Pages with background color or light colored printing.
- Pages with small type or poor printing; and or
- Pages with continuous tone material or color photographs.

Due to various output media available these conditions may or may not cause poor legibility in the microfiche or hardcopy output you receive.

☐ If this block is checked, the copy furnished to DTIC contained pages with color printing, that when reproduced in Black and White, may change detail of the original copy.

SUMMARY

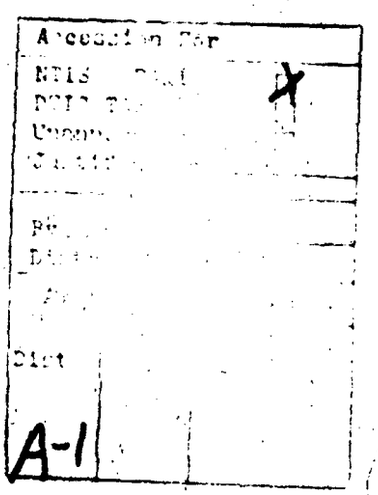

1. INTRODUCTION

To obtain the greatest effectiveness in the operation of complex machines and mechanical systems, on-condition maintenance strategies are being widely employed to minimise operating and overhaul costs, without adversely affecting reliability and availability. Access to, and use of effective methods for monitoring the condition of these systems and their component parts are essential prerequisites to the adoption of on-condition maintenance, and developments in condition monitoring techniques are currently of considerable interest, especially in areas where machine availability is vital. Service equipment, such as helicopter transmissions and turbine engines, is one important area where monitoring methods are being sought in order to detect performance deterioration, damage or incipient failure, and if possible to diagnose the source of the problem and predict its sequence of development.

Data sources for condition monitoring include direct physical inspection (provided the machine can be shut down periodically for this purpose), non-destructive material inspection techniques, examination of lubricating oil and oil borne wear debris, and the analysis of dynamic values of various parameters generated while the machine is in operation. Of the latter, the most commonly used parameter is machine vibration, although noise, shaft torque and other parameters can be used when they provide significant data. Analysis methods for dynamic signals, such as vibration, aim to derive the maximum condition information from the available data, and methods to enhance the usefulness of this information are constantly sought.

Vibration analysis has been extensively used for evaluating the condition of gear transmissions since distinct, discrete meshing frequencies can be identified; spectrum analysis using the Fourier Transform analyser has virtually become a standard technique for this purpose. Rolling element bearings are equally vital machine components, but the vibrations generated by both sound and damaged bearings are much more complex and discrete frequencies are not so readily identified and distinguished. This paper examines some of the vibration analysis techniques particularly applicable to the monitoring of rolling element bearings, and describes the findings of some supporting experimental investigations.

2. SOURCES OF VIBRATION IN ROLLING ELEMENT BEARINGS

Under normal operating conditions rolling element bearings always generate some degree of vibration and noise, albeit at very low level for a properly installed bearing in good condition. Sources of vibration include imperfect rolling motion during rotation, acoustic emission, and external vibration transmitted via the bearings.

2.1 Imperfect Rolling Motion

Motion which is not perfectly regular is the major source of bearing vibration. Causes of irregularity can be classified into areas of manufacture, application and operation, and deterioration in service.

2.1.1 Manufacturing Faults

Departures from perfect geometry are the main items in this category. These include out of roundness of inner or outer race, lack of sphericity of balls, and unequal ball diameters. A possible secondary cause is lack of uniformity of bearing materials; e.g. varying local modulus due to inclusions etc.

2.1.2 Faulty Application, Installation or Operation

Some faults in this classification result directly in imperfect rolling motion; others have obvious mechanical effects. The former category includes assembly misalignment and race distortion, as well as brinelling of the bearing races (caused by overloading or impact either during assembly or operation). Looseness or similar faults produce direct mechanical impact effects.

Poor or inadequate lubrication can lead to friction and sticking with irregular motion or vibration. At the highly stressed Hertzian contact area, if there is no separating layer or lubricant, the contacting surfaces will weld together and then be broken or sheared apart. Since the contact area is very small only a trace of lubricant is required but this trace is essential (the main purpose of greater oil supply is to remove heat from the bearing, preventing deterioration of components due to overheating). Wear particles or other minute debris in the oil produce vibration effects similar to defective lubrication, since very small particles can penetrate the lubricant film, effectively resulting in metal to metal contact.

2.1.3 Deterioration of Bearing Components in Service

Continued repetitive loading of a bearing will lead to surface fatigue, manifested as pitting, spalling or flaking of races, balls or rollers. Other progressive surface damage mechanisms include corrosion, fretting, abrasive wear (due to contaminants in the oil or some other external source), and other wear mechanisms associated with defective lubrication. All these faults can be regarded as departures from ideal rolling geometry and, depending on whether they occur in the inner race, outer race, ball or roller, generate vibration with the same characteristic periodicities, or repetition frequencies, as geometric irregularities.

Early detection and evaluation of this progressive type of damage, which if continued leads to total bearing failure, is the prime reason for monitoring bearing vibration.

2.2 Other Vibration Sources

2.2.1 Acoustic Emission

Acoustic emission is generated by very small scale plastic deformation or crack propagation in high stress regions. Slip, dislocation movements, or fracture release energy manifested as a propagating stress wave. In rolling bearings, the high stress levels are found in Hertzian stress regions just below the contacting surfaces between ball and race. Significant acoustic emission levels thus provide an indication of sub-surface fatigue crack growth, likely to be followed soon after by surface failure such as pitting or spalling.

2.2.2 External Vibration

Measurements of bearing vibration are complicated because part of the signal detected may be generated elsewhere in the machine. It is often difficult to distinguish the external sources from intrinsic bearing vibration, especially as the bearings form the transmission path between vibrations originating on the rotating assembly and the stationary bearing housing or machine casing where sensors are located. Furthermore, both external and intrinsic sources may excite resonances of races characteristic purely of the bearing, making their discrimination virtually impossible.

3. CHARACTERISTICS OF VIBRATION OF DAMAGED BEARINGS

The various types of surface damage in bearings, associated with deterioration processes result in geometric changes in the surface form or topology of the bearing elements. Manufacturing errors result in similar departures from true geometric shape; the major difference between such errors and damage being one of scale. Initially at least, surface damage due to fatigue and similar processes is at a local, almost microscopic, scale; for example a typical initial size of the fatigue pit is about 0·2 mm. Damage caused by corrosion or fretting covers a larger area, but local surface roughness remains of small size.

The nature of surface irregularities produced by damage governs the mechanism and characteristics of vibration generated by these features. The small size of the irregularities means that contact between rolling element and irregularity is of very short duration; effectively it is in impact action. A simple model of this contact action first given in [1] clarifies the significant parameters.

3.1 Impact Action

Fig. 3.1 shows a ball which is assumed to roll into a defect with instantaneous rotation centre fixed at A, until it impacts the far side of the defect at B with velocity u_s. If the ball rolls without slip on the inner race at C, then for a small defect size x,

$$u_s = v_I \frac{x}{d_B} = w_I \frac{d_I}{2} \frac{x}{d_B},$$

where

v_I = velocity at point C

w_I = rotational velocity of inner race

d_I = inner race diameter

d_B = ball diameter.

The energy transferred to the outer race at impact point B is proportional to the square of the velocity. Hence,

$$u_s^2 = w_I^2 \frac{x^2}{4} \frac{d_I^2}{d_B^2} \tag{3.1}$$

The response of the impacted bearing race, as measured by stress, particle motion (e.g. acceleration) or other parameter, is proportional to the energy at impact. Equation (3.1) shows that the parameters governing this response include the defect size, bearing geometry and speed. Bearing load does not directly affect the response, provided that the ball/defect contact conditions shown in Fig. 3.1 are maintained, i.e. the ball must fully engage the defect. Under some conditions, such as light load, full contact between ball and track may not be maintained, preventing full engagement of the defect, and the impulse response will then be reduced.

A measure of impact duration is the total time in which the ball is in contact with the impact point B. During this phase it is assumed that the ball rolls out of the defect with fixed centre of rotation B, so to clear the defect the ball centre P, having velocity v_P, must roll a distance x_P along the pitch circle d_P (see Fig. 3.1).

$$v_P = \frac{v_I}{2} = \frac{w_I d_I}{4}$$

$$x_P = \frac{x}{2} \frac{d_P}{d_o}$$

The time of contact t_R is:

$$t_R = \frac{x_P}{v_P} = \frac{x}{2} \frac{d_P}{d_o} \frac{4}{w_I d_I}$$

or, since

$$d_P^2 = d_o d_I \text{ approx.}$$

$$t_R = \frac{2x}{w_I d_P} \tag{3.2}$$

For typical rolling bearing applications in engines and transmissions t_R is of the order of tens of microseconds; e.g. for the bearing tests described in this report with a defect size $x = 0{\cdot}2$ mm, $t_R = 15$ microseconds. The actual rise-time of the impact will be a small fraction of the total time of contact, and consequently stress wave frequencies excited by the impact can extend into the megahertz region.

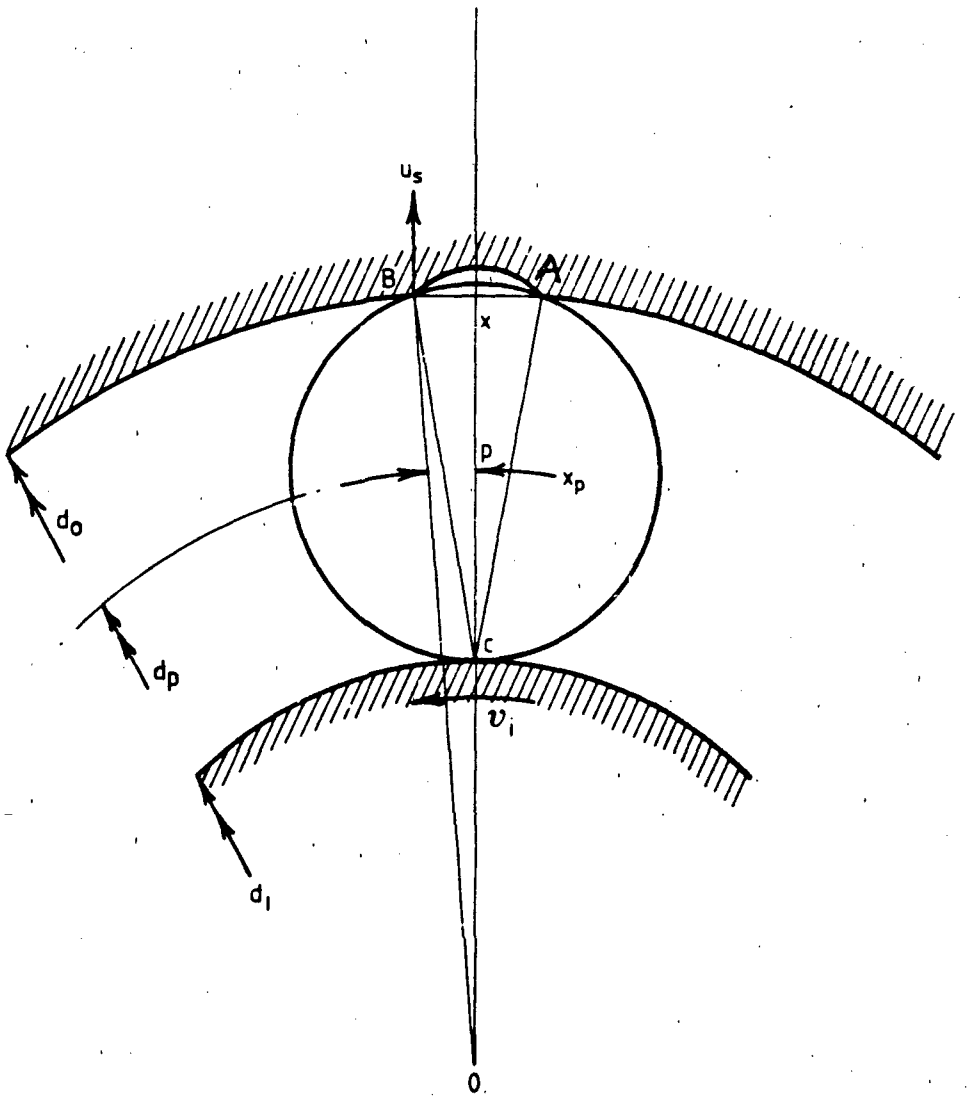

FIG 3.1 BALL CONTACT WITH DEFECT

3.2 Stress Wave Propagation and Response

When a rolling element contacts a defect it produces an impact which transfers energy into the bearing race. This impact energy, in the form of a stress wave, propagates outwards from the impact point at sonic velocity. When the stress wave reaches the interface between the bearing race and another component, the major part of the incident energy is reflected back into the bearing race and a small proportion is transmitted through the interface into the adjacent component. Damped resonant oscillations of the bearing race and adjacent component, and other components in the transmission path, are set up by multiple reflections of the propagating wave.

The short impact duration and resulting brief rise-time of the stress wave front means that a wide range of natural modes and frequencies can be excited in the bearing race. The simpler modes of the race are most readily excited, and because the race components are physically small, corresponding natural frequencies are high relative to general machine resonances.

The transmitted signal is attenuated as it passes through each interface, especially at high frequencies (50 kHz or greater) where the attenuation becomes severe. High frequency attenuation varies a great deal with details of design, fitting of components and installation practices. One reason for this is that at an interface contact is made at only a few engaging asperities and the true contact area is only a small fraction of the apparent area. Elsewhere the components are separated, and at high frequencies the separation distance can exceed the vibration amplitude, so that most of the surfaces do not make contact. The constraint applied by the contact depends on a fortuitous combination of factors including surface finish, accuracy and tightness of fit, presence of grease or lubricant (which can act as a couplant transmitting pressure waves between surfaces), so that the transmissibility is not readily predictable.

The foregoing discussion has referred to stress waves generated by the impulse action of a rolling element contacting a defect. It applies equally when acoustic emission mechanisms produce stress waves. As previously discussed, propagating fatigue cracks can generate acoustic emission, and since the motions involved are very small with correspondingly short durations, frequencies produced can extend into the megahertz range, albeit at low signal level. The low amplitude means that attenuation in the transmission path is a highly important consideration, and satisfactory measurement of acoustic emission requires that the transducer be located in a position with a favourable transmission path from the bearing.

3.3 Contact Frequencies and Load Modulation

So far, phenomena following an impact when a single ball or roller contacts a defect have been described. In an operating bearing a series of impacts occurs as successive balls contact the defect, generating a sequence of damped oscillation bursts superimposed on a random vibration background as shown in Fig. 3.2(*a*). The repetition frequency of the impacts and associated oscillation bursts depend on whether the defect is in the outer or inner race, or ball. If it is assumed that the balls roll without slip, repetition frequencies can be predicted theoretically [2] from the

TABLE 1

Contact Frequencies in Ball and Roller Bearings

f_I = frequency of rotation of inner race Other notation as in Fig. 5.2	
Outer race defect	$\frac{N}{2} f_I \left(1 - \frac{d_B}{d_P} \cos\theta\right)$
Inner race defect	$\frac{N}{2} f_I \left(1 + \frac{d_B}{d_P} \cos\theta\right)$
Ball or roller defect	$f_I \frac{d_P}{d_B} \left(1 - \left(\frac{d_B}{d_P} \cos\theta\right)^2\right)$

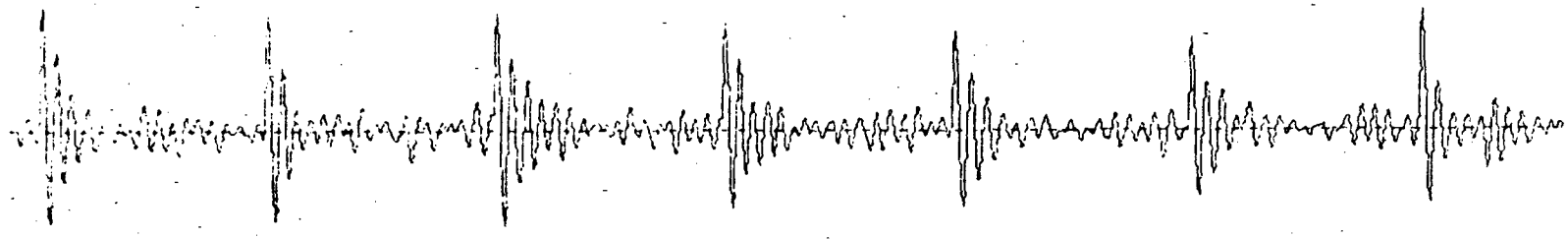

(a) Load Direction Fixed

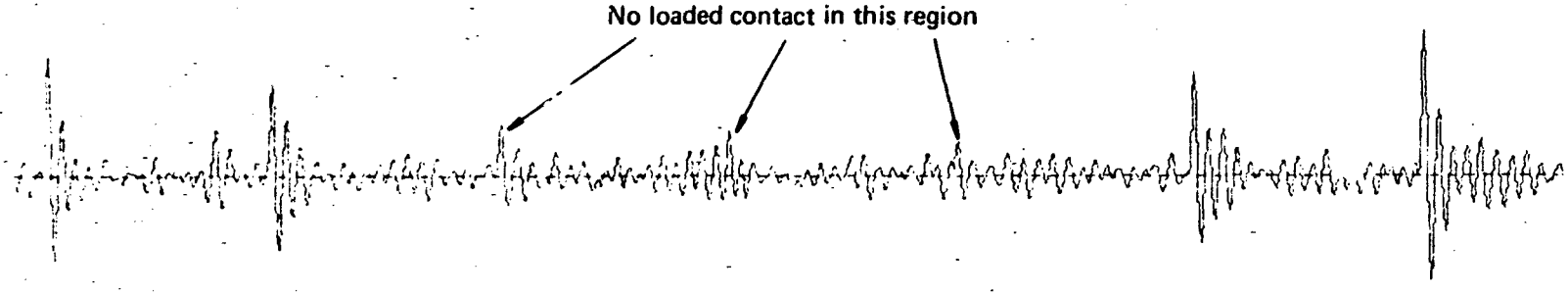

(b) Load rotating

FIG 3.2 VIBRATION OF DAMAGED BEARING

formulae given in Table 1 (slip modifies the predicted values). Manufacturing irregularities and faults such as lobing or ovality, can produce additional frequencies with interaction effects leading to numerous possible sum and difference frequencies as described in [3].

If the orientation of the load on the bearing remains fixed relative to the defect, successive pulse bursts are of roughly equal amplitude, as shown in Fig. 3.2(*a*). However, if the load orientation rotates relative to the defect, the impact amplitude is reduced in the unloaded region, so successive pulse amplitudes are modulated as shown in Fig. 3.2(*b*). A similar effect occurs in the less common event of a ball or roller defect, although the resulting modulation pattern is more complicated.

4. VIBRATION ANALYSIS METHODS FOR BEARING MONITORING

4.1 Conditions of Measurement

The most effective vibration analysis methods for rolling element bearings are those which utilise the particular characteristics of bearing vibration. Selection of such methods is of greatest importance when measurements must be performed under unfavourable conditions. Ray [4] states that for favourable conditions of measurement:

(i) The machine must not have any source of impulsive vibration other than bearings.

(ii) Bearing speed and load must be of sufficient magnitude to generate impulses.

(iii) There should be a direct transmission path from the bearing to the transducer mounting, with only one interface between bearing race and mounting face on the casing, and the mounting should be reasonably central relative to the bearing load zone.

Favourable conditions may be realized on simple machines such as pedestal bearings and pumps. Most complex machines however lack favourable conditions in one or more respects, with measurement difficulties ranging from slight to severe. In particular, adverse conditions are found in aircraft gas turbine engines and helicopter transmissions.

4.2 Signal/Noise Ratio Improvement

Adverse conditions result in a poor signal to noise ratio, since they may lead to:

(i) Low signal—caused by excessive attenuation in the transmission path, or low bearing load or speed,

(ii) High noise (i.e. unwanted interfering vibration) from sources in the machine other than bearings.

Unfortunately techniques such as synchronous time averaging, which are of great value in improving signal/noise in gear transmissions where meshing frequencies are an integral multiple of shaft speeds, are not applicable to bearings.

The most useful available technique is bandpass filtering which entails viewing the signal through a frequency 'window'. The filter window is selected to encompass frequencies generated by impulses and to exclude other machine vibration as far as possible. For maximum signal/noise ratio, the window should preferably be centred on one of the system resonances (which will be excited by impulses) or the resonance of the measuring transducer. The latter method is evidently independent of application and has been adopted in some commercial measuring systems.

4.3 Level Measurement—Time and Frequency Domains

Because vibration generated by rolling element bearings is highly complex, simple measurement of total (rms) vibration level is useful for monitoring bearings only when measuring conditions are highly favourable. The extra discrimination of octave or 1/3 octave analysis does not significantly enhance the effectiveness of level measurement.

Standard narrowband spectrum analysis techniques, normally implemented on a Fourier transform analyser, do not provide the clarification that might be expected. Most of the bearing vibration energy occurs in a band of frequencies around the pulse excited resonances; these frequencies depend on the structure or transducer and are not related to the bearing ball passing frequencies. Spectral lines at ball passing frequencies can be identified in some cases, but often tend to be submerged in the general noise level. The small defects associated with early bearing damage do not produce major changes in energy in any particular part of the spectrum, so spectrum analysis, except in favourable conditions, is only capable of detecting substantial bearing damage.

If after bandpass filtering, which removes extraneous low frequency and noise signals, the vibration signal is enveloped, high frequency structural or transducer resonances are removed, but impulse repetition frequencies remain. Frequency spectrum analysis of the enveloped signal clearly reveals ball passing frequencies with the amplitude of these components a function of the impulse energy. Trends in the amplitude of such components can reveal change or deterioration in the bearing, and the frequency value enables the origin of the signal to be attributed to particular bearings.

4.4 Pulse Measurement

A direct indication of bearing condition implemented in a number of instruments, is obtained by measuring the total energy of the impulse bursts, using a frequency window matched to the pulse oscillations. In the shock pulse measurement system of SKF, the oscillations in each pulse are enveloped and then integrated; the total area or energy is termed shock value. A peak hold circuit indicates maximum shock value of a pulse train. The system also incorporates a comparator with an adjustable threshold setting for shock value, so that the rate of shocks exceeding the present level can be determined--effectively giving a cumulative distribution of shock values. This distribution has been found to give a better correlation with bearing condition than maximum shock value [5].

Other methods used for measuring pulses determine average energy in a pulse train. Background noise is excluded by measuring only the signal exceeding a certain threshold level, which may be set either manually or automatically.

4.5 Pattern Recognition v. Level Measurement

All methods so far described essentially measure the amplitude of the vibration signal. This applies irrespective of the prior processing used to enhance the significance of the signal, and irrespective of whether it is measured in the time or frequency domain. Amplitude or level measurement has two significant limitations:

(i) Vibration level varies with several independent parameters such as bearing load and speed. For different records to be comparable they must be acquired under the same operating conditions.

(ii) Some vibration is always present, even with a machine whose bearings are in new condition, so deterioration or damage can only be determined by comparison of current records with those taken from a similar machine whose bearings are known to be in good condition. Generally this is achieved by taking 'baseline' records when the machine is virtually new, then observing trends as successive records are taken during the life of the machine.

Pattern recognition methods, unlike level measurement, characterize intrinsic features of the vibration signal which forms its own reference. Generally, vibration patterns are relatively independent of machine operating parameters, so reproducing identical test conditions for comparison of records becomes less critical. In addition, the need for a baseline signature is obviated, as the methods are inherently independent of signal level.

Experience has shown that while pattern recognition methods are very sensitive to change and thus provide early indication of damage, their major limitation, when applied to bearing

signatures, arises when damage is increasing. Under these circumstances, the pattern tends to revert to that of the undamaged signal, albeit with much higher vibration levels. To cope with this situation, pattern analysis may need to be complemented by level methods.

4.6 Probability Distribution

The distinctive feature of vibration generated by damaged bearings is a periodic series of impulse generated oscillation bursts, sometimes modulated because of load variation effects. A random background vibration combines with the impulsive oscillations, tending to obscure the impulsive pattern as signal/noise ratio deteriorates.

Direct measurement of pulse energy is satisfactory when signal/noise is adequate but with a less favourable ratio more sensitive methods are required. Such methods include spectrum analysis of the signal envelope, which determines pulse amplitude and periodicity, and analysis of statistical properties (in particular those derived from the probability density distribution) of the vibration signal.

Probability density $p(x)$ of a time varying signal $x(t)$ is defined such that the probability of the signal value lying between x and $x+dx$ is $p(x)dx$. Since the vibration of an undamaged bearing consists of the combination of numbers of separate independent effects, the central limit theorem indicates that its probability density will tend towards Gaussian. This theoretical prediction is confirmed in practice; Fig. 4.1(a) shows the probability density distribution of a bearing in good condition, with a superimposed Gaussian curve. The same data is plotted in Fig. 4.1(b) with a logarithmic probability scale, and the Gaussian distribution appears as a parabola.

Deterioration and damage in a bearing lead to changes in the probability density. Damped impulsive oscillations in the time domain signal, of significant magnitude relative to the Gaussian noise of the undamaged bearing, lead to greater occurrence of extreme signal levels manifested by changes in the tails of the probability density distribution. The higher probability of extreme values is shown in Fig. 4.2(a) and more clearly in the logarithmic plot in Fig. 4.2(b).

Of the various statistical measures used to quantify the shape of probability density curves, one most easily measured is the crest factor—the ratio of peak value to standard deviation (rms). For a periodic signal this provides an absolute definition; but for a signal with random components peak value must be defined as the value exceeded at some defined relatively low probability level. (The existence of this probability may not be apparent in analogue peak or crest factor measurement, but it is implicit in the time decay constants of the measuring circuit).

Crest factor measurement provides a useful preliminary indication, but more sensitive methods are available for use in adverse conditions. An approach which is simple but sensitive utilizes the statistical moments M_n of the probability distribution $p(x)$. The moment M_n of order n is defined as:

$$M_n = \int_{-\infty}^{\infty} (x-\bar{x})^n \, p(x)\, dx \qquad (4.1)$$

As defined the first moment is zero and the second moment is familiar as the variance, s^2. Odd moments provide a measure of the asymmetry or skewness of the distribution; even moments measure its spread with the higher order moments responding to occurrence of extreme values in the tails of the distribution. The fourth moment M_4 has been found to be sufficiently sensitive without responding excessively to occasional measurement perturbations. This moment is normalised relative to standard deviation; the ratio $M_4/M_2^2 = M_4/s^4$ is called kurtosis, K.

The kurtosis of a signal with Gaussian probability distribution is 3; vibration measurements on good bearings give kurtosis values close to 3. As bearing damage develops, with the generation of impulsive oscillation bursts (e.g. Fig. 3.2) kurtosis values rise, as shown in the corresponding probability density plots (Figs 4.1 and 4.2).

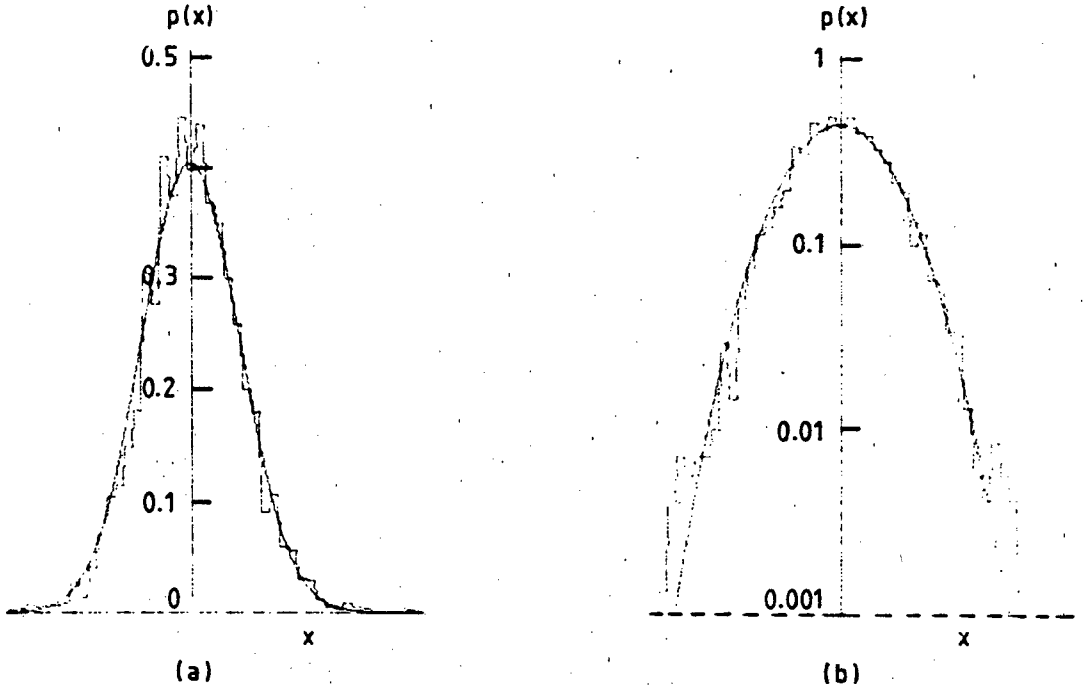

K = 3.2

FIG 4.1 PROBABILITY DENSITY DISTRIBUTIONS – SOUND BEARING –

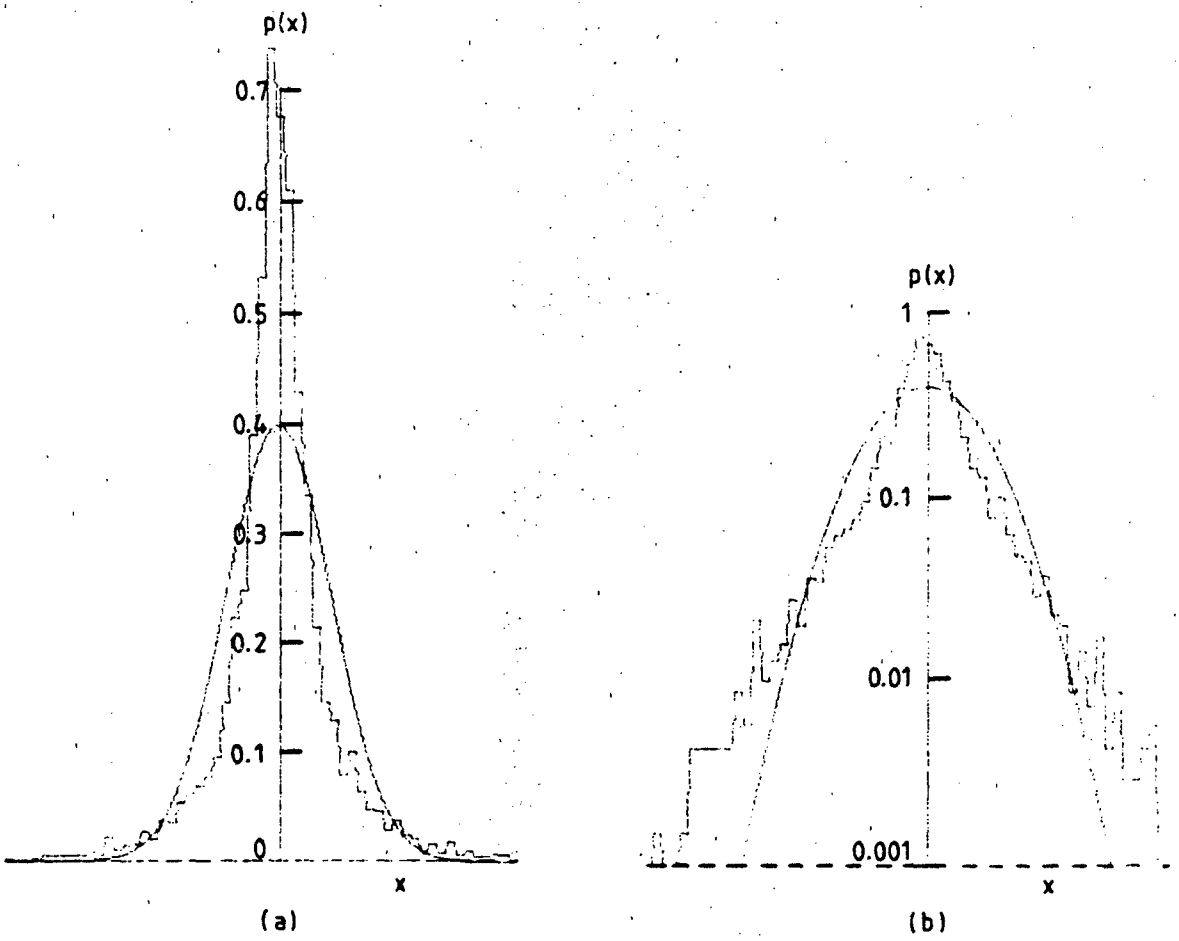

K = 6.5

FIG 4.2 PROBABILITY DENSITY DISTRIBUTIONS – DAMAGED BEARING –

5. EXPERIMENTAL INVESTIGATIONS

A number of bearing and gear rigs have been in use for some time for the purpose of evaluating condition monitoring methods. Initially, kurtosis measurements were made on angular contact bearings, which were being used in other tests for the evaluation of shock pulse measurement [5]. After promising initial results, a program was initiated to test a number of deep groove bearings to failure, with the aim of evaluating kurtosis measurement and comparing its effectiveness as a condition monitoring technique for bearings with other methods such as shock pulse, rms acceleration and envelope spectrum measurement. In addition comparison of transducers with different resonances, including acoustic emission, would be made.

5.1 Bearing Test Rig

The rig comprises two bearing housings, one containing the 30 mm test bearing, the other containing two angular contact bearings arranged in tandem which react the test load. Axial load is applied to the outer race of the test bearing by screwing a large nut into the housing, thereby putting the shaft in compression with a balancing tension in a surrounding tube, which is fitted with a strain gauge bridge for load measurement.

Cooling is obtained by jet impingement of a synthetic oil, and power is supplied to the rig by a Ward–Leonard set with a DC motor providing a variable speed drive.

A photograph of the rig is shown in Fig. 5.1, highlighting the principal features and the location of various transducers.

5.2 Test Bearings

Two types of ball bearings, of 30 mm bore, were used:

(i) Angular contact bearing—ABEC 9 precision class (Barden 106B×48).

(ii) Deep groove ball bearing (SKF 6006/C3).

The principal dimensions of both bearings are shown in Fig. 5.2. Table 5.1 gives contact or repetition frequencies for the bearings at the test speed of 6000 rpm, calculated from the formulae given in Table 1.

TABLE 5.1

Ball Passing Frequencies

Component	Frequency (Hz) Angular Contact	Deep Groove
Ball Passing—Outer Race	587	453
Ball Passing—Inner Race	813	647
Ball Rolling	583	549
	Based on shaft frequency 100 Hz (6000 rpm)	

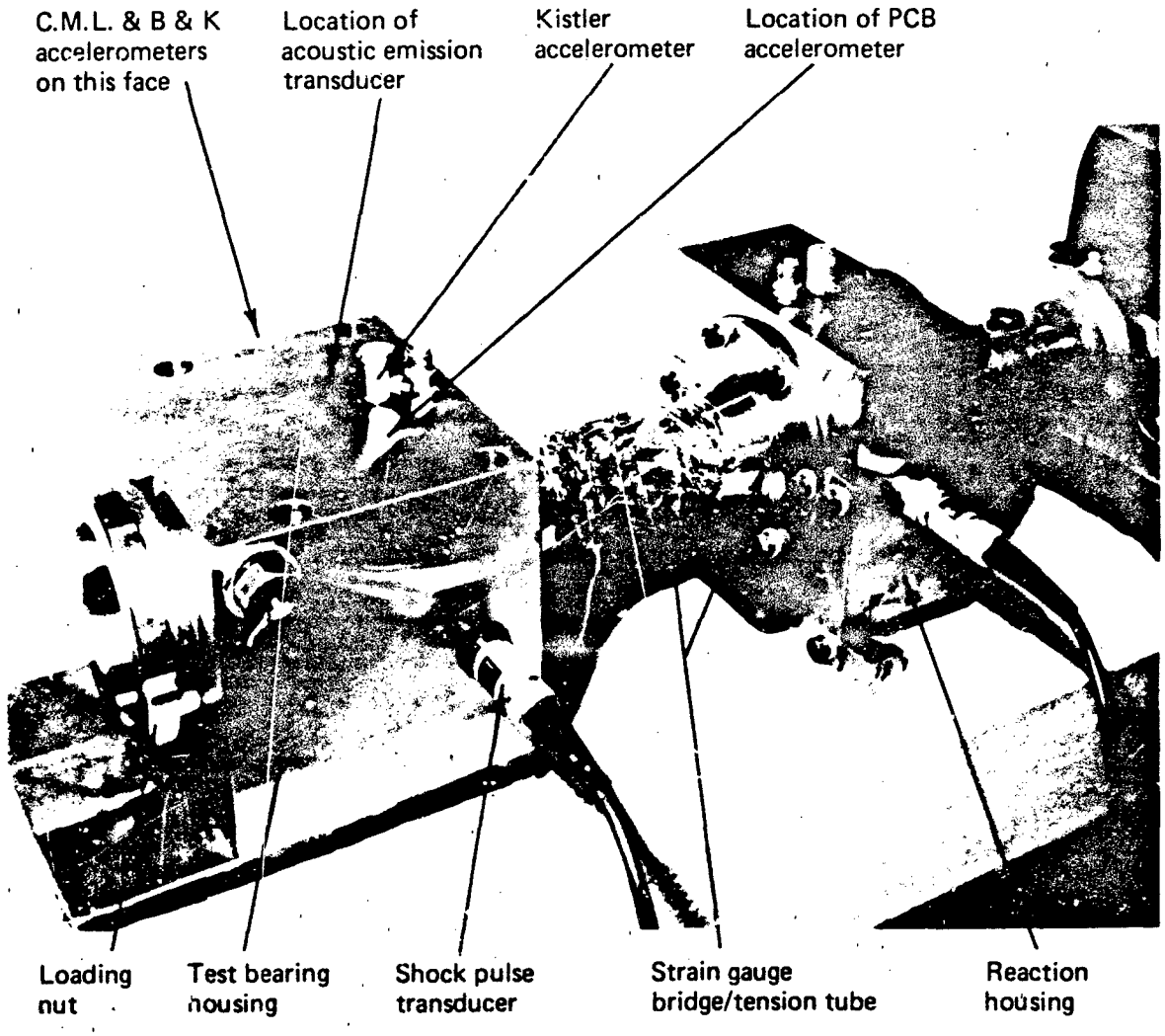

FIG 5.1 BEARING RIG

The inner and outer races of the bearings are bonded to steel sleeves, which are supported in the housing and on the shaft at three contact points as shown in Fig. 5.3. Resonant frequencies have been calculated for the bearing components and the bearing/sleeve assembly (assuming ideal bonding) for lower modes using formulae in [6], and are given in Table 5.2.

TABLE 5.2

Natural Frequencies (kHz) of Bearing Components

Mode type	No. of diametral nodes	Angular contact				Deep groove			
		Alone		With sleeve		Alone		With sleeve	
		Inner	Outer	Inner	Outer	Inner	Outer	Inner	Outer
Race—In-plane Flexure	0	49·1	32·1	40·6	27·8	48·7	32·3	40·3	27·9
	2	8·2	3·5	16·4	8·4	8·7	3·8	16·6	8·7
	3	23·1	9·8	46·5	23·8	24·5	10·8	47·1	24·6
Race—Transverse Flexure	2	7·9	3·4	15·9	8·1	8·4	3·7	16·1	8·4
	3	22·7	9·7	45·7	23·4	24·1	10·6	46·3	24·2
Ball—Ellipsoidal	—	437·0				414·0			

5.3 Instrumentation

A diagram of the instrumentation arrangement is shown in Fig. 5.4. Not all equipment illustrated was in use at the one time; in the preliminary tests on the angular contact bearings, a single accelerometer was used and its output, after signal conditioning and capture on the digital waveform recorder, was processed on the ARL DECsystem10 site computer. In the later tests on the deep groove bearings, additional accelerometers, including an acoustic emission transducer, a shock pulse measuring system and an on-line kurtosis meter were used. Much faster data processing was provided with the addition of a dedicated VT103 microcomputer to the system.

5.3.1 Kurtosis Measurement

Kurtosis was calculated as follows on the DECsystem10 and VT103 computers using co..diti.. ..ta records captured by the digital recorder. If a random sample of N points, v.. ..taken from the time signal $X(t)$ (uniform sample intervals may be used provided t.. ..period is unrelated to any periodicities in the signal) the formula for statistical moments o.. equation (4.1) becomes:

$$M_n = \frac{1}{N} \sum_{i=1}^{N} (Xi - \bar{X})^n \qquad (5.1)$$

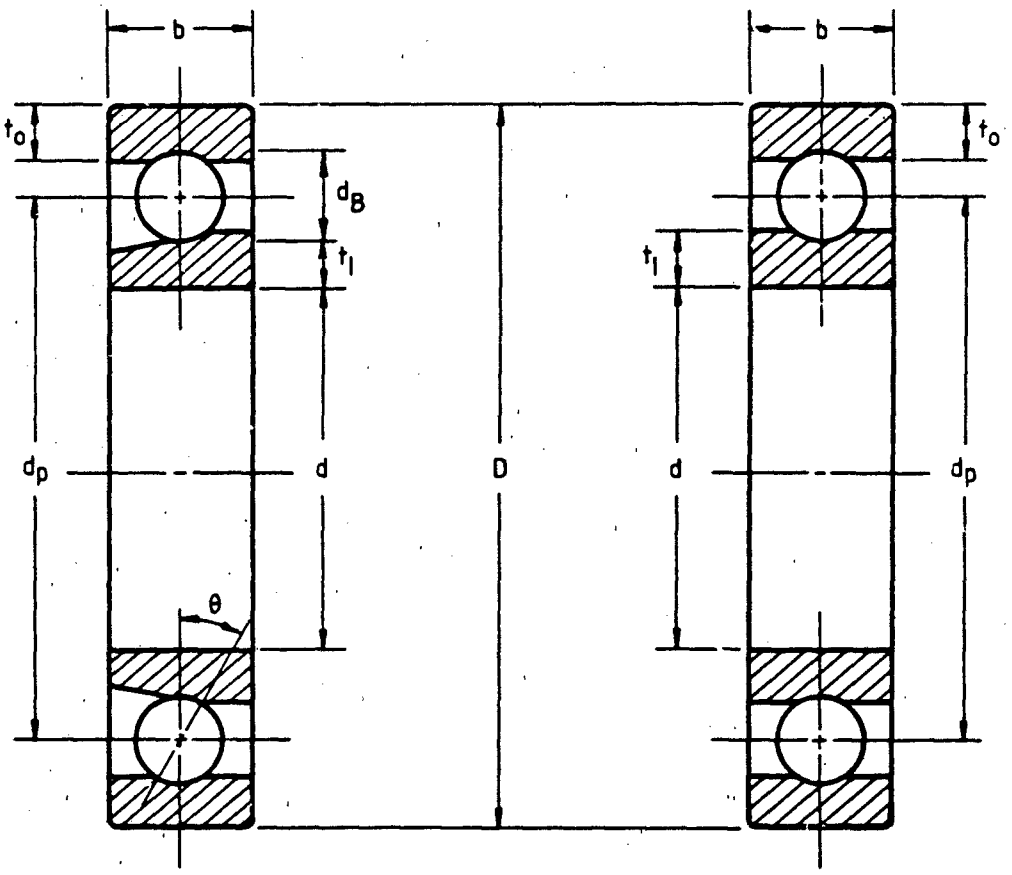

(a)
Angular contact (BARDEN)

(b)
Deep groove (SKF)

		Dimensions (mm)	
		(a)	(b)
Bore	d	30	30
Outside diameter	D	55	55
Pitch diameter	d_P	42.5	42.5
Mean thickness	t_l	3.6	3.9
Inner and outer	t_o	3.6	3.9
Width	b	13	13
Ball diameter	d_B	7.1	7.5
Contact angle	θ	15°	–
No. of balls	N	14	11

FIG 3.2 BEARING DIMENSIONS

and so kurtosis is:

$$K = \frac{M_4}{(M_2)^2} = \frac{N \sum_{i=1}^{N} (Xi - \bar{X})^4}{\left\{ \sum_{i=1}^{N} (Xi - \bar{X})^2 \right\}^2} \tag{5.2}$$

At high sample rates (i.e. when examining spectra of high frequency windows) the total sample time was less than one shaft revolution—sometimes only one or two impulse events—so concatenated records were averaged until acceptable convergence was obtained, using the formula:

$$\bar{K} = \frac{L \sum_{j=1}^{L} M_{4j}}{\left\{ \sum_{j=1}^{L} M_{2j} \right\}^2} \quad \text{(for records of equal length)} \tag{5.3}$$

The Kurtosis meter (K-meter) implements this measurement process in one instrument. Input signals are bandpass filtered and then digitized. The limits of each frequency window or band (the same limits as those used on the bandpass filter prior to computer calculation of kurtosis) are given in Table 5.3. The K-meter incorporates a microprocessor which computes kurtosis, rms acceleration and velocity. Output of the envelope of each band is provided for external spectrum analysis, but the gain of the envelope circuit is variable and is not calibrated.

K-meter operation and readout is oriented toward the non-technical user: using kurtosis and rms acceleration values, an algorithm in the micro-processor gives a one-shot diagnosis of bearing condition—'Good', 'Early', 'Advanced' or 'High Damage'.

TABLE 5.3

Frequency Bands

Band No.	Frequency Cut-off kHz	
1	2·5	5
2	5	10
3	10	20
4	20	40
5	40	80

5.3.2 Transducers

A secondary objective formulated after the initial tests was to compare the effectiveness of various transducers in detecting bearing damage; so in the main series of tests four transducers were used, measuring acceleration and acoustic emission. Characteristics of these transducers are given in Table 5.4. Full characteristics were not available for the transducer supplied with the Shock Pulse Meter, but its nominal resonance frequency is known to be about 32 kHz.

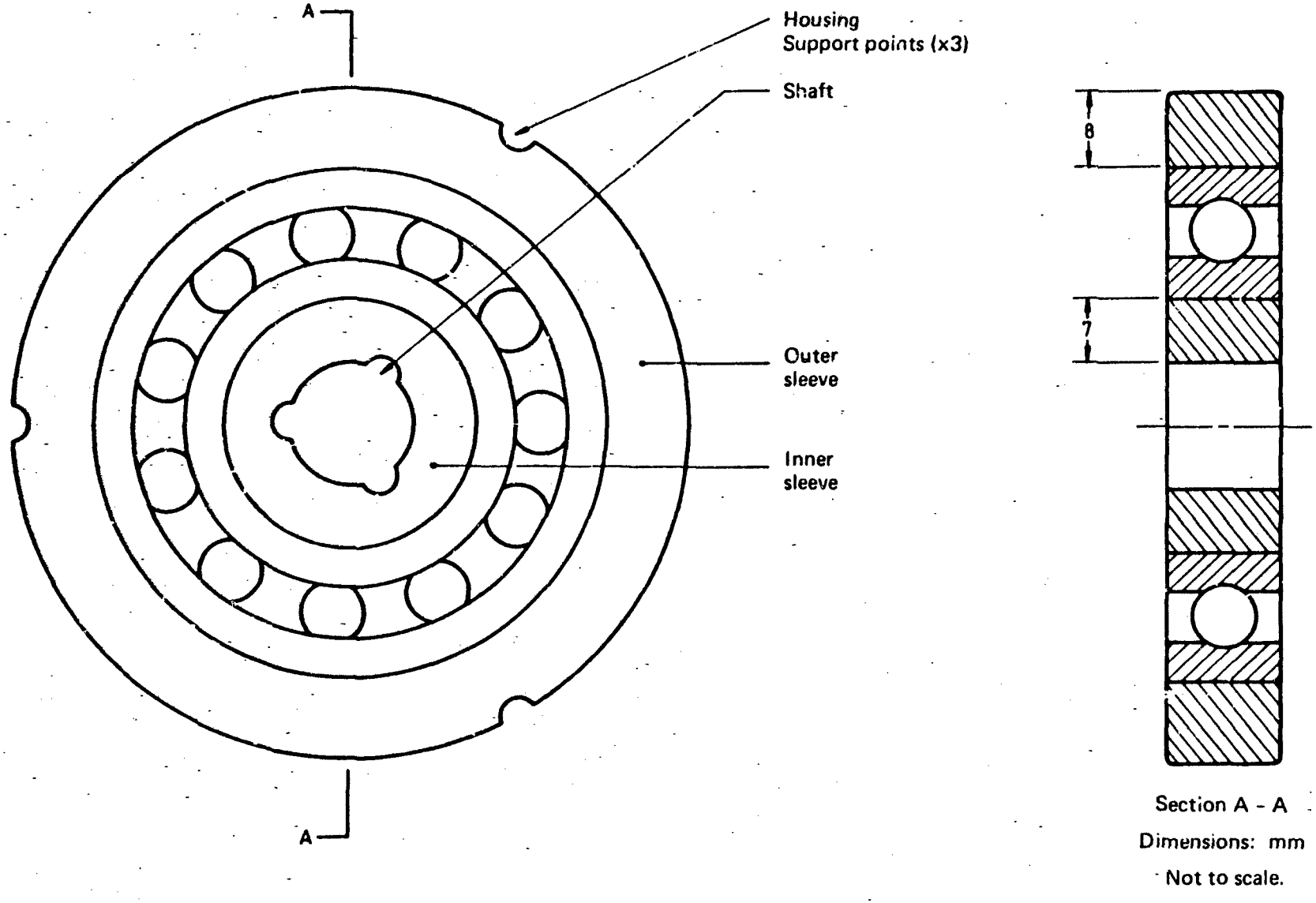

FIG 5.3 BEARING AND SLEEVE ARRANGEMENT

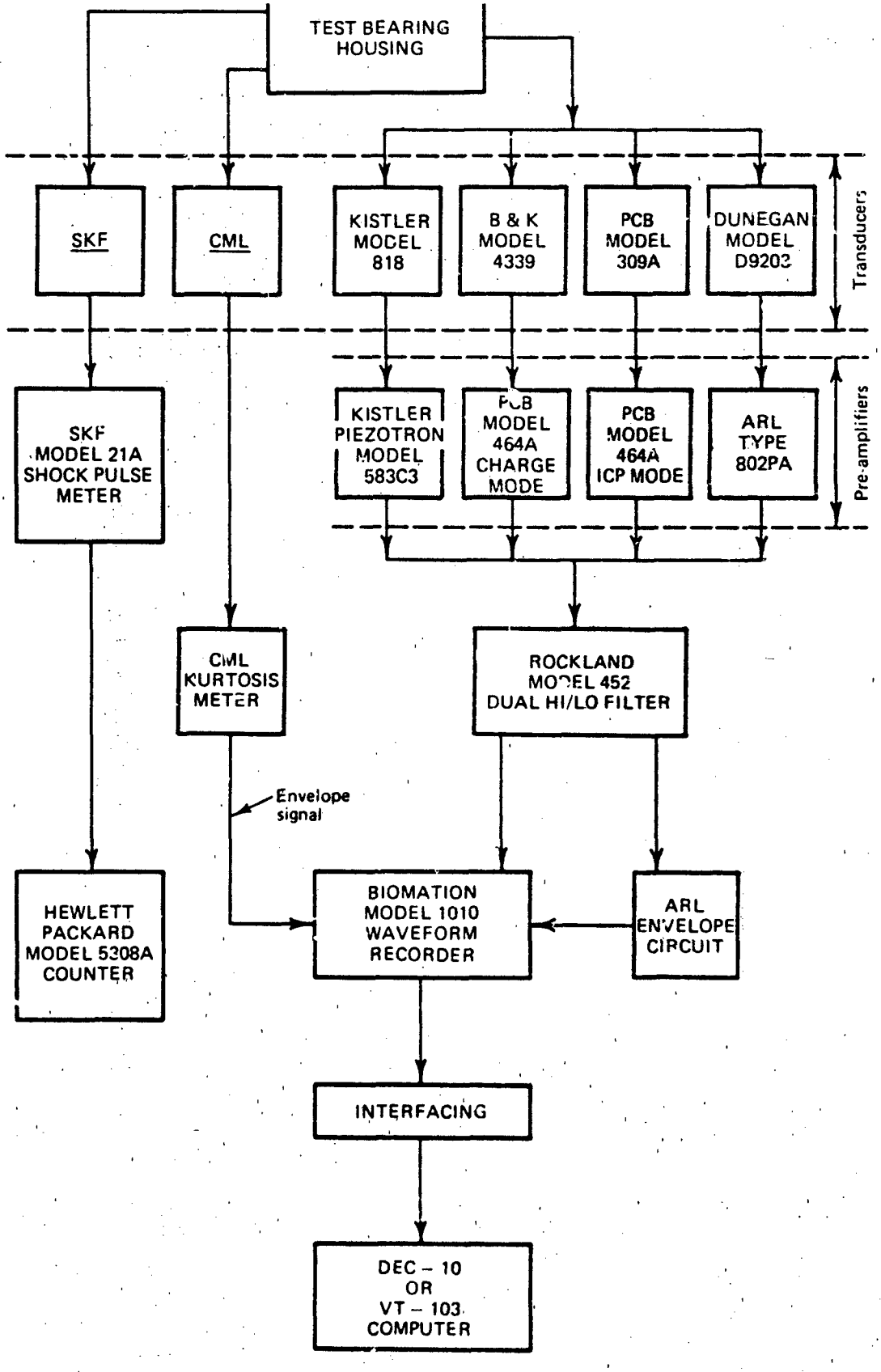

FIG 5.4 INSTRUMENTATION SYSTEM

TABLE 5.4

Transducer Characteristics

Manufacturer	Type	Model	Sensitivity	Nominal Mounted Resonance—kHz
Kistler	Accelerometer	818	9·85 mV/g	34
Bruel & Kjaer	Accelerometer	4339	11·0 pc/g	57
PCB	Miniature Accelerometer	309A	5 mV/g	120
Dunegan/Endevco	Acoustic Emission	D9203	−64dB re 1V/μbar	> 200
CML (K-meter)	Accelerometer	—	100 mV/g	28

5.3.3 Other Instrumentation

Other instruments shown in Fig. 5.4, excepting the Shock Pulse Meter, are standard types and need no detailed description. The principle of shock pulse measurement is outlined in Section 4.4; a more detailed description of its implementation is given in [5].

6. RESULTS AND DISCUSSION

6.1 Angular Contact Bearing Tests

Several high precision angular contact ball bearings, as shown in Fig. 5.2, which had already sustained varying degrees of damage, were available for kurtosis measurement. The results of these tests are presented in Figures 6.1–6.4, which include plots of kurtosis in various frequency bands under different conditions of rotational speed and axial load, and for increasing degrees of damage.

One bearing was tested at a speed of 6000 rpm and a load of 4500 N. After 65 hours the bearing had sustained spalling damage of the kind illustrated in Fig. 6.1. Such damage causes substantial impulsive action and these effects are well illustrated in the kurtosis trend plots in Fig. 6.2.

A second bearing, which had already sustained spalling damage to the inner race, was tested under low load of 445 N and varying speed conditions. Measurements were also taken from sound bearings located in the reaction housing and the results are shown in Fig. 6.3. Testing continued at 6000 rpm and increased load of 4500 N; these results are shown in Fig. 6.4.

It can be seen that sound bearings produce kurtosis values close to 3, regardless of load and speed conditions. For damaged bearings, kurtosis varies with these conditions in a complex manner, though in all cases there is a definite indication of damage with kurtosis values significantly greater than 3 in at least some of the frequency bands.

At low speeds impact energies are smaller (eqn 3.1), and impulse amplitudes may also be reduced because of imperfect ball/track contact at low loads. Together these effects may lead to impulse levels being significantly reduced relative to background noise, so in the low frequency bands kurtosis values reveal no damage (Fig. 6.3). Continuing higher kurtosis values in the high frequency bands, under the same conditions, are more difficult to explain. Other impulse generating mechanisms associated with propagating bearing damage, and having greater energy content in the high frequency bands, may be significant in this situation.

Figs 6.4(*a*) and 6.4(*b*) show that, starting in the lower frequency bands and progressing to the higher, the kurtosis of a severely damaged bearing tends to revert to the undamaged value of 3, albeit with a much higher general vibration level (not shown on these plots). This characteristic has been widely observed (it is seen in many of the results later in this report) and must be taken into account when kurtosis measurement is used for bearing condition monitoring.

(a) Inner race spall size: .75 mm x .5 mm

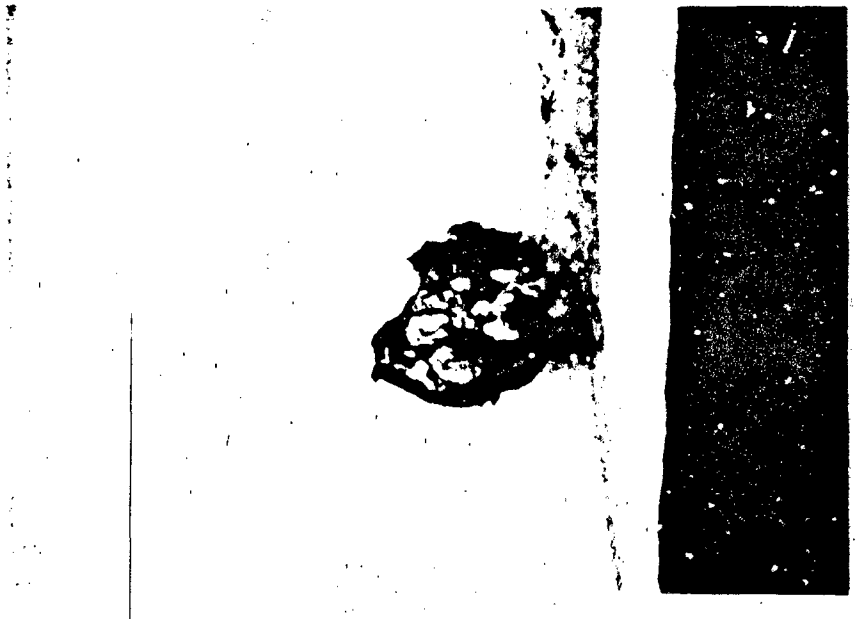

(b) Outer race spall size: 2.5 x 2.0 mm

FIG 6.1 DAMAGE TO BEARING AFTER 65 HOURS RUNTIME

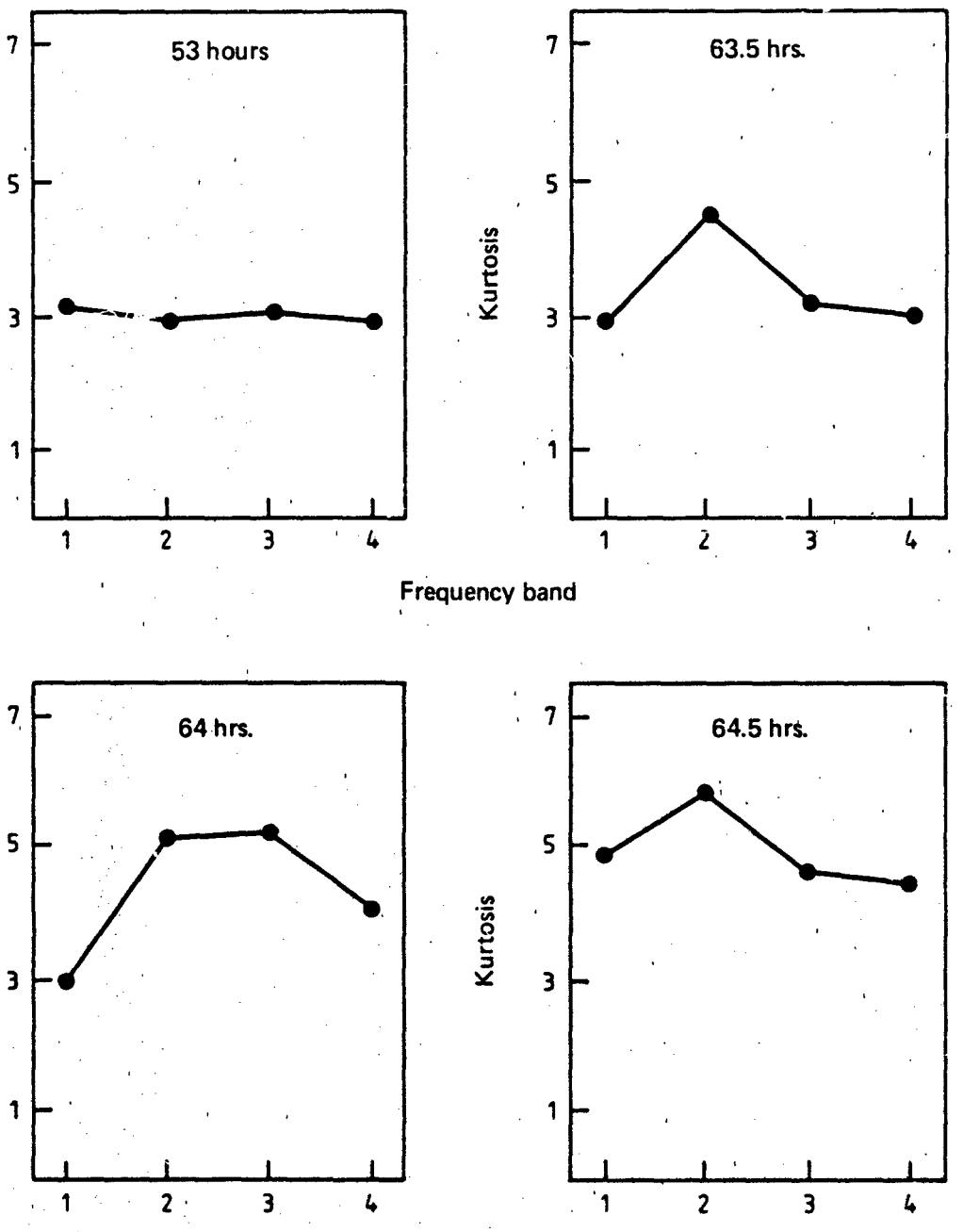

FIG 6.2 KURTOSIS Vs. FREQUENCY BAND PLOTS FOR A NEW BEARING AT TIME 0 HOURS UNTIL 65 HOURS, RUNNING AT 4500 N LOAD AND 6000 RPM.

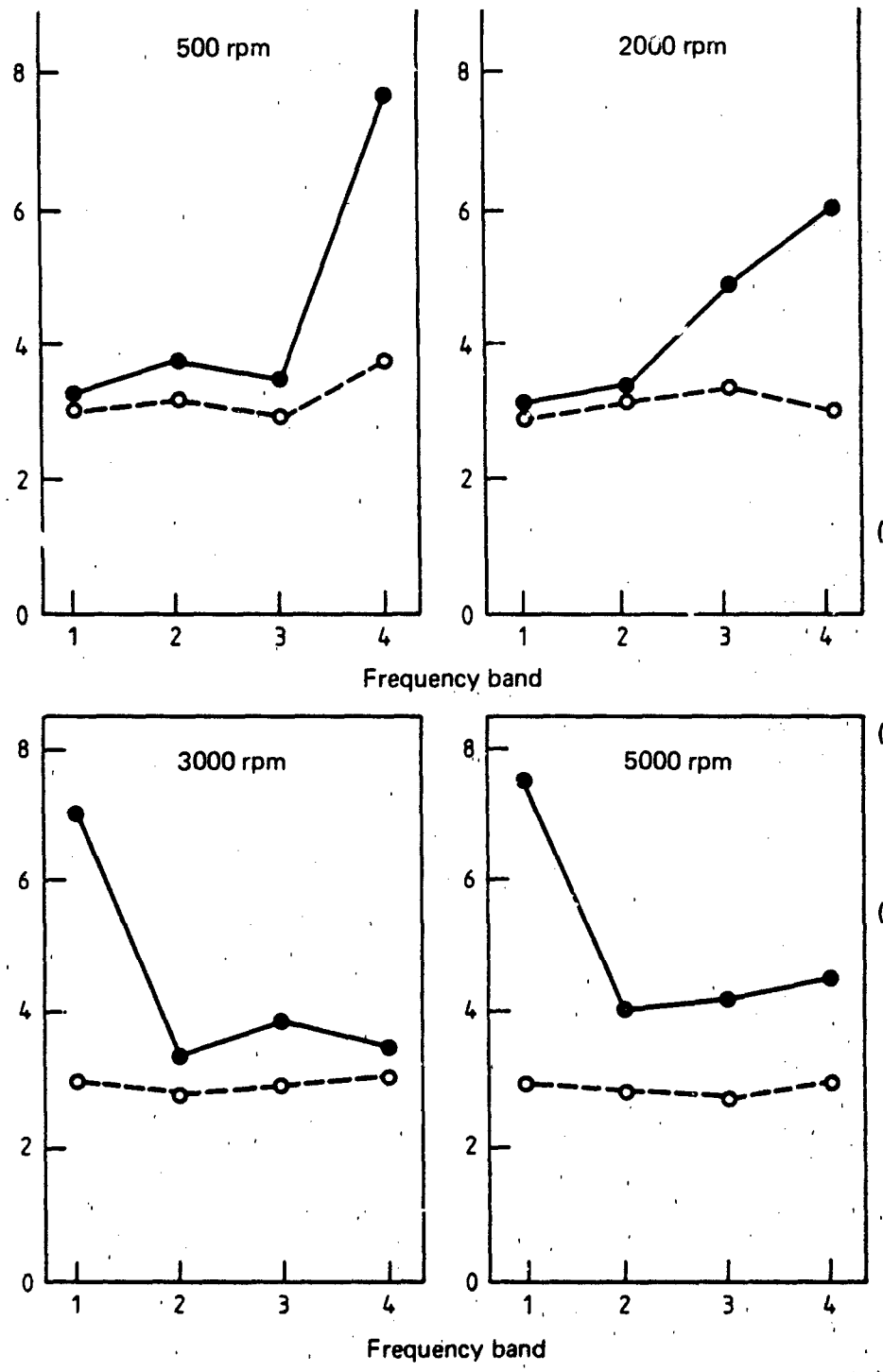

FIG 6.3 KURTOSIS (K) Vs. FREQUENCY BAND AT VARIOUS SPEEDS FOR SOUND AND DAMAGED BEARINGS.

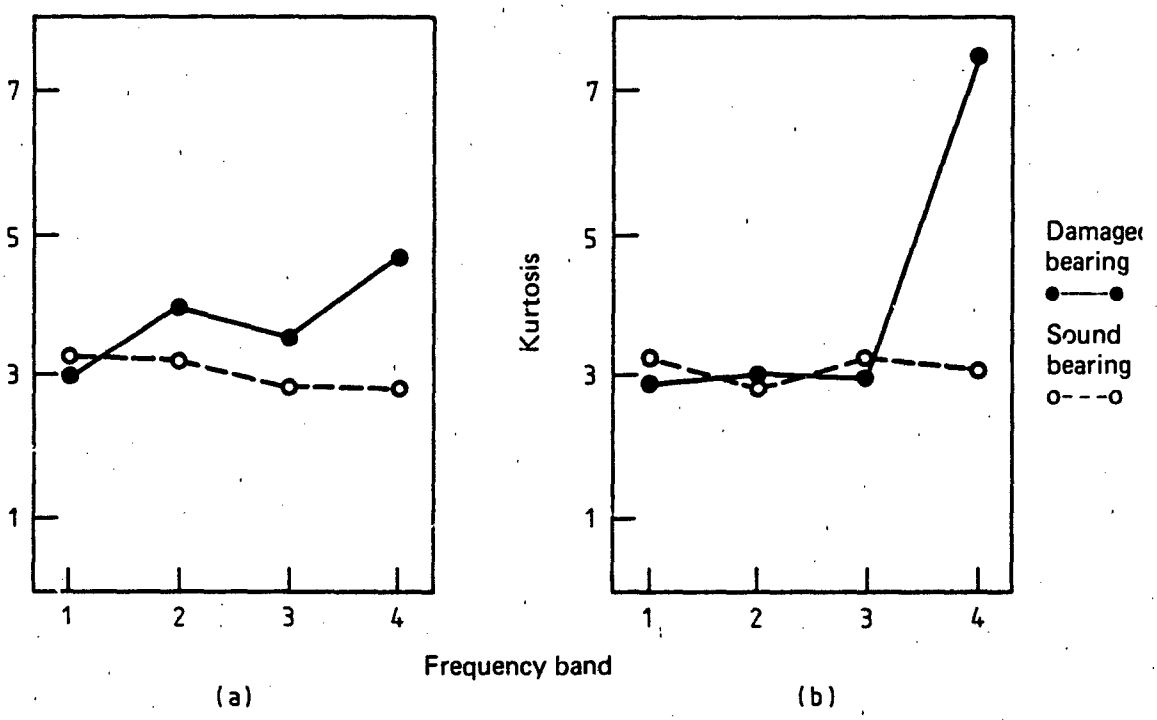

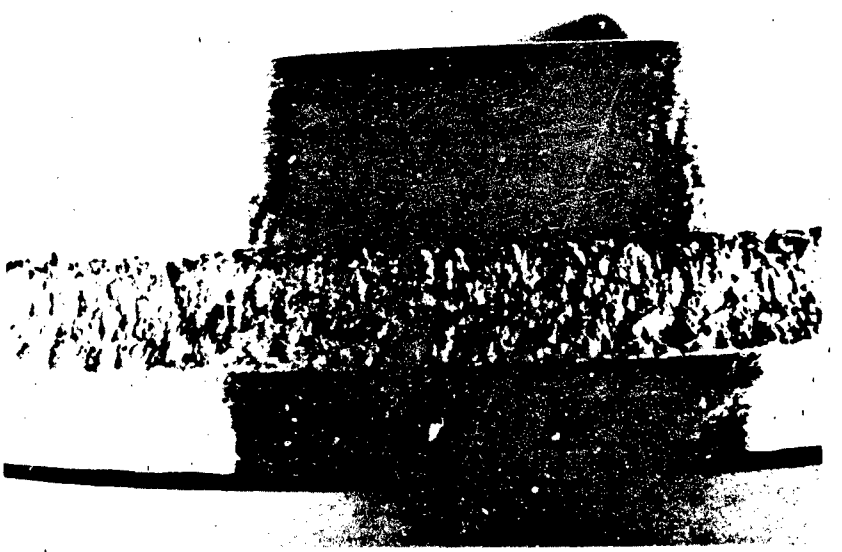

(c)

FIG. 6.4

(a) Damaged bearing of Fig 6.3: Load = 4500N, Speed = 6000 rpm

(b) Same bearing, 15 minutes later (131.75 hours)

(c) Inner race of bearing at 131.75 hours.

When damage consists only of a few discrete pits or spalls, the oscillations generated by one impulse decay back to the background noise level before the next impulse generating defect is encountered, and this impulsiveness is manifested by high kurtosis values of the signal. But with severe damage, such as Fig. 6.4(*c*), there are multiple closely spaced impulse actions, and the oscillations produced by one impulse do not have sufficient time to decay back to the noise level before the next impulse is encountered. The total vibration signal consists of the cumulative response to this impulse sequence, which because of the random nature of the impulses tends towards a Gaussian probability distribution with kurtosis approaching 3. This effect is most pronounced in the low frequency bands, because these signals have the longest decay times.

The existence of transducer and structural resonances affects results in certain frequency bands. Impulse action will excite resonances both in the rig and in the transducer, and relatively high vibration signals can be detected at structural and transducer resonances. Herein is the main significance of these resonant frequencies; frequency bands or 'windows' centred on these values should record reasonable signal levels for kurtosis measurement. For example, Fig. 6.2 suggests the presence of a structural resonance in band 2 (5–10 kHz), since increased kurtosis values were first detected in this band.

Values of natural frequency for the bearing components have been computed (Table 5.2), but which frequency will be most readily excited depends on a precise, almost microscopic definition of the conditions of constraint and so cannot be predicted. A similar computation was made for the bearing housing using a finite element model, revealing a number of possible modes in the frequency range (Table 6.1), but again it is not possible to predict which modes will be excited.

TABLE 6.1

Bearing Housing Assembly Natural Frequencies (kHz) from Finite Element Model

Boundary Conditions—Base Restrained in Plane	
Symmetric Mode	Antisymmetric Mode
7·3	7·2
11·5	13·0
14·8	14·8
15·1	15·4
15·7	18·1
19·8	20·8
20·5	21·5
22·4	23·1

To resolve this uncertainty, experimental measurements were made of the impact response of the bearing/housing system. Two different types of transducer were used, enabling structural and transducer resonances to be distinguished. Results are shown in Fig. 6.5, and a major structural resonance at 8·5 kHz is evident, corresponding to the relatively simple bearing race mode with 2 diametral nodes (Table 5.2). Other structural resonances seen in these response curves could also be useful in selecting frequency windows for vibration measurement.

6.2 Deep Groove Ball Bearing Tests

Four standard commercial quality deep groove ball bearings, as shown in Fig. 5.2, were available for testing. At first only shock pulse measurement and kurtosis estimation by computer were available, but the K-meter became available early in the test series, thus providing an extra

transducer with alternative kurtosis and level estimation, and a signal envelope output for spectrum analysis. Since the envelope output has a variable gain, no significance could be attached to the absolute level of spectral lines, but late in the test program, a locally developed circuit was obtained, giving a calibrated envelope output for spectrum analysis.

Kurtosis, g rms levels, shock pulse distributions and envelope spectra for these bearings (designated A, B, C, D) are plotted in Appendices A, B, C, D and E. A description of bearing condition at times of inspection is given in Appendix G, with accompanying photographs.

The four bearings, which were operated at the same speed and load (6000 rpm and 6600 N), had widely different lives. Life to the first indication of damage varied from 1·4 to 136 hours, and to the conclusion of testing from 2·5 to 152 hours. However, damage patterns during the tests were similar for all bearings. The following discussion is primarily centred on the results from bearing C, since this bearing was fitted with the greatest range of transducers and measuring systems. Generally, results for the one bearing are typical of all, but comparisons with other bearings are made where appropriate.

6.2.1 Kurtosis and Level Trends

Changes in kurtosis values as bearings deteriorated in operation followed a fairly typical pattern. First damage indications were increasing kurtosis in low frequency bands, with progressive damage leading to a fairly steady plateau with high kurtosis values in all bands, and finally, kurtosis values reducing, especially in the low bands, with extensive damage. This pattern is illustrated by bearing C where kurtosis values greater than 3 were first observed at about 11 hours with the Kistler transducer (Fig. A.7) and the K-meter (Fig. A.8) and with the PCB transducer (Fig. A.9) when first fitted at 12 hours. Physical inspection of the bearing at this time revealed a spall about 1 × 3 mm in the inner race. With further testing, kurtosis values remained high, but after 17·7 hours they tended to reduce to undamaged values, primarily in the lower frequency bands. Inspections at 15 hours revealed that the inner race spall had grown to about 2 × 3·5 mm, with 'bruise' marks (due to crushing of re-entrained wear particles) all round the outer race. At 18·5 hours, there were two large spall areas, 8 mm and 11 mm long separated by about 2 mm on the inner race, with severe bruising over the remainder of the inner and outer races. The test was concluded at 20 hours with about 180° of the inner race completely failed, two more spalls beginning on the remaining section of the race, severe bruising and one spall on the outer race, and spalling and pitting apparent on the balls (Figs G.5–G.9).

Simultaneous measurements of total (rms) vibration showed levels increasing slowly in the early damage phase, and much more rapidly as bearing damage became severe (Figs B.7, B.8, B.9). The first noticeable increase in level with bearing C occurred after 14 hours (Fig. B.8), some 3 hours after the first registered change in kurtosis.

6.2.2 Shock Pulse Distributions

Shock pulse distribution curves revealed a definite and consistent change with early damage (Fig. D.3—bearing C at 11·5 hours) and progressive changes with increasing and severe damage.

6.2.3 Envelope Spectra

Envelope spectra of deteriorating bearings followed a pattern similar to kurtosis. Spectra of undamaged bearings revealed random spectral distributions with no identifiable frequency peaks. Once early damage occurred, the spectra changed markedly and the various characteristic ball passing frequencies became apparent. With progressive damage, amplitudes at these frequencies increased relative to background noise. When the damage became severe, the threshold noise increased but unlike kurtosis, which at this stage tended to revert to undamaged values, spectral lines at the characteristic frequencies were still clearly evident, albeit at reduced magnitudes. Fig. E.2 clearly illustrates the pattern of rise and fall in relative magnitudes of spectral lines at ball passing frequencies, while Figs E.3–E.5 show a similar pattern for absolute magnitudes when the locally made circuit was used on bearing D.

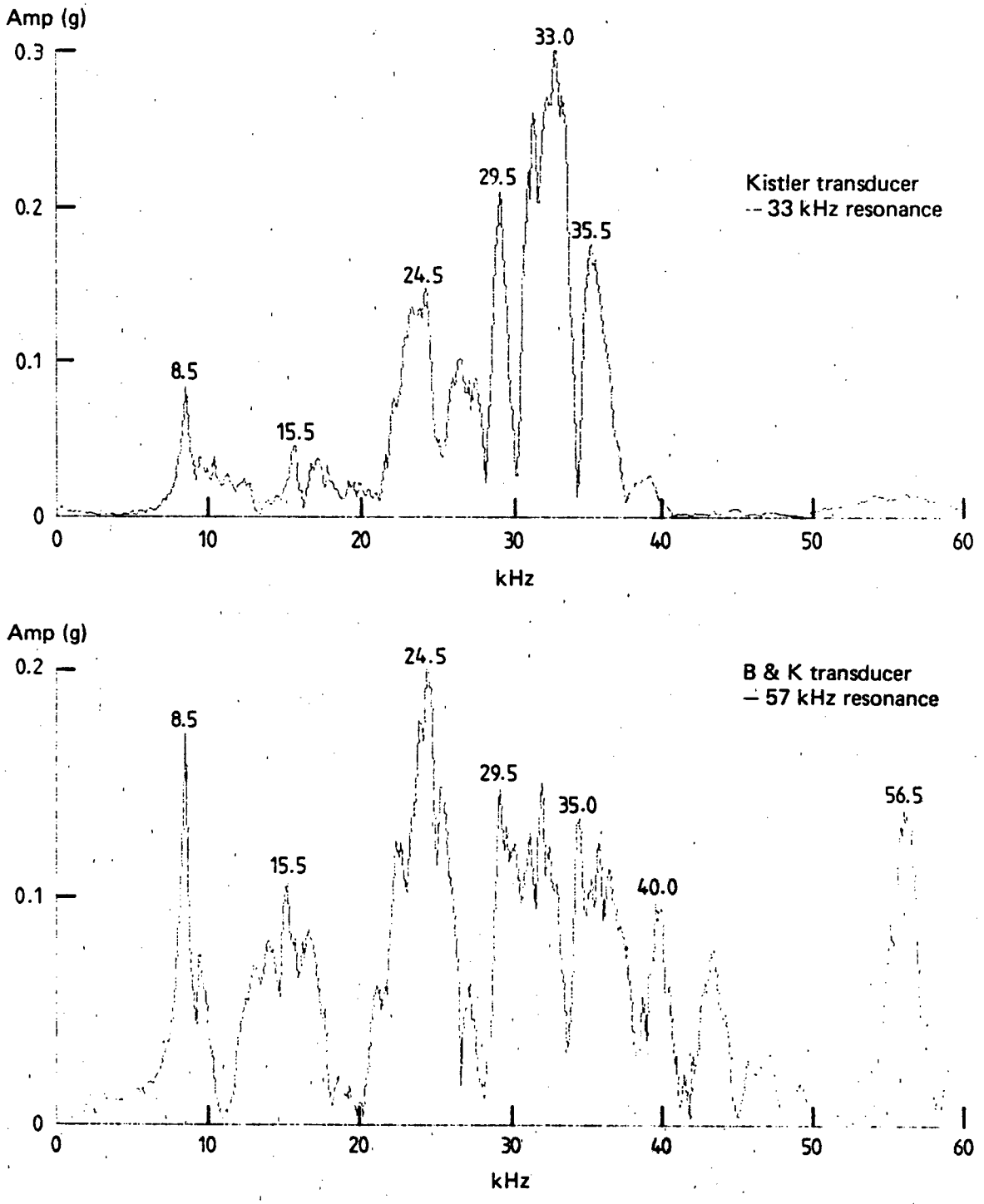

FIG 6.5 HOUSING IMPULSE RESPONSE

Nearly all spectra show contact frequencies for outer or inner races (ref. Table 5.1). In addition, a series of other frequencies separated by shaft frequency (100 Hz) intervals are evident, especially when damage becomes extensive. This indicates strong shaft frequency modulation of the signal, possibly due to eccentric shaft rotation as extensive damage has been found to loosen the bearing.

The last spectrum with bearing B severely damaged (105 hours—Fig. E.1(*c*)) reveals some anomalies. The outer race frequency component evident in Figs E.1(*b*) and E.1(*c*), has disappeared and a strong frequency component at 530 Hz has appeared. Although this frequency very nearly corresponds to the ball rolling frequency, examination of the bearing at the conclusion of the test revealed little or no damage to the balls. This tends to exclude the ball rolling frequency as the source of the 530 Hz component and a satisfactory explanation for its appearance and the disappearance of the outer race component requires further investigation.

6.2.4 Time Domain Signals

Figs F.1–F.4 show time traces of signals from bearing C at 1 and 14·5 hours runtime, in various frequency bands. Differences between the undamaged and damaged states are evident, with structural, accelerometer and event frequencies apparent in the latter state. One feature is the larger number of oscillations following each impulse in the 5–10 kHz and 20–40 kHz bands (where there are major structural and accelerometer resonances) compared with the number in the 2–5 kHz and 10–20 kHz bands.

6.2.5 Comparison of Accelerometers

Comparison of kurtosis and rms values from the four different accelerometers used did not reveal major differences. Any effects which may be due to the different resonance frequencies of these transducers are largely submerged in the structural resonances of the test rig and inherent scatter of measurement. All are adequately effective in detecting early damage provided the pattern over all bands is used. Envelope spectra are also very little effected by the particular accelerometer and frequency band which is used.

6.2.6 Acoustic Emission

Unlike the accelerometers, the acoustic emission transducer produced some significantly different results. Differences were not noted with the first bearings tested (A and B) despite periodical sampling of all signals; sampling intervals were not appropriate and shock pulse measurement was relied on for the earliest indication of damage. Results for bearings C and D show that the acoustic transducer produced increased kurtosis values significantly before any indication from the accelerometers.

On bearing C the acoustic transducer indicated higher kurtosis at about 5 hours operating time, some 6 hours before the first indications from other sensors (Fig. C.3 cf. Fig. A.8). Subsequently bearing D was observed very carefully. Unfortunately it failed very quickly but even so acoustic indications at 0·5 hours preceded K-meter indications by over 0·5 hours (Fig. C.4 cf. Fig. A.10).

Another feature of the acoustic signals is the reduction of kurtosis values below Gaussian levels (to about 1·8) in conditions of severe damage. This effect occurred with all bearings, but only when general signal levels were very high. Although the equipment appeared to be operating within nominal limits, it is suspected that the transducer and measuring system may not be linear under extreme conditions.

7. CONCLUSIONS

Vibration analysis methods which utilize high frequency impulsively excited signals provide an effective means of detecting early damage in rolling element bearings. Such methods have an inherent discriminatory capability since in many machines rolling bearings are the only components producing impulses which excite the high frequency resonances.

In a series of tests investigating alternative signal processing methods—kurtosis, spectral analysis of the enveloped signal and shock pulse distribution—all were found to produce clear indications of early or moderate damage. With damage increasing to severe, kurtosis values tended to revert to undamaged levels, envelope spectra became more random and difficult to interpret and shock pulse distribution curves showed a progressive, though gradual change. Total vibration levels, which did not respond significantly to early damage, increased substantially with severe damage and so usefully complemented the other measurements.

Comparison of a number of accelerometers having different resonance frequencies indicated no significant difference in effectiveness in detecting bearing damage. However, an acoustic emission transducer provided indications of damage sooner than the accelerometers. In the early stages of failure fatigue cracks develop in the region of greatest Hertzian stress just below the surface and subsequent propagation of these cracks generates acoustic emission signals. It is most likely that the acoustic emission transducer detected these signals prior to the development of surface pits or spalls which produce the characteristic impulsive vibrations capable of being detected by accelerometers. It should be realised that this promising result was obtained on a simple bearing rig with a reasonably direct transmission path from bearing to transducer, and further investigation is required to establish the effectiveness of acoustic emission measurement in practical situations where the transmission path is less direct. Once such procedures are established it may be possible to use acoustic emission methods to locate the precise source of bearing failure when this cannot be achieved by other means.

The bearing rig used in the series of tests provided favourable measurement conditions, and though all monitoring methods investigated utilize the discriminatory capacity of high frequency signals, there are differences in selectivity which become more important when endeavouring to monitor in the adverse conditions frequently encountered in practice.

Shock pulse measurement is less discriminating as it measures the area of the impulse peaks, comparing the distribution of energies with a baseline distribution from a similar bearing in good condition. Kurtosis calculation, by using the fourth power of amplitude, emphasizes the 'peakiness' characteristic of the signal pattern, and requires no baseline since bearings in good condition generate a Gaussian signal which forms a standard reference.

Spectra of the signal envelope make the greatest use of the characteristics of the signal pattern. The amplitude of characteristic spectral lines is significant, and in addition a clear distinction is seen between the discrete lines produced by damaged bearings and the relatively random spectra of sound bearings. The significance of individual spectral lines is examined elsewhere [7], but regardless of the details of the pattern, the emergence of discrete lines provides the clearest confirmation of bearing damage, so that this method is arguably the most effective and versatile of all methods investigated in this paper.

ACKNOWLEDGEMENTS

The authors wish to acknowledge the assistance given by Mr A. J. Davis in the operation of the rig and recording of experimental data.

REFERENCES

[1] Boto, P. A. (1971). 'Detection of Bearing Damage by Shock Pulse Measurement', Ball Bearing Journal (SKF) Vol. 167, pp. 1–7.

[2] Taylor, J. I. (1980). 'Identification of Bearing Defects by Spectral Analysis', Trans. ASME Journ. Mech. Des. Vol. 102, pp. 199–204, April 1980.

[3] Meyer, L. D., Ahlgren, F. F., and Weichbrodt, B. (1980). 'An Analytical Model for Ball Bearing Vibrations to Predict Vibration Response to Distributed Defects', Trans. ASME Journ. Mech. Des., Vol. 102, pp. 205–210, April 1980.

[4] Ray, A. G. (1980). 'Monitoring Rolling Contact Bearings under Adverse Conditions', 2nd International Conference, Vibrations in Rotating Machinery, I. Mech. E. Conference Publications 1980–84, pp. 187–194.

[5] Parmington, B. (1983). 'Application of the Shock Pulse Method to Monitoring Rolling Element Bearing Deterioration', ARL Mechanical Engineering Report—to be published.

[6] Ensor, L. C., and Febg, C. C. (1975). 'A Study of the Use of Vibration and Stress Wave Sensing for the Detection of Bearing Failure', Engineering Report No. 75—18C, ENDEVCO, San Juan Capistrano.

[7] McFadden, P. D., and Smith, J. D. (1984). 'Model for the Vibration Produced by a Single Point Defect in a Rolling Element Bearing', Journal of Sound and Vibration, Vol. 96, No. 1, 1984.

APPENDIX A

Kurtosis Trend Plots

Kurtosis trends: bearings A–D with

(1) Kistler accelerometer

(2) Bruel & Kjaer accelerometer

(3) PCB accelerometer

(4) K-meter

KEY: Frequency bands:

1 . . . 2–5 kHz*

2 . . . 5–10 kHz

3 . . . 10–20 kHz

4 . . . 20–40 kHz

5 . . . 40–80 kHz

* 2·5–5·0 kHz for K-meter.

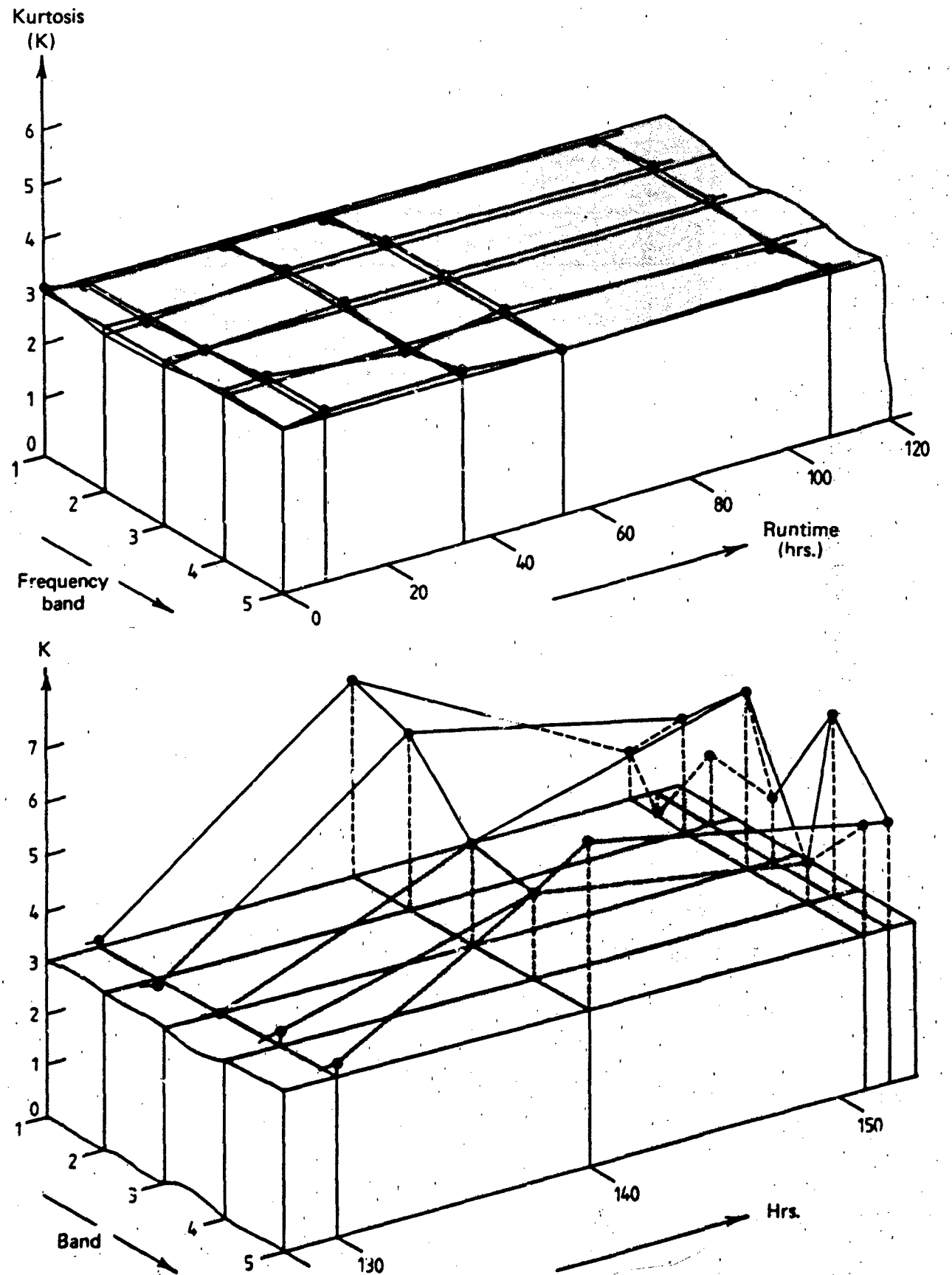

FIG A.1
KURTOSIS – BEARING A
KISTLER ACCELEROMETER

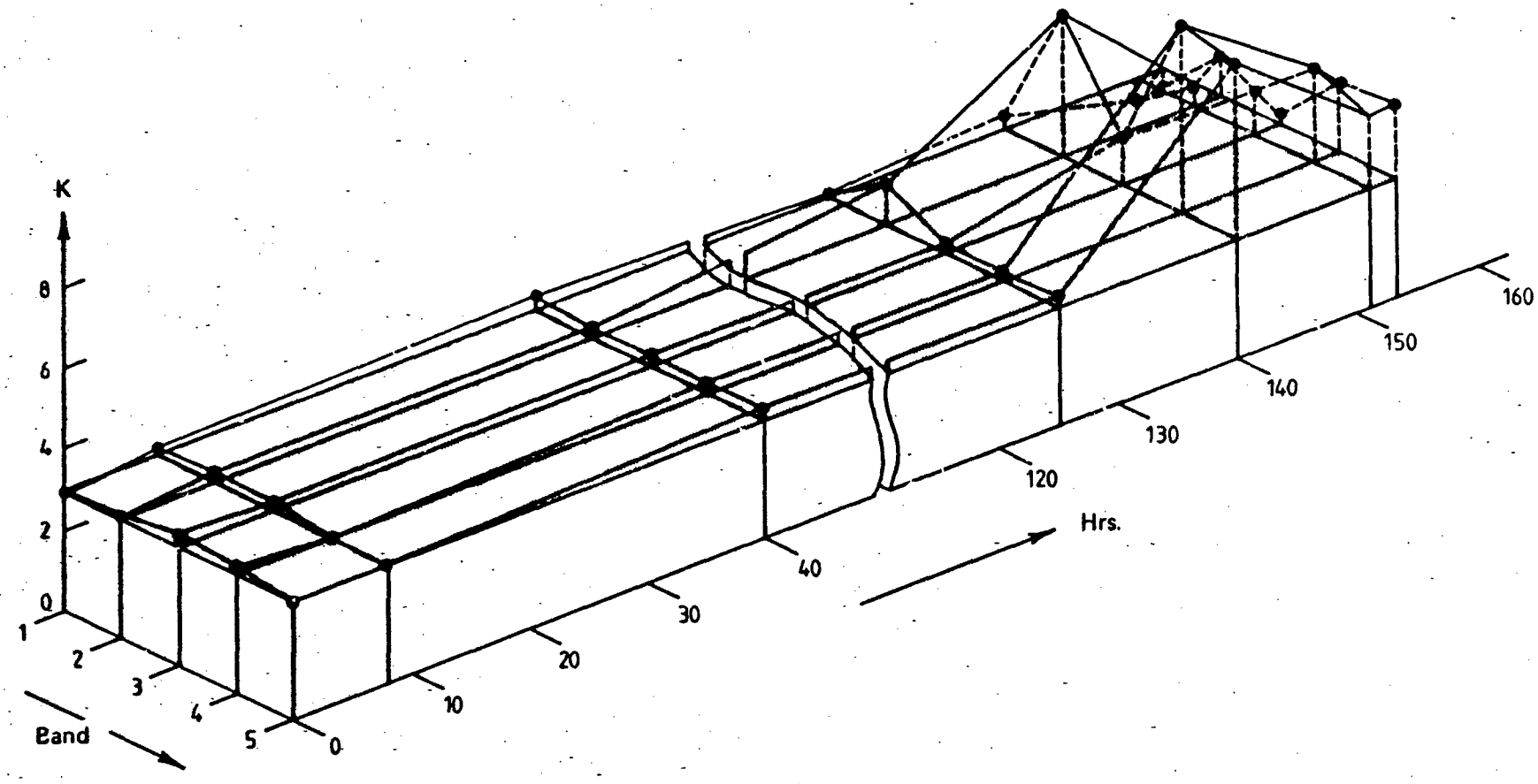

FIG A.2
KURTOSIS – BEARING A
– BRUEL & KJAER ACCELEROMETER

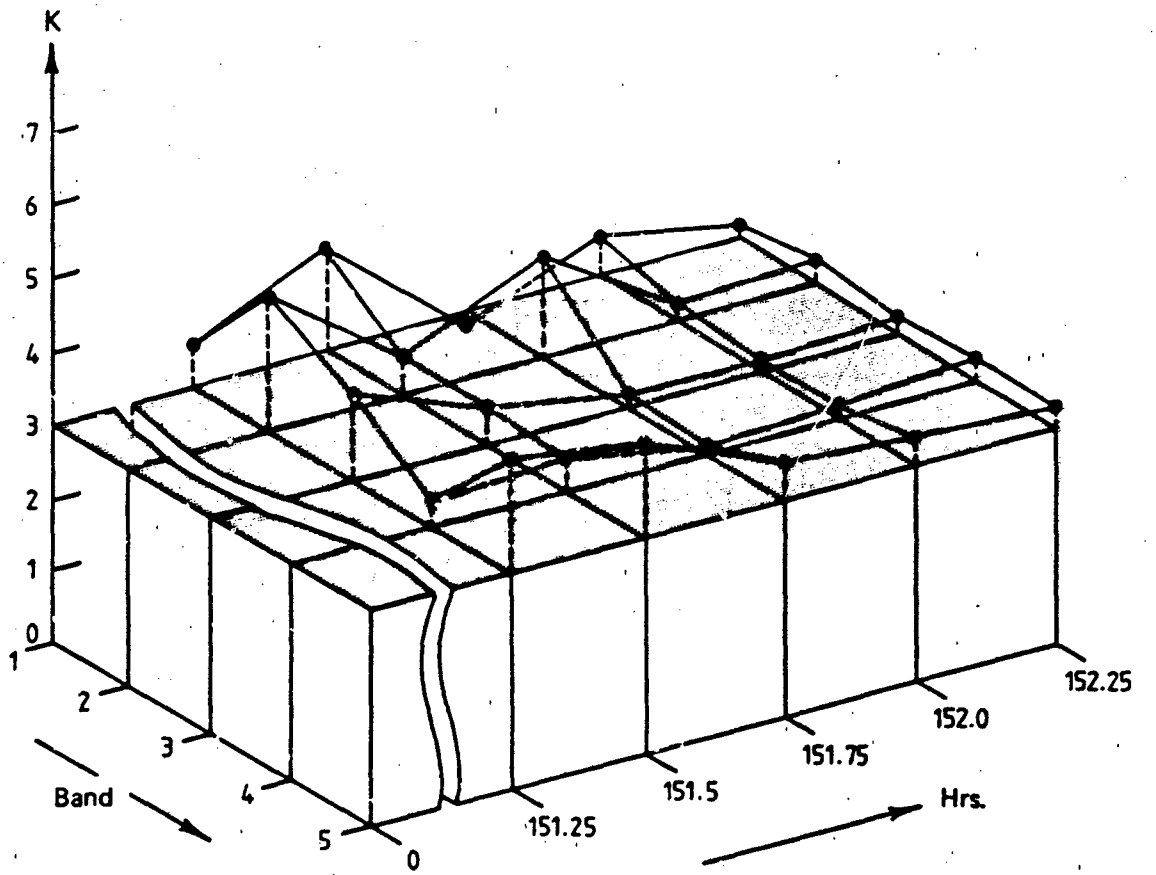

FIG A.3
KURTOSIS – BEARING A
– K - METER

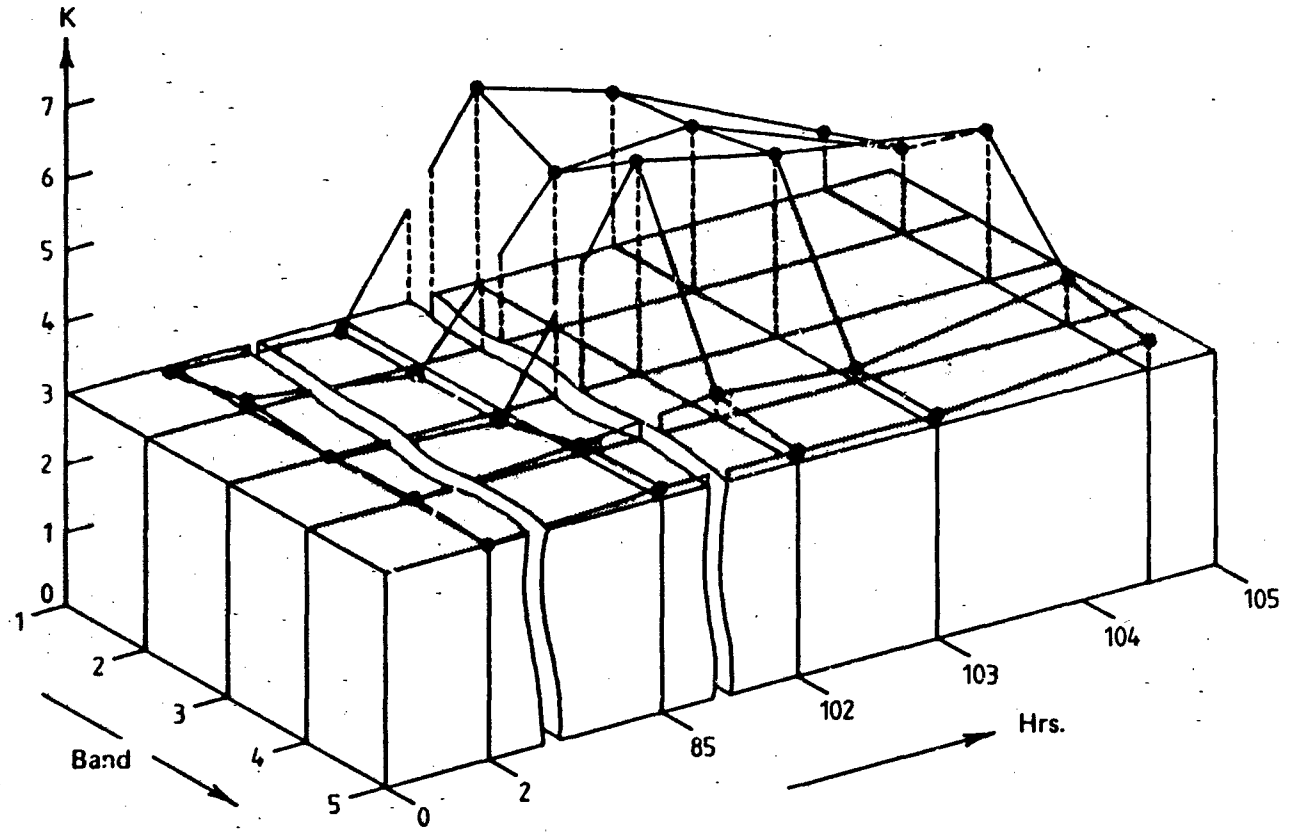

FIG A.4
KURTOSIS – BEARING B
– KISTLER ACCELEROMETER

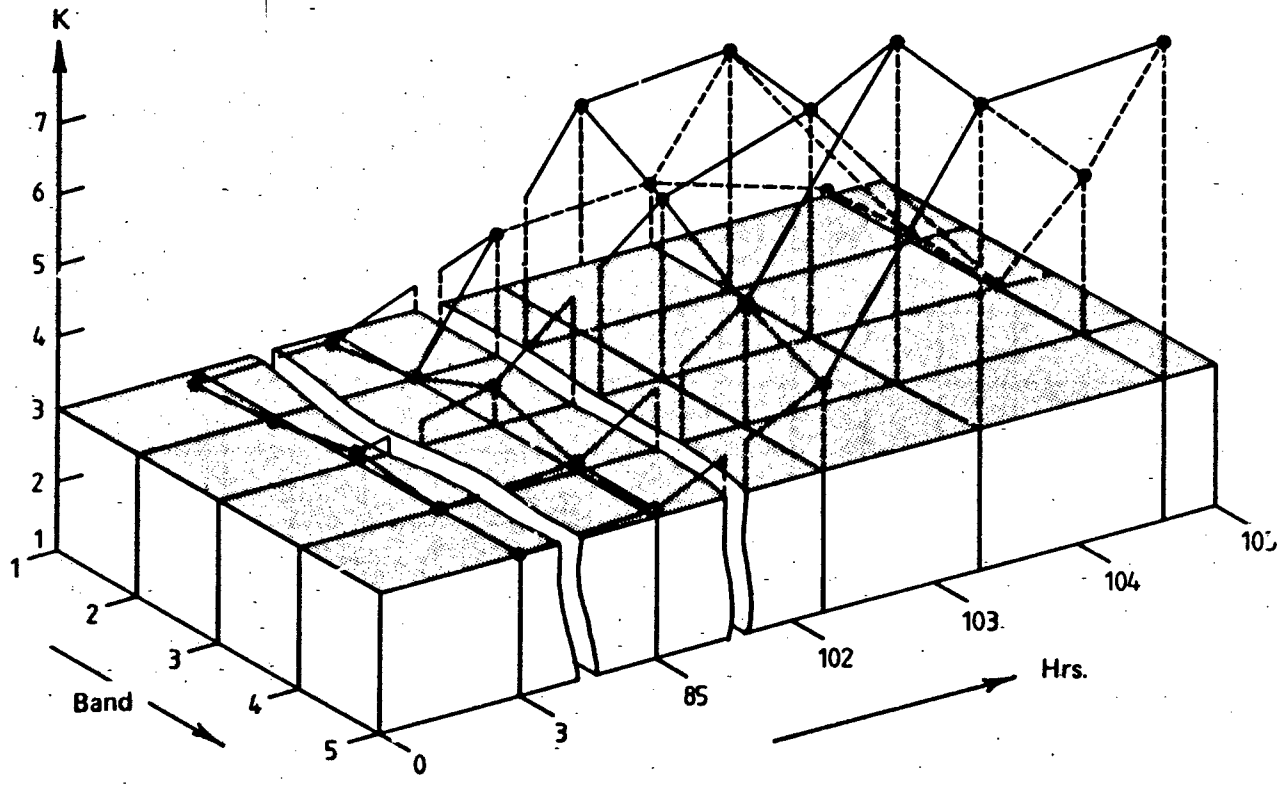

FIG A.5
KURTOSIS – BEARING B
BRUEL & KJAER ACCELEROMETER

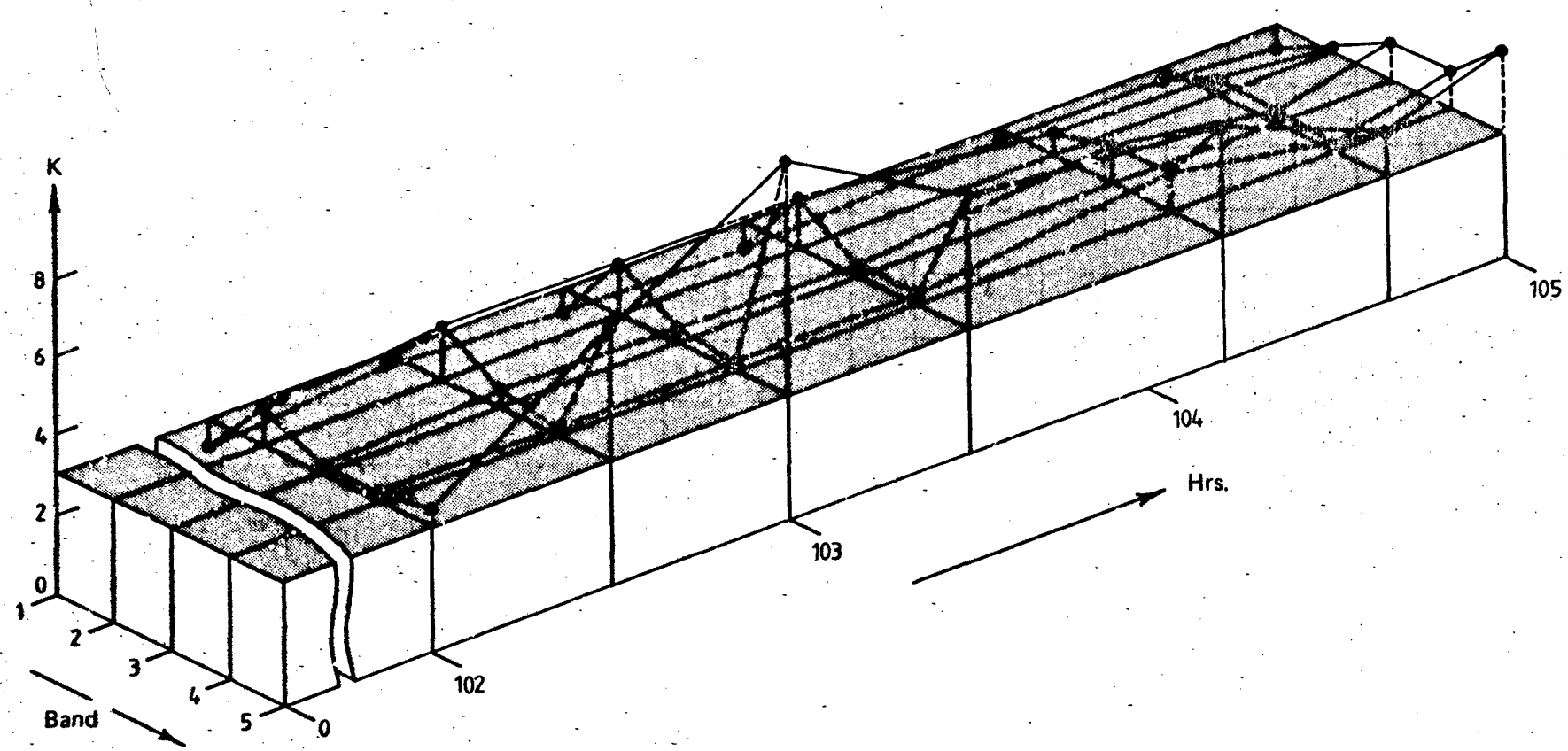

FIG A.6
KURTOSIS – BEARING B
– K - METER

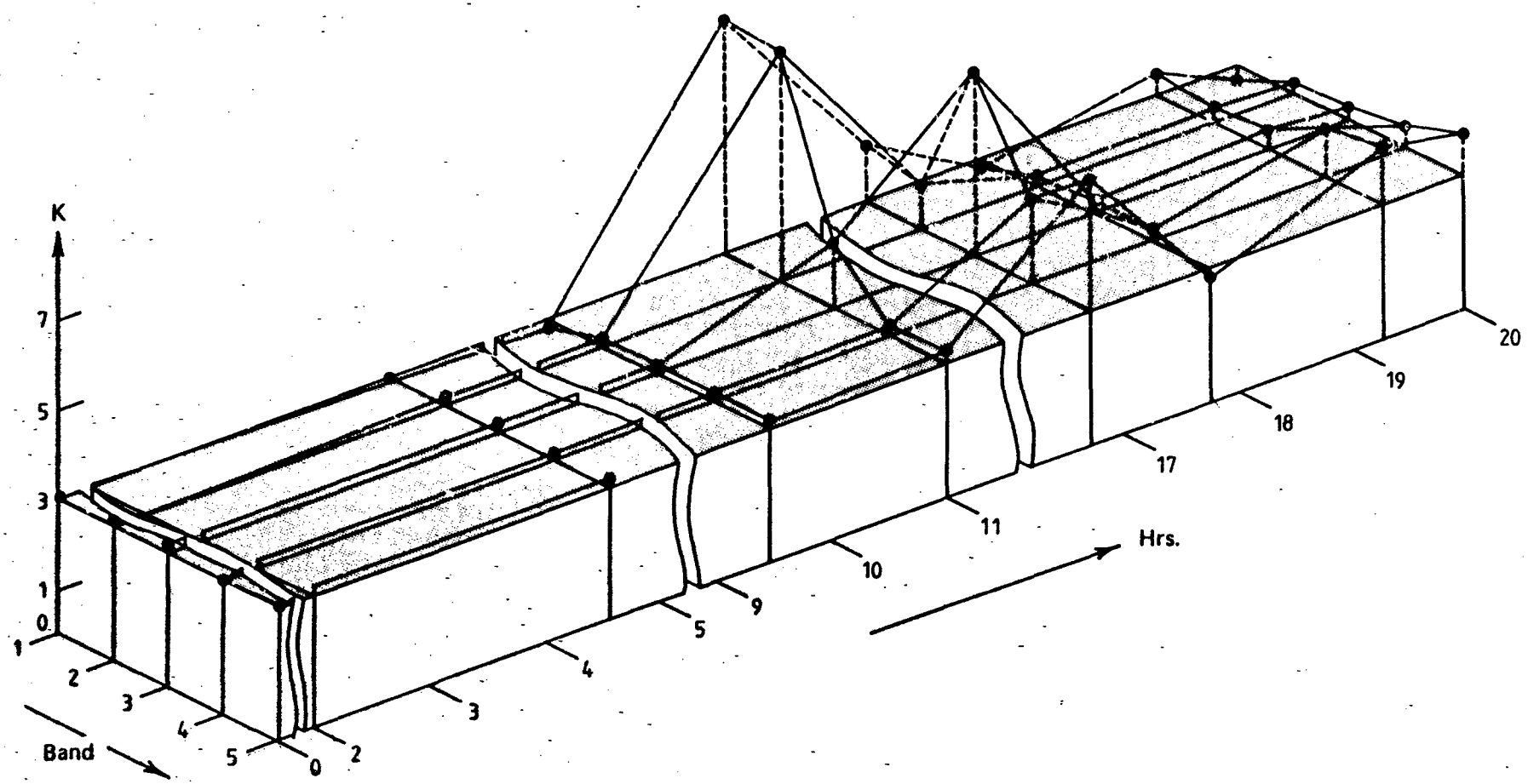

FIG A.7
KURTOSIS – BEARING C
– KISTLER ACCELEROMETER

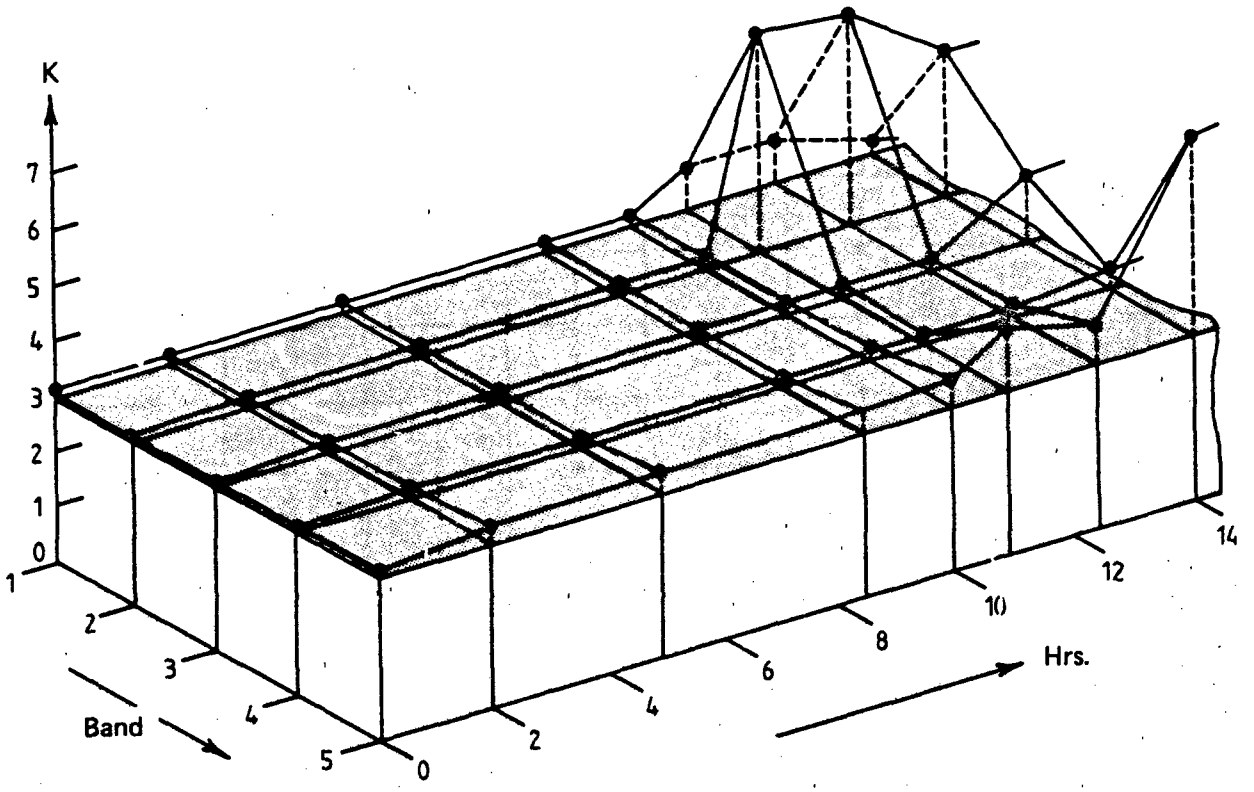

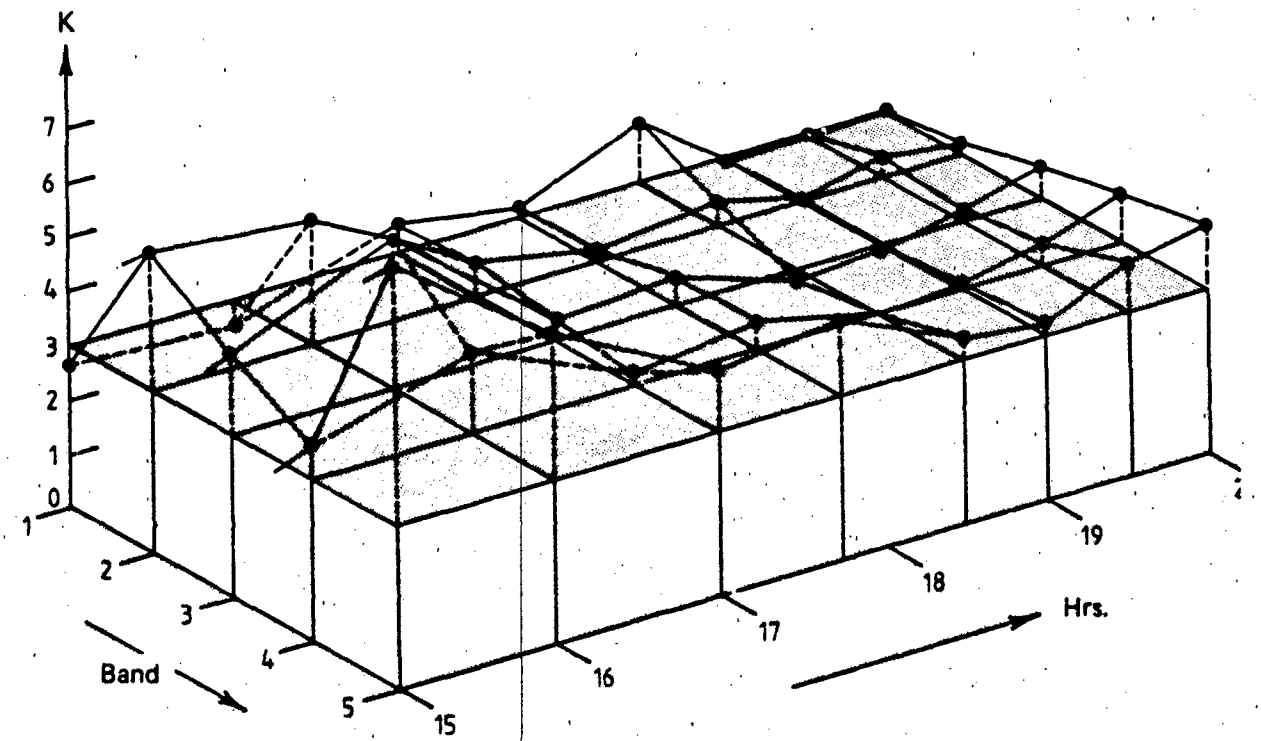

FIG A.8
KURTOSIS – BEARING C
– K. METER

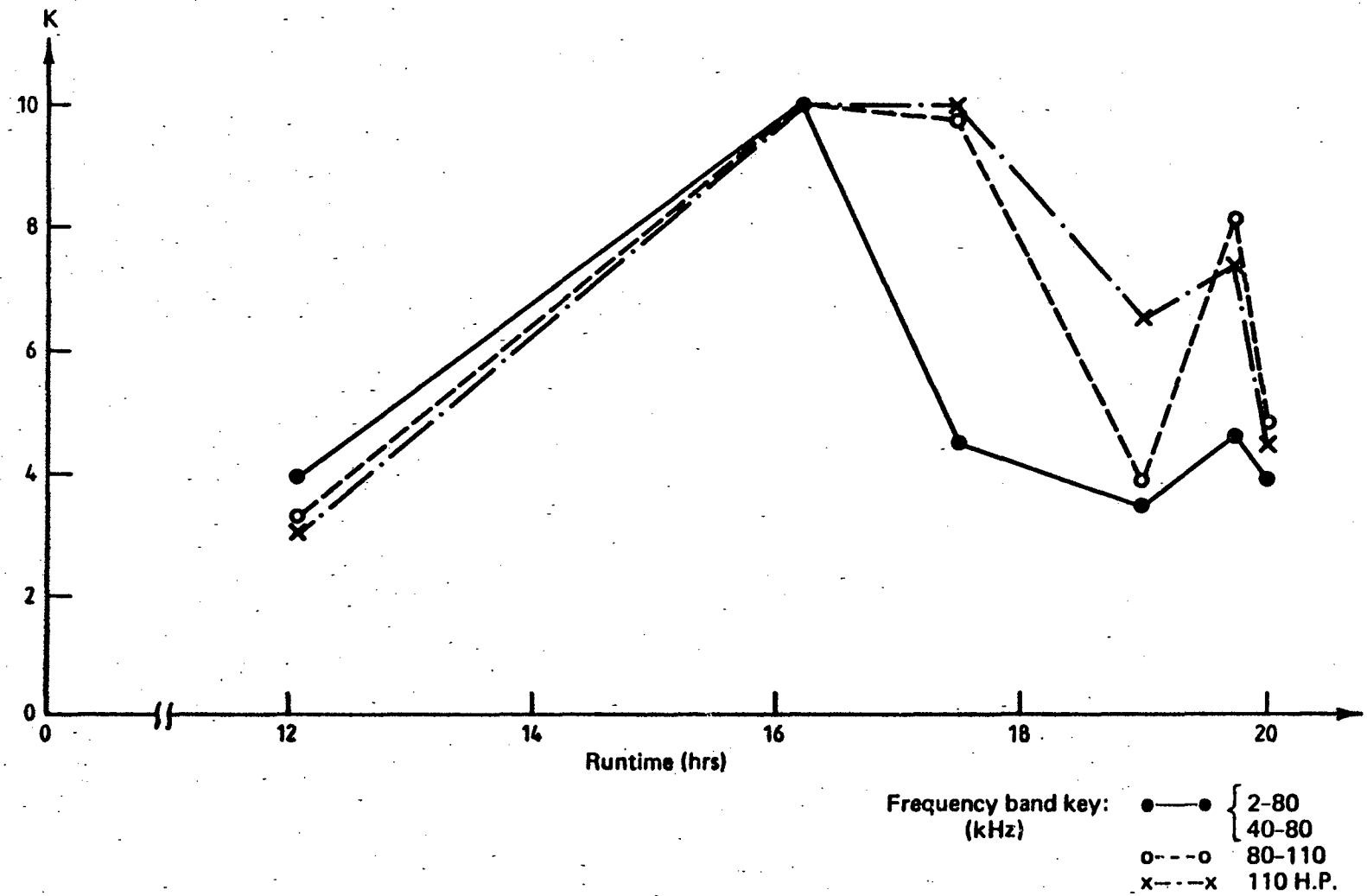

FIG A.9
KURTOSIS – PCB ACCELEROMETER
BEARING C

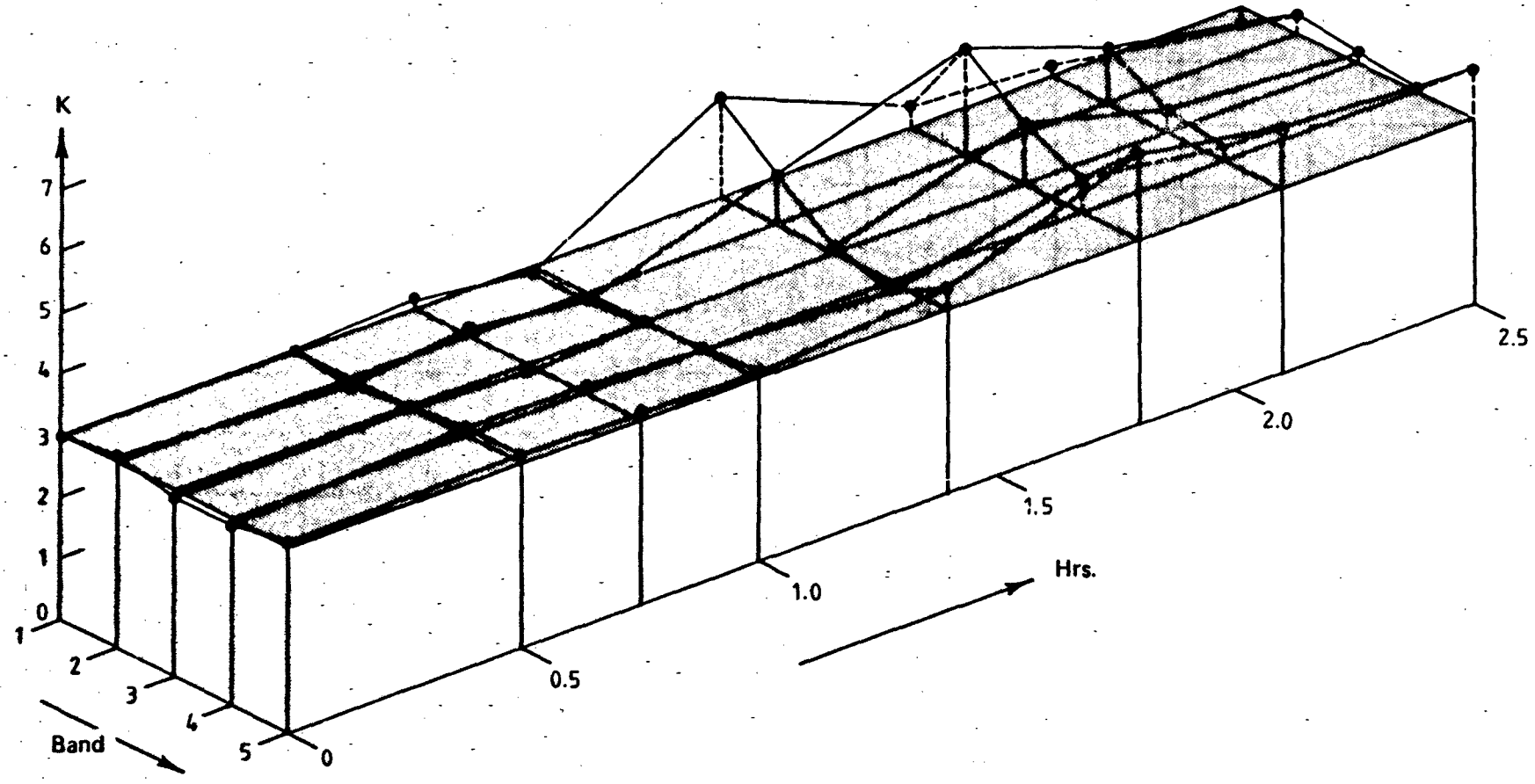

FIG A.10
KURTOSIS – BEARING D
– K - METER

Runtime (hrs.)	Frequency band (kHz)						
	2-5	5-10	10-20	20-40	40-80	80-110	110 H.P.
0.1	3.02	3.03	2.98	3.31	3.0	3.19	3.2
1.5	4.28	3.67	3.86	6.01	6.22	9.13	15.0

FIG A.11
KURTOSIS – BEARING D
– PCB TRANSDUCER

APPENDIX B

RMS Acceleration Trend Plots

g rms trends: bearings A–D with

(1) Kistler accelerometer

(2) Bruel & Kjaer accelerometer

(3) PCB accelerometer

(4) K-meter

KEY: (Same as Appendix A)

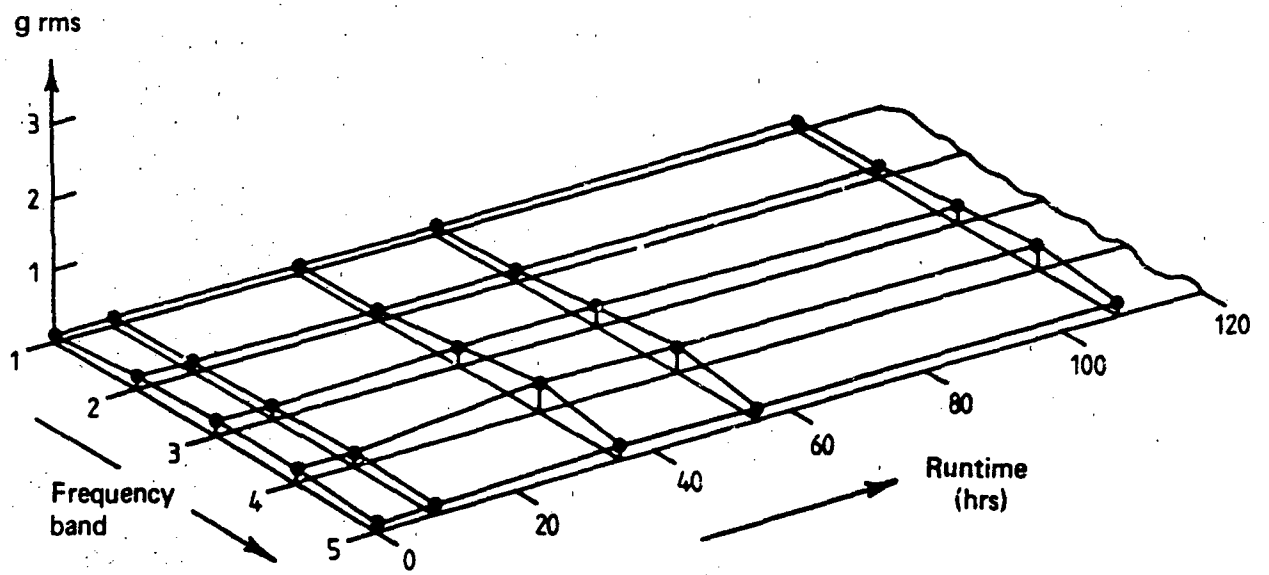

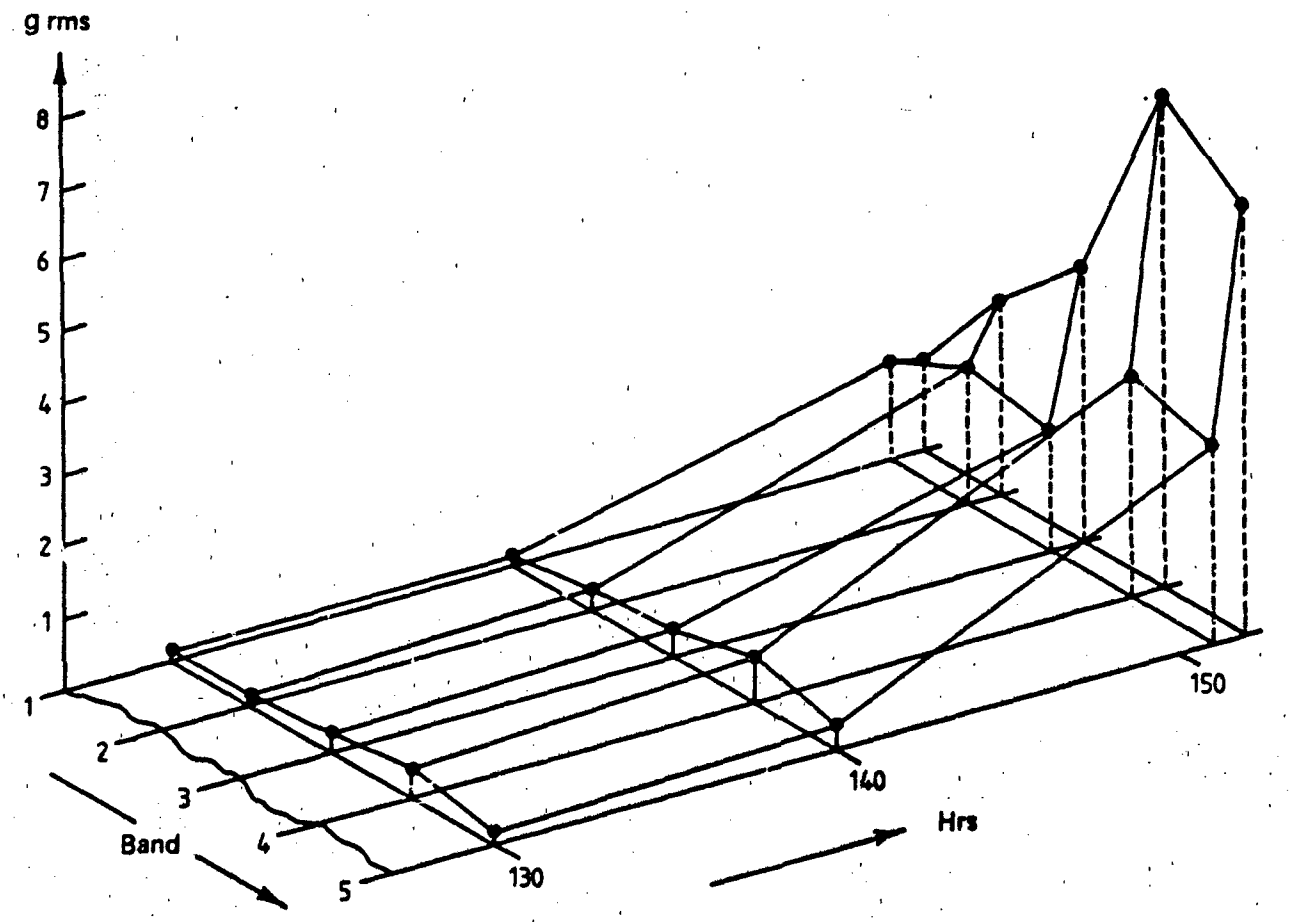

FIG B.1
g rms – BEARING A
– KISTLER ACCELEROMETER

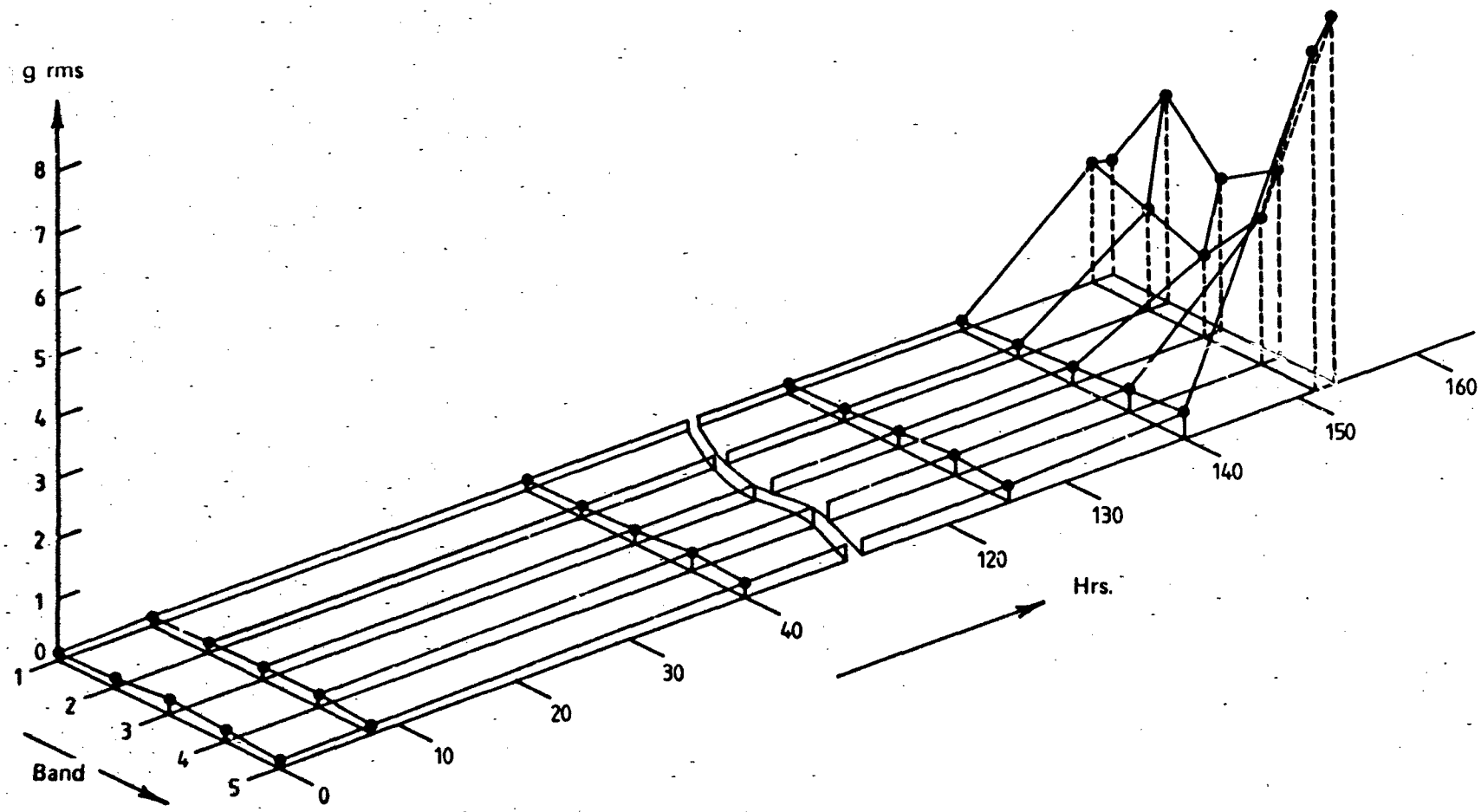

FIG B.2
g rms – BEARING A
BRUEL & KJAER ACCELEROMETER

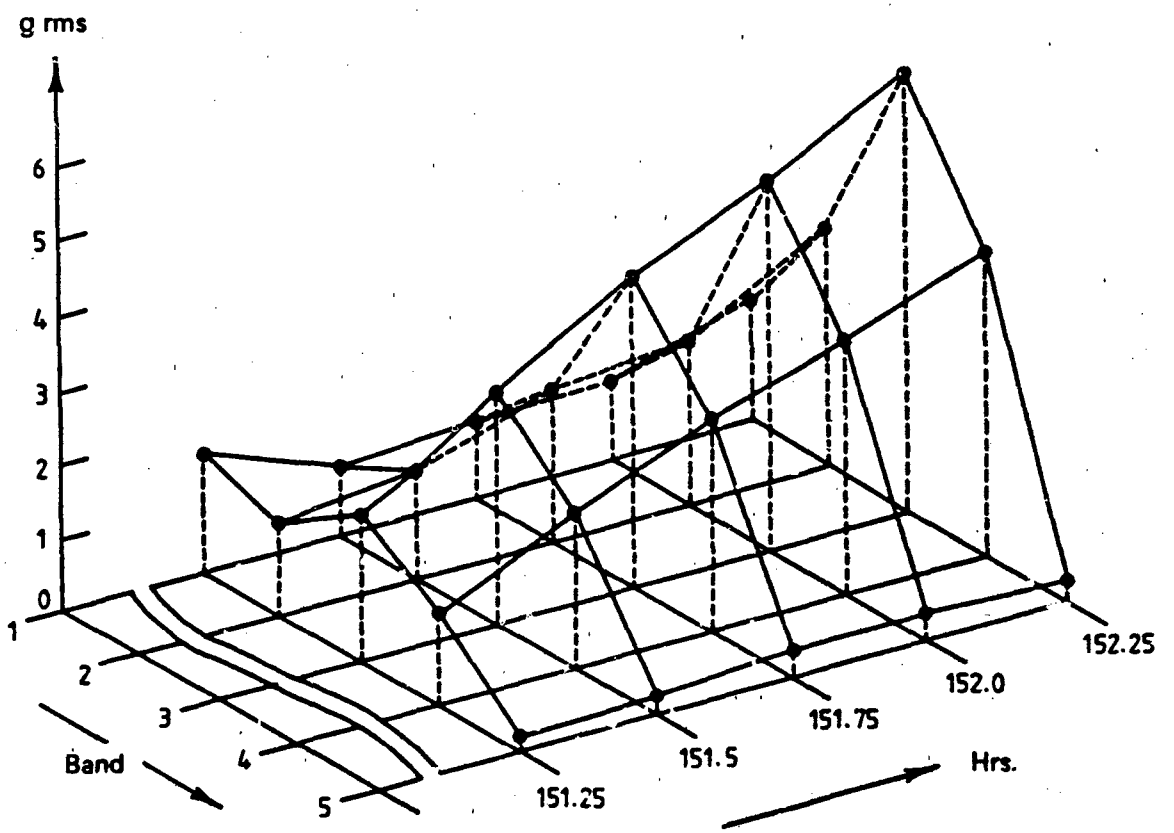

FIG B.3
g rms – BEARING A
K - METER

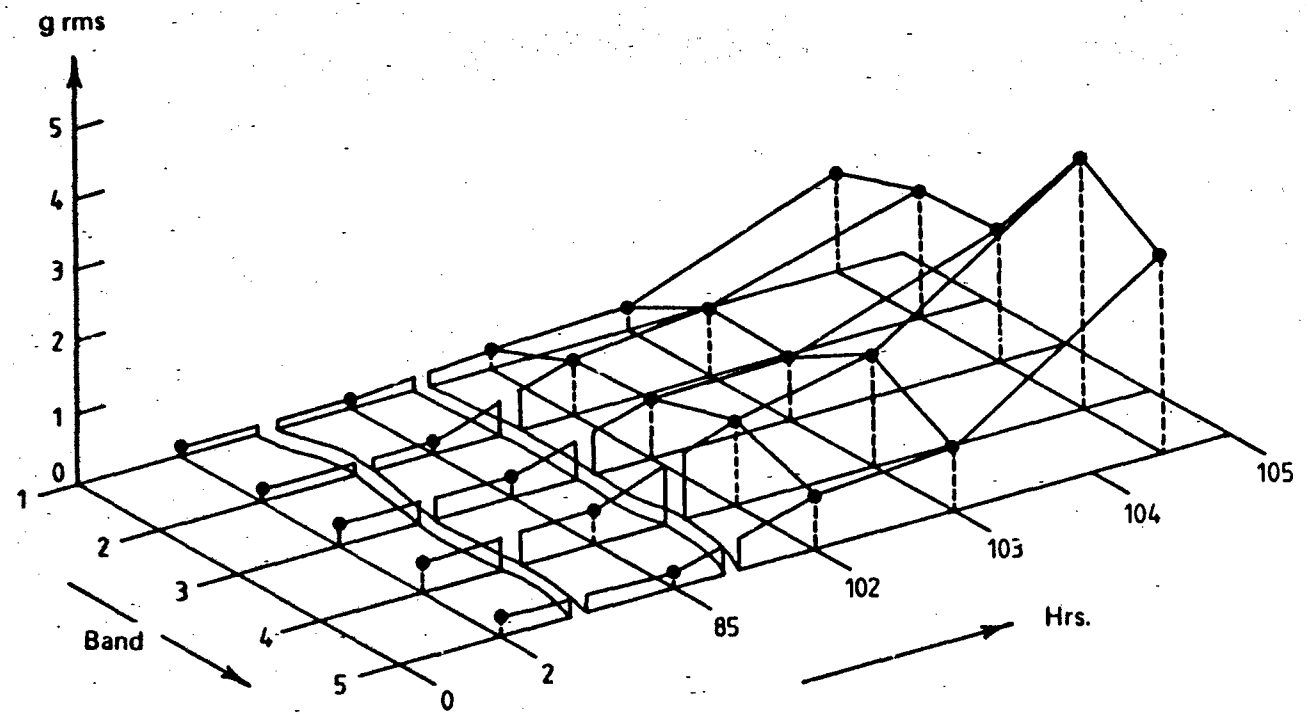

FIG B.4
g *rms* – BEARING B
– KISTLER ACCELEROMETER

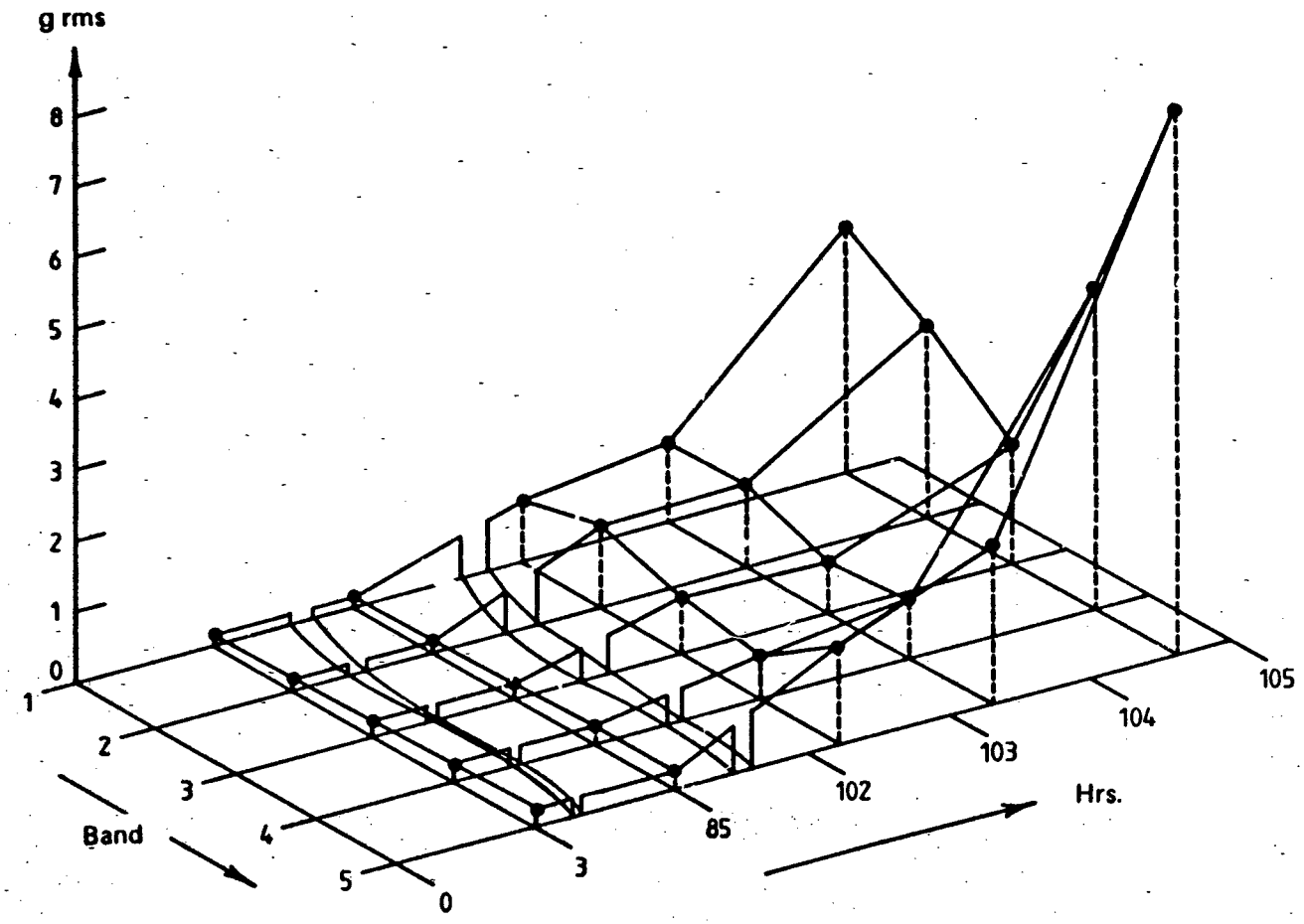

FIG B.5
g rms – BEARING B
BRUEL & KJAER ACCELEROMETER

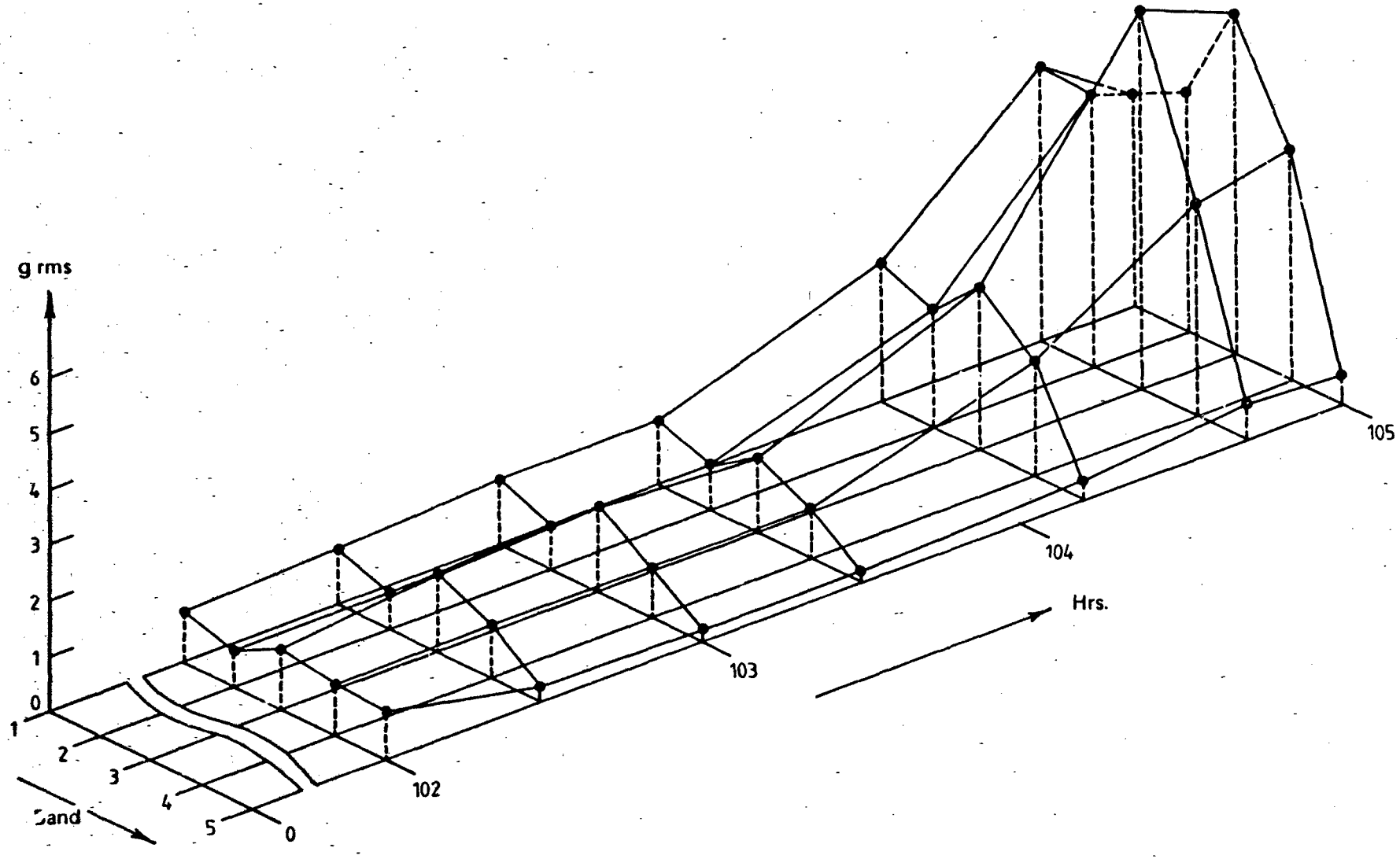

FIG B.6
g rms – BEARING B
– K - METER

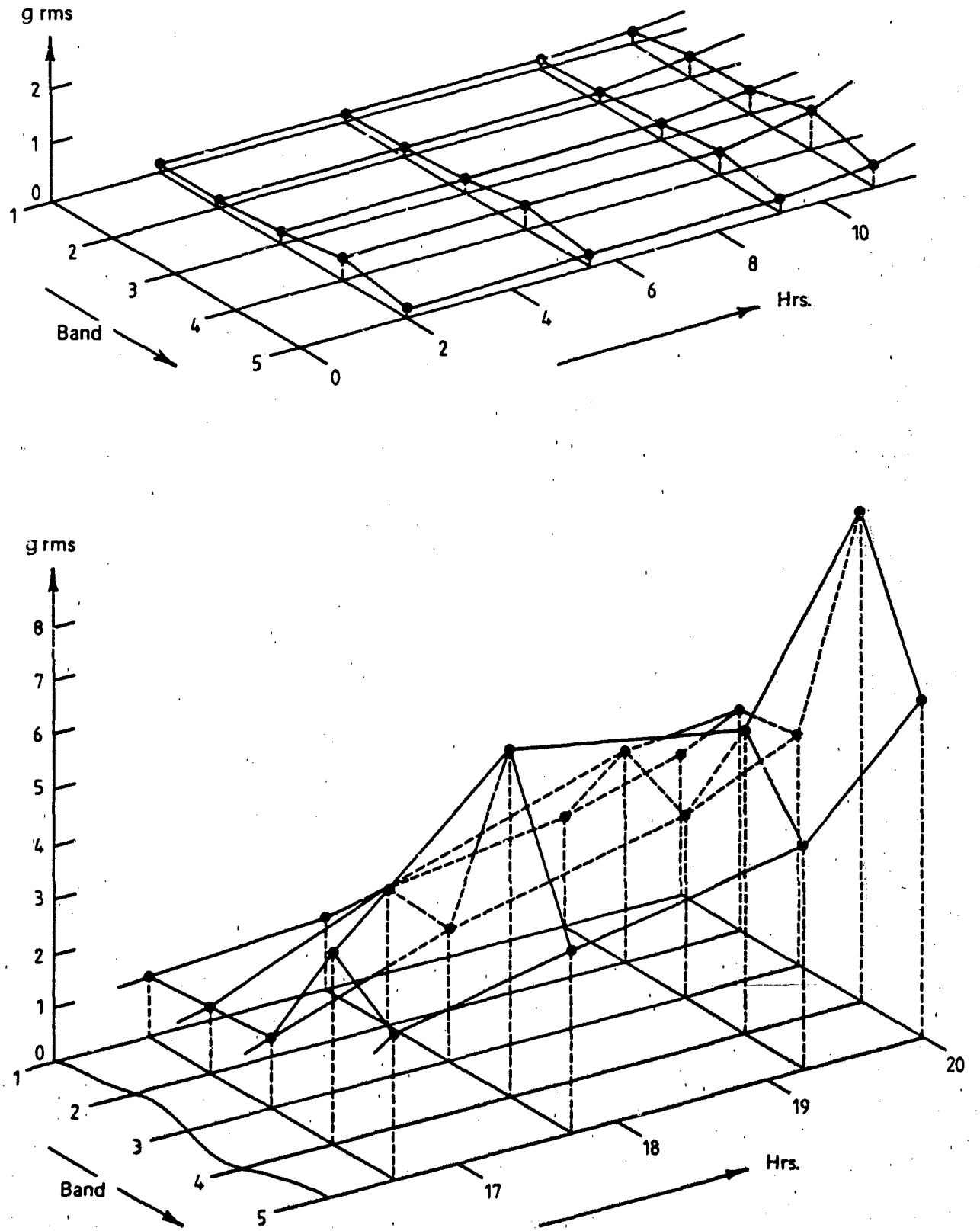

FIG B.7
g rms – BEARING C
KISTLER ACCELEROMETER

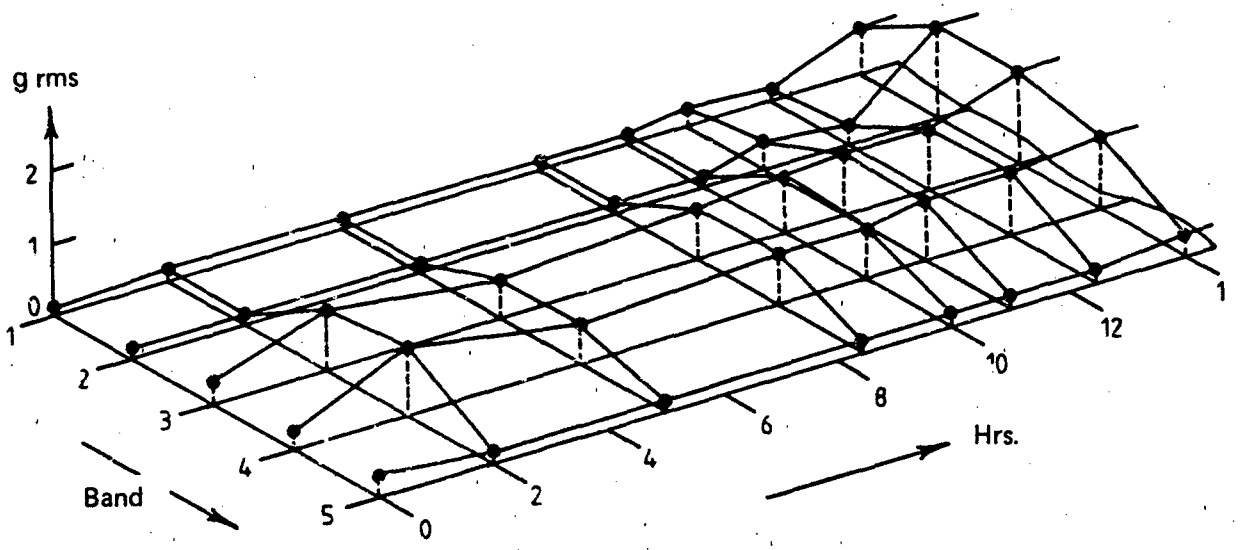

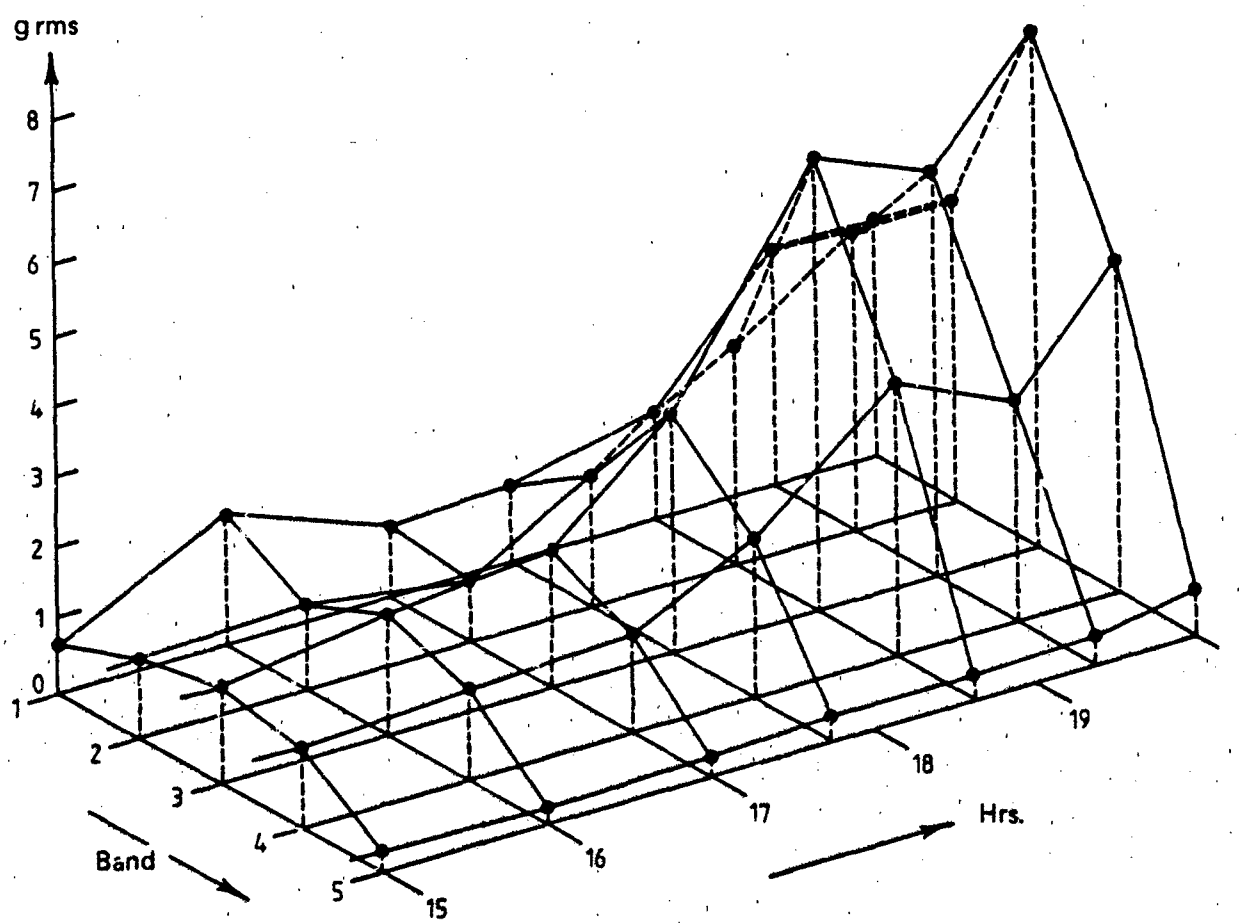

FIG B.8
g rms – BEARING C
– K - METER

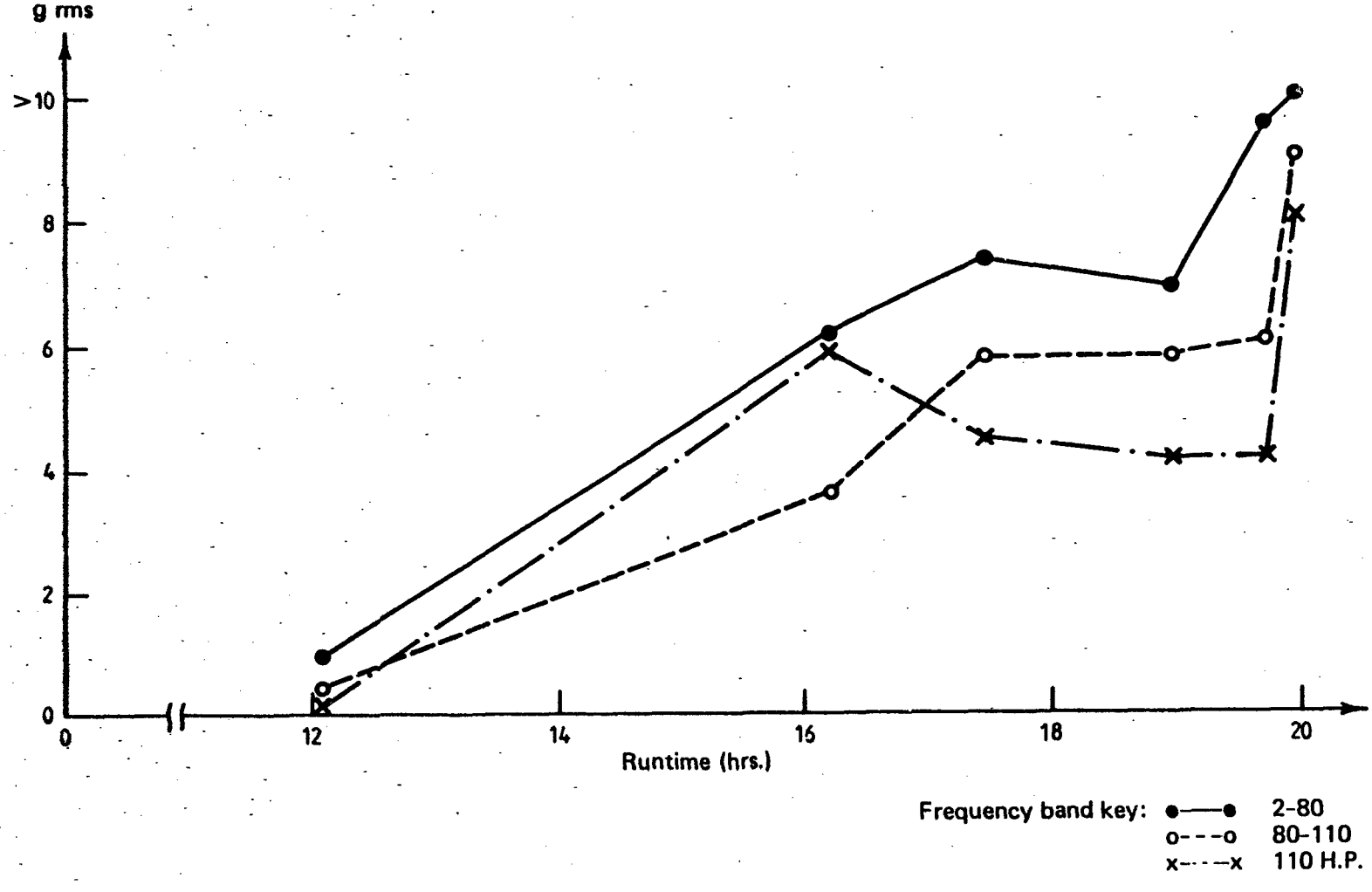

FIG B.9
g rms – P.C.B. ACCELEROMETER
BEARING C

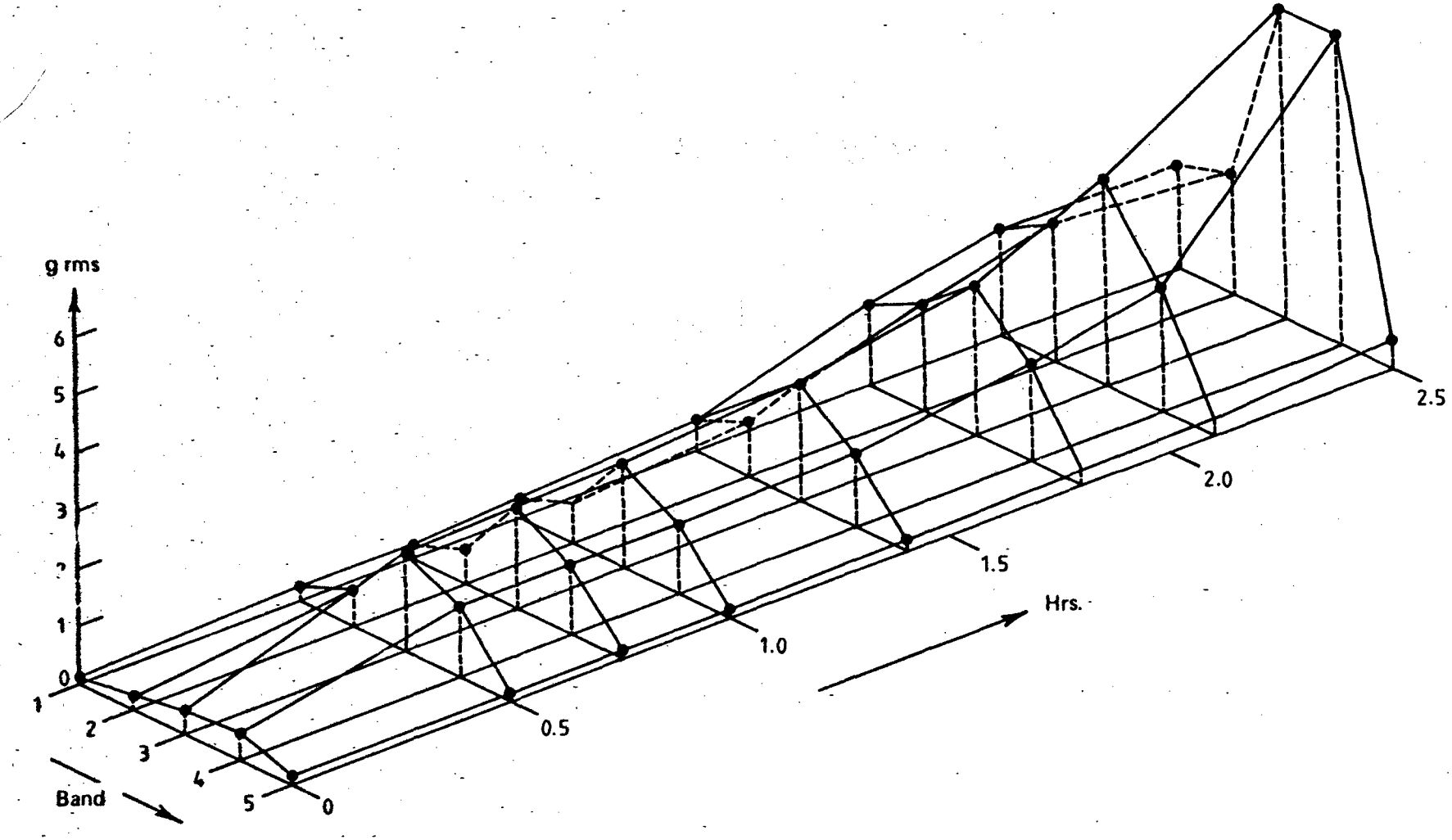

FIG B.10
g rms – BEARING D
K - METER

Runtime (hrs.)	Frequency band (kHz)						
	2-5	5-10	10-20	20-40	40-80	80-110	110 H.P.
0.1	.2	.74	.69	.67	2.61	1.89	.41
1.5	.72	1.25	.90	.95	4.08	4.63	4.94

FIG B.11
g rms – BEARING D
– PCB ACCELEROMETER

APPENDIX C

Acoustic Emission Trend Plots

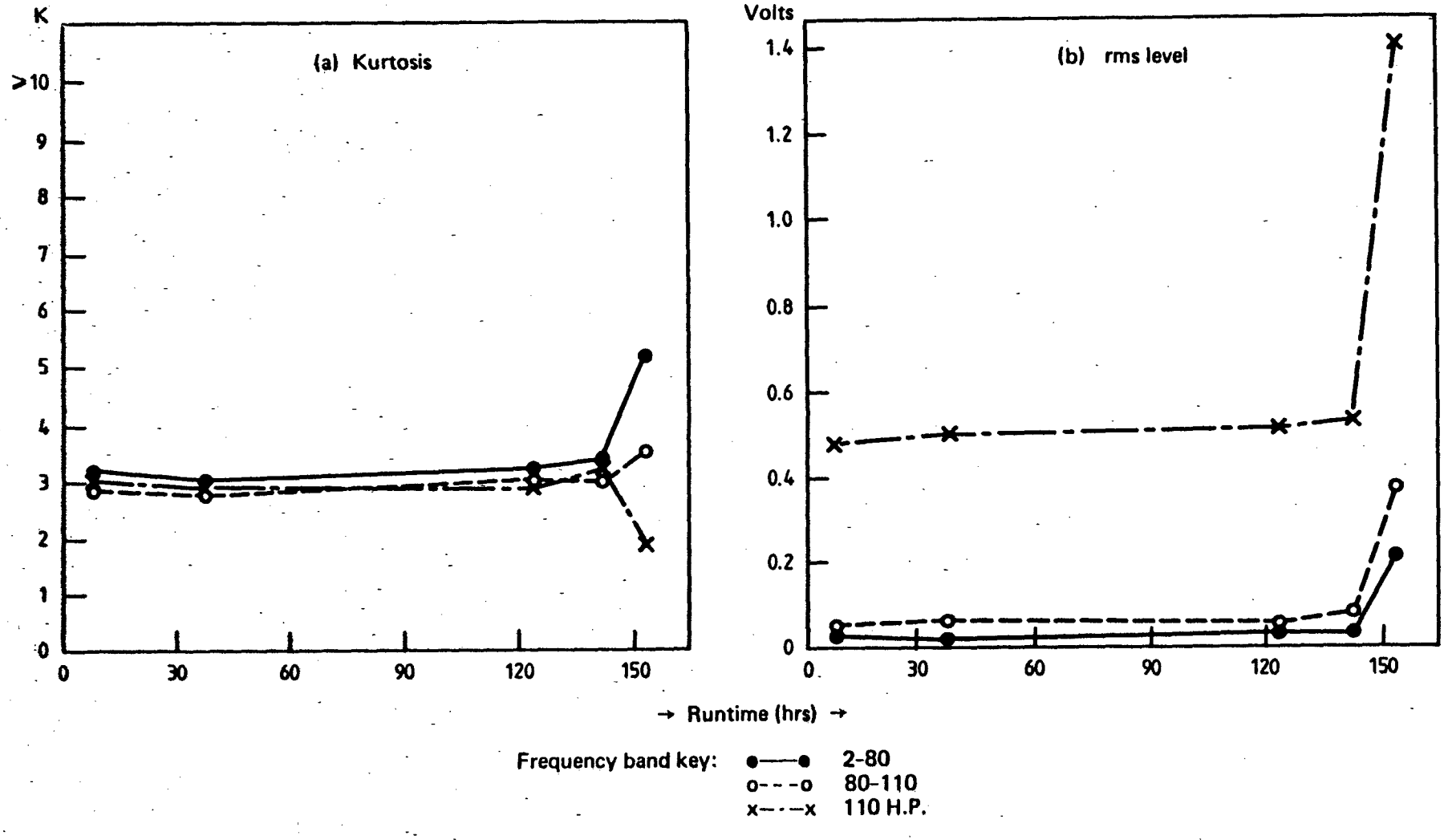

FIG C.1
BEARING A
ACOUSTIC EMISSION

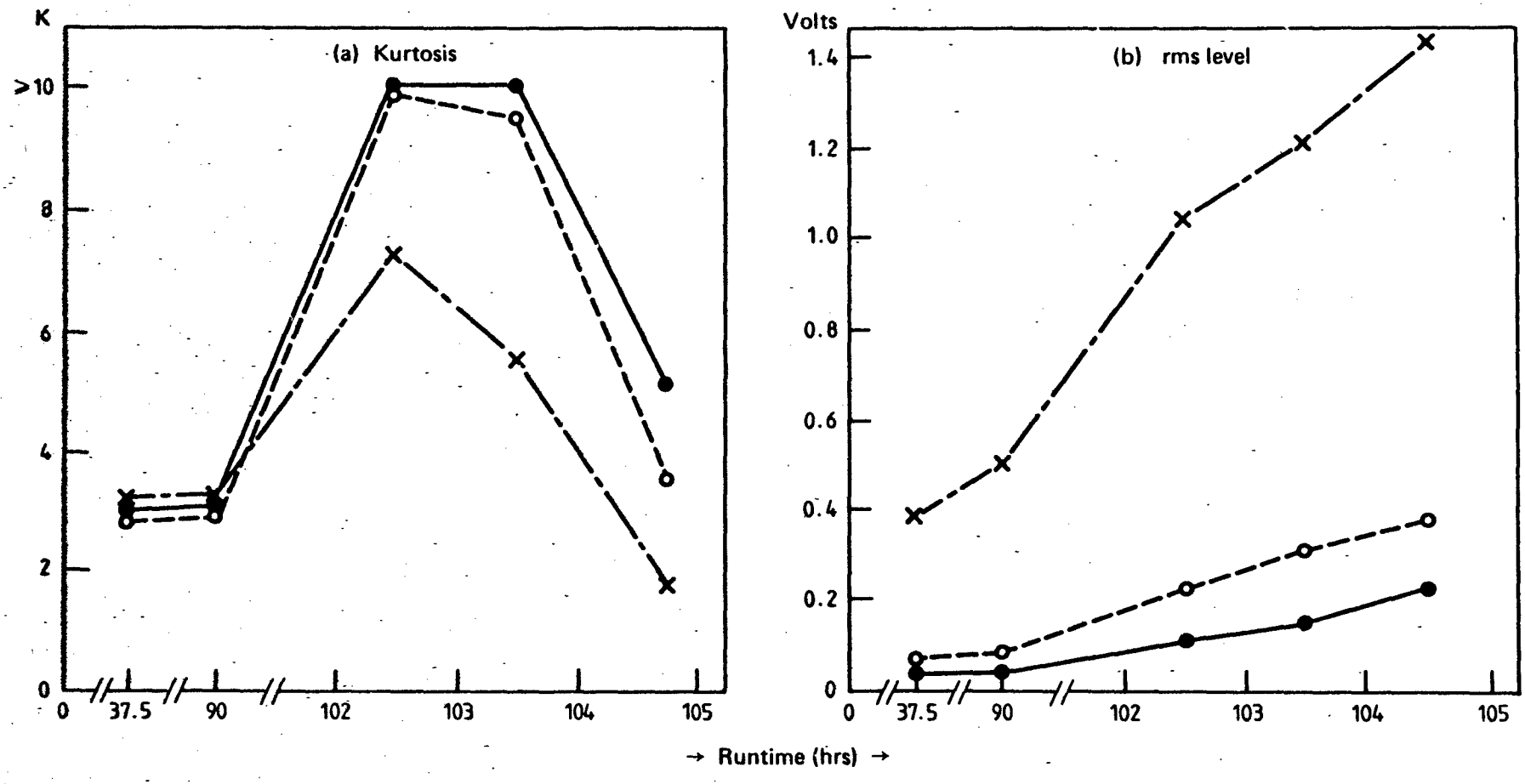

FIG C.2
BEARING B
ACOUSTIC EMISSION

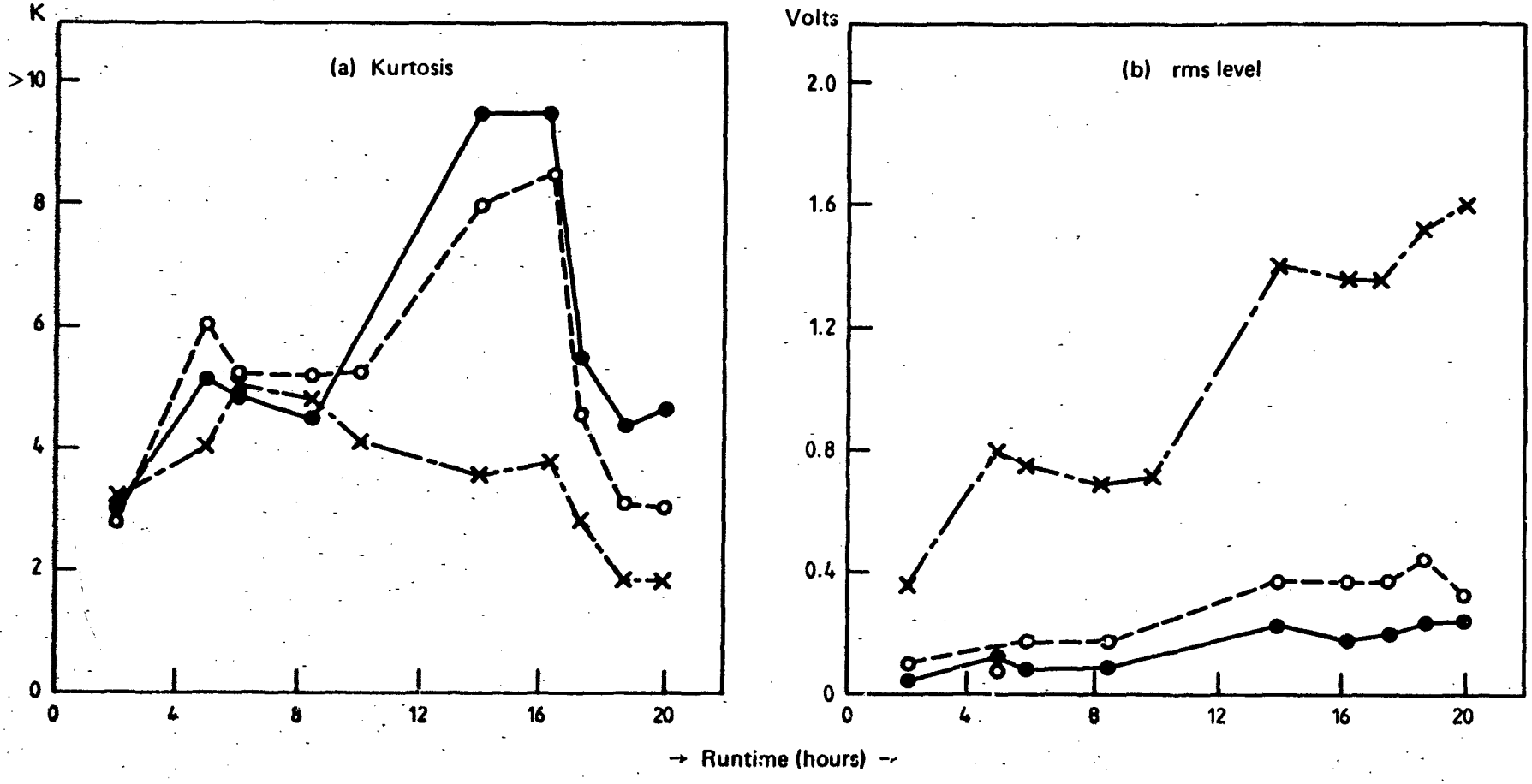

FIG C.3
BEARING C
ACOUSTIC EMISSION

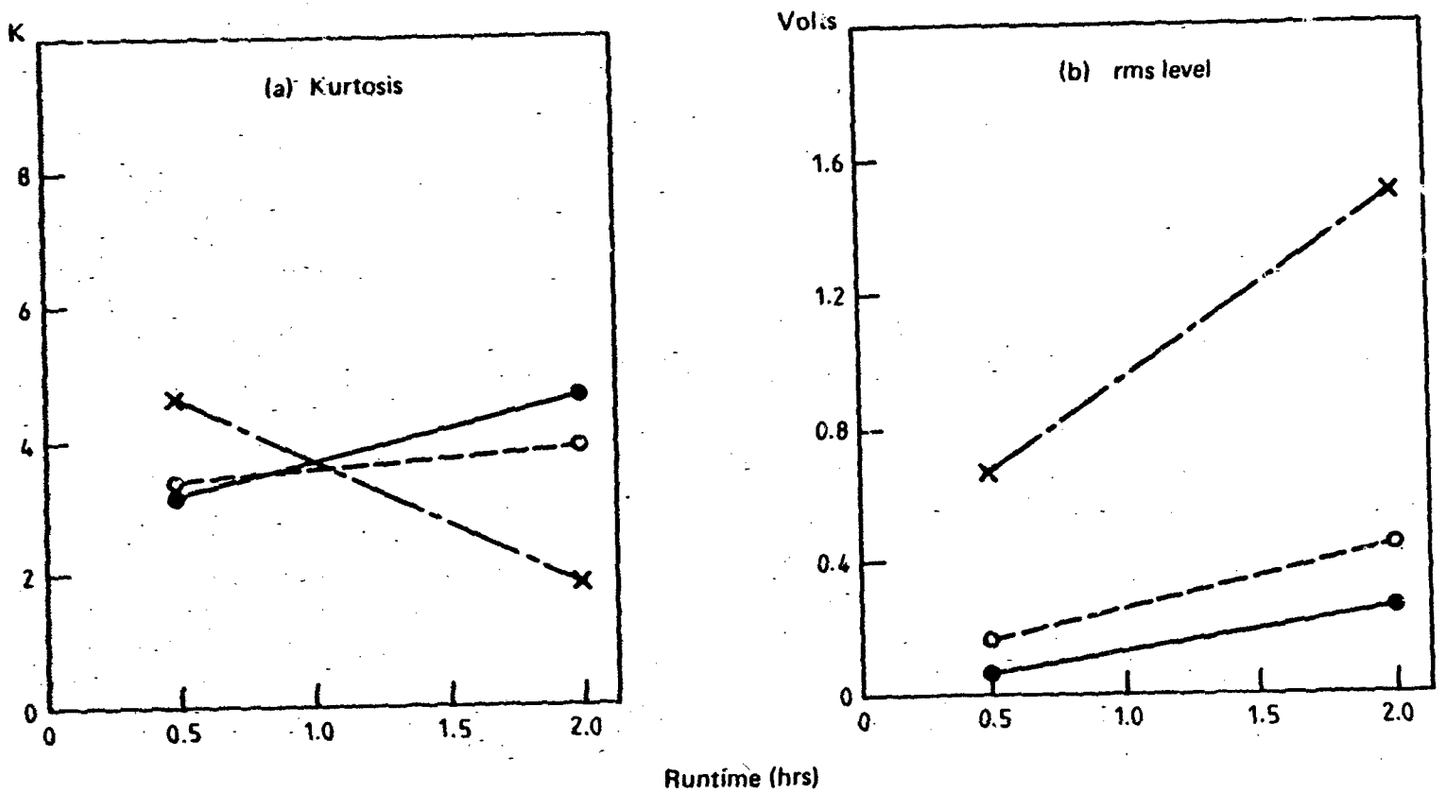

Frequency band key:
- ●——● 2-80 kHz
- o---o 80-110 kHz
- x---x 110 H.P. kHz

FIG C.4
BEARING D
ACOUSTIC EMISSION

APPENDIX D

Shock Pulse Distribution Curves

Shock value determined as in paragraph 4.4.

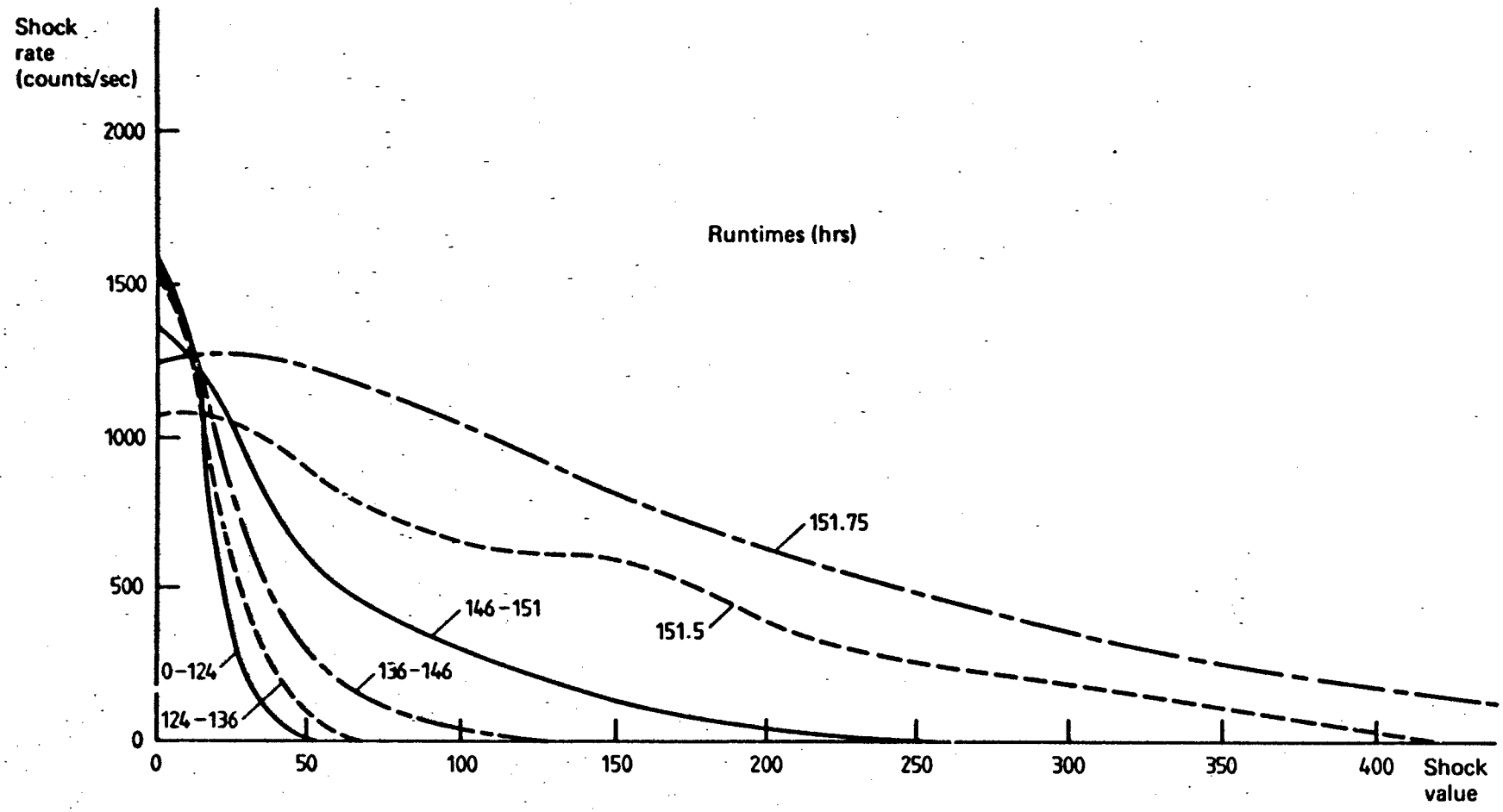

FIG D.1
BEARING A

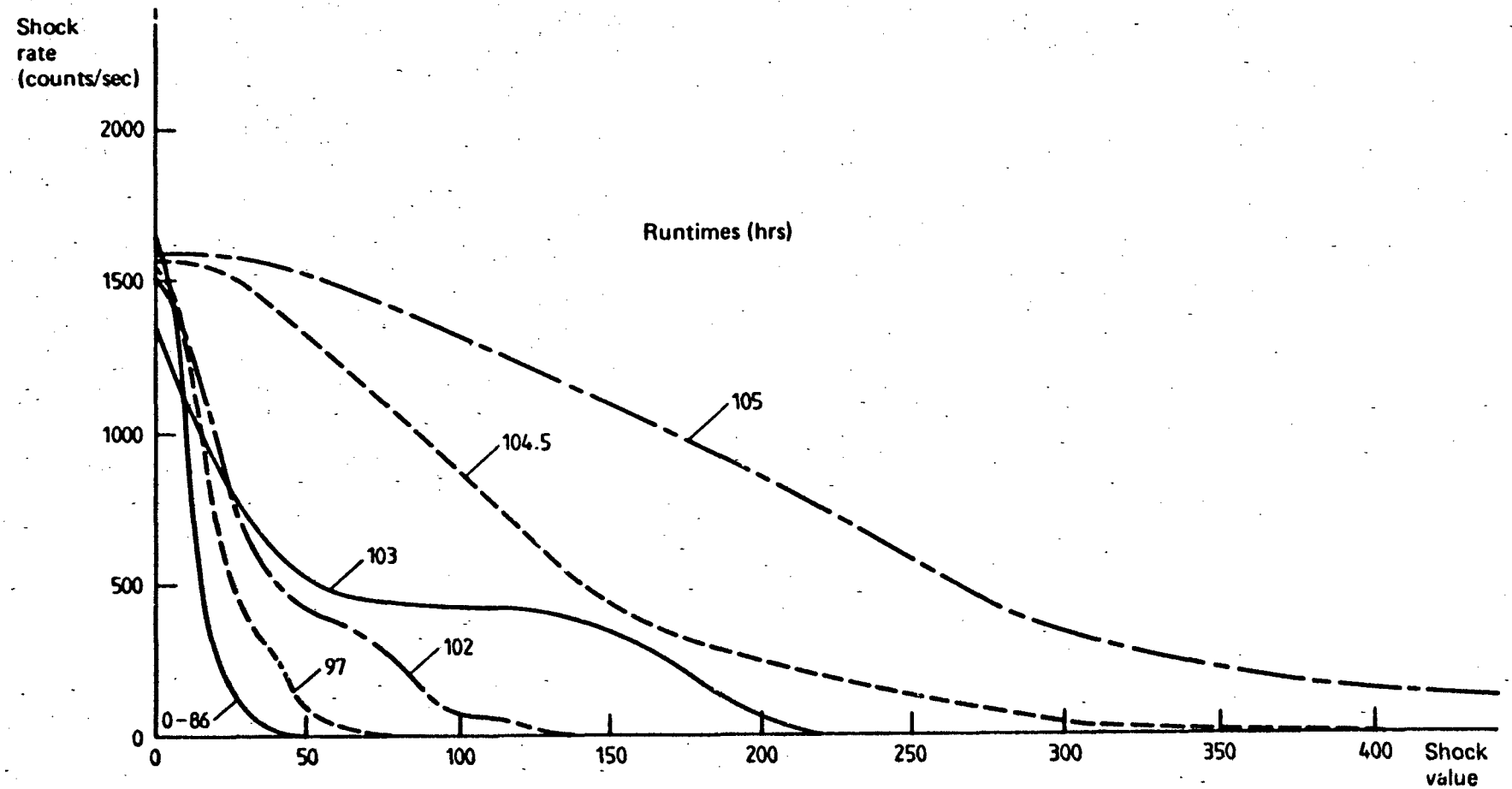

FIG D.2
BEARING B

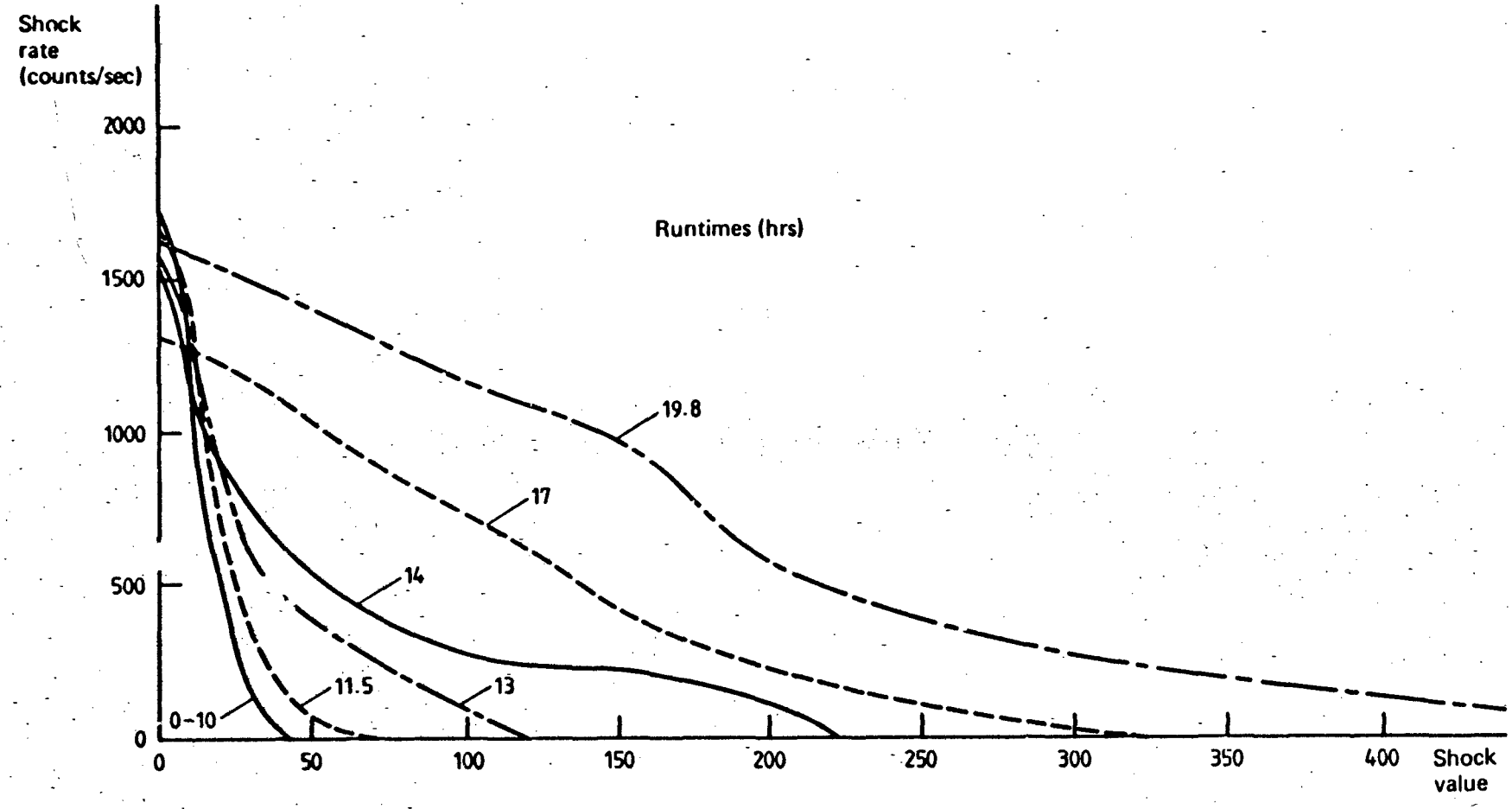

FIG D.3
BEARING C

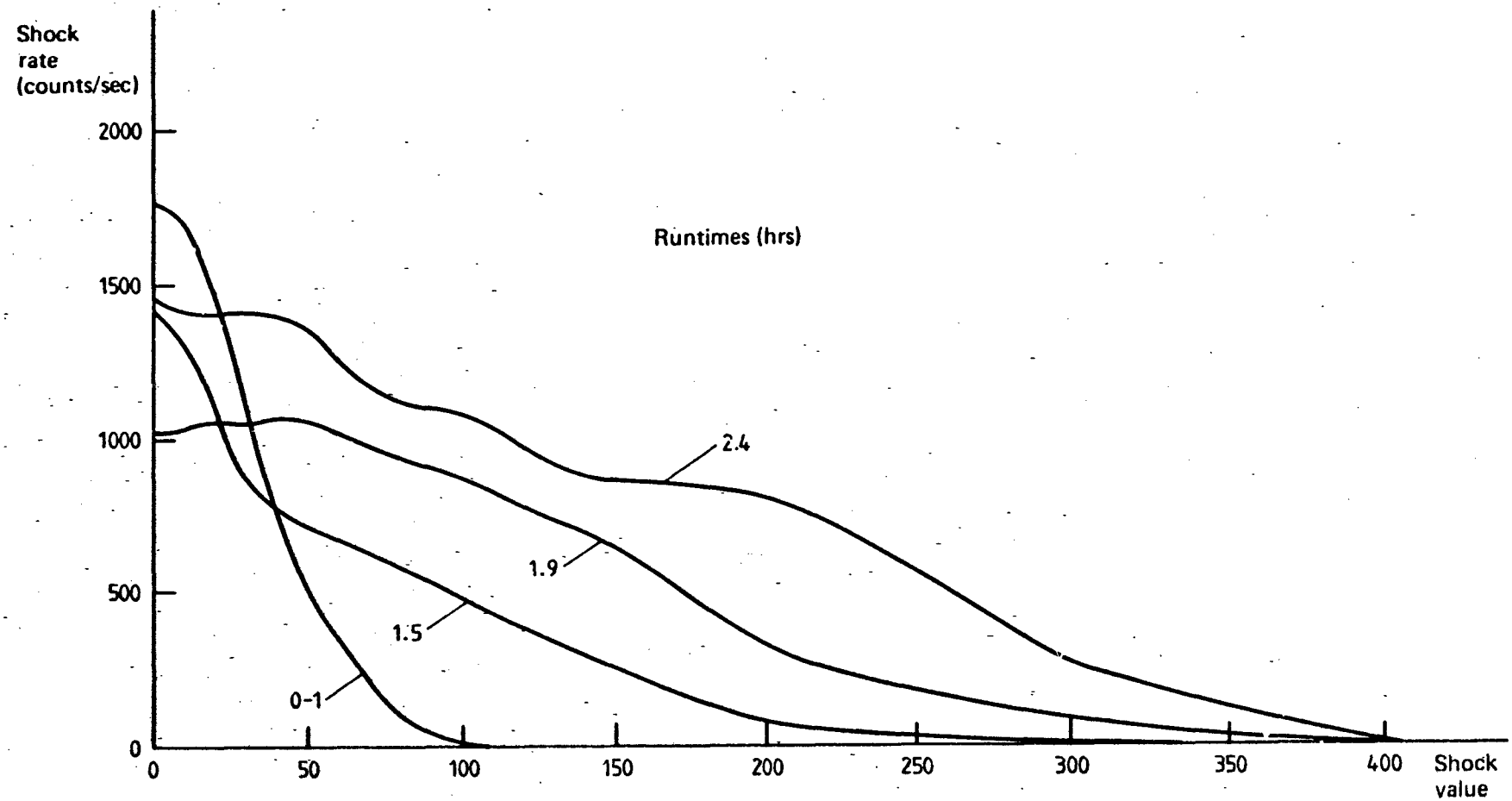

FIG D.4
BEARING D

APPENDIX E

Envelope Spectra

Envelope Spectra using

(1) ARL developed circuit

(2) K-meter

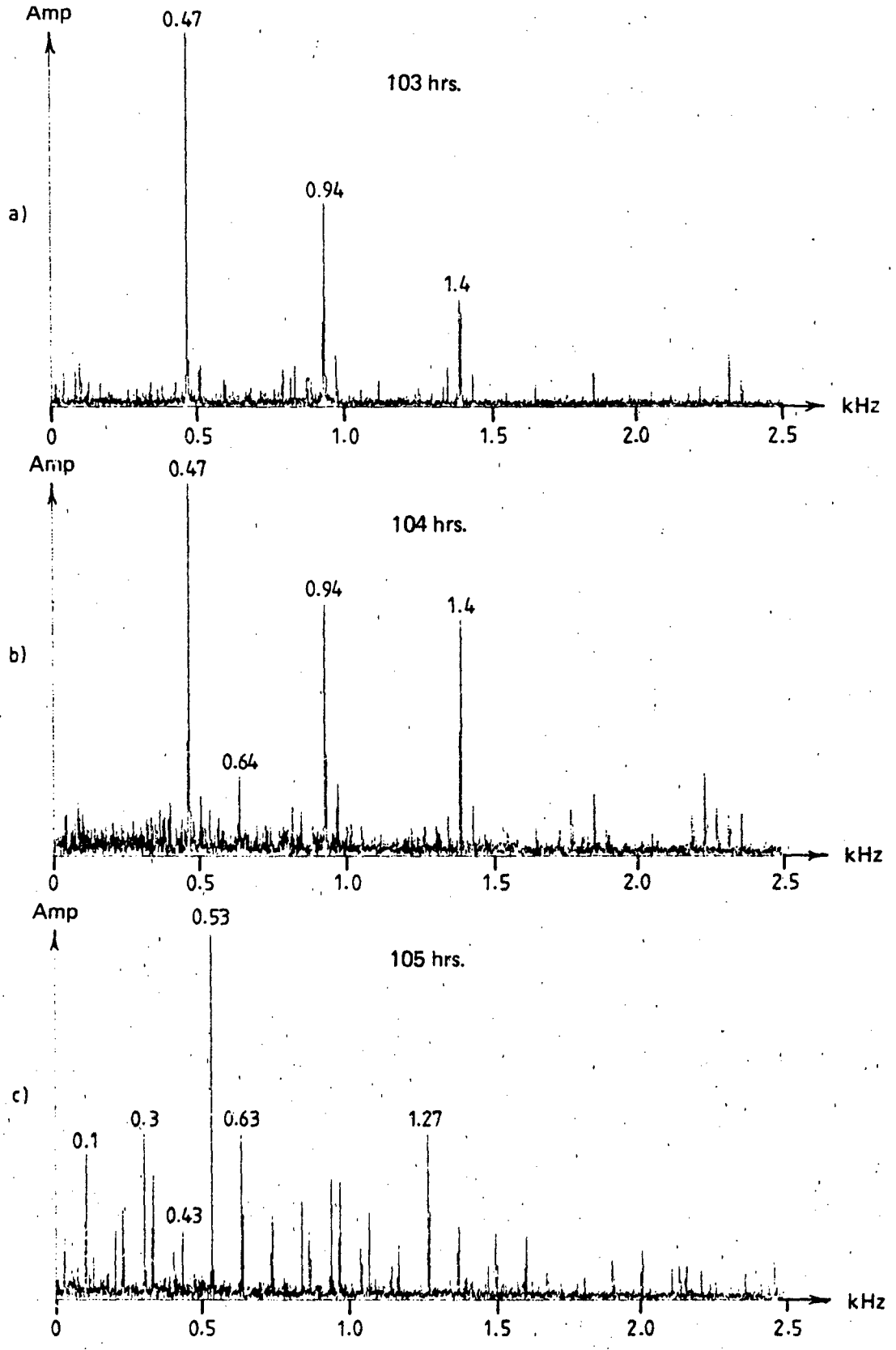

FIG E.1
Bearing B
K - meter: 0-10 kHz band

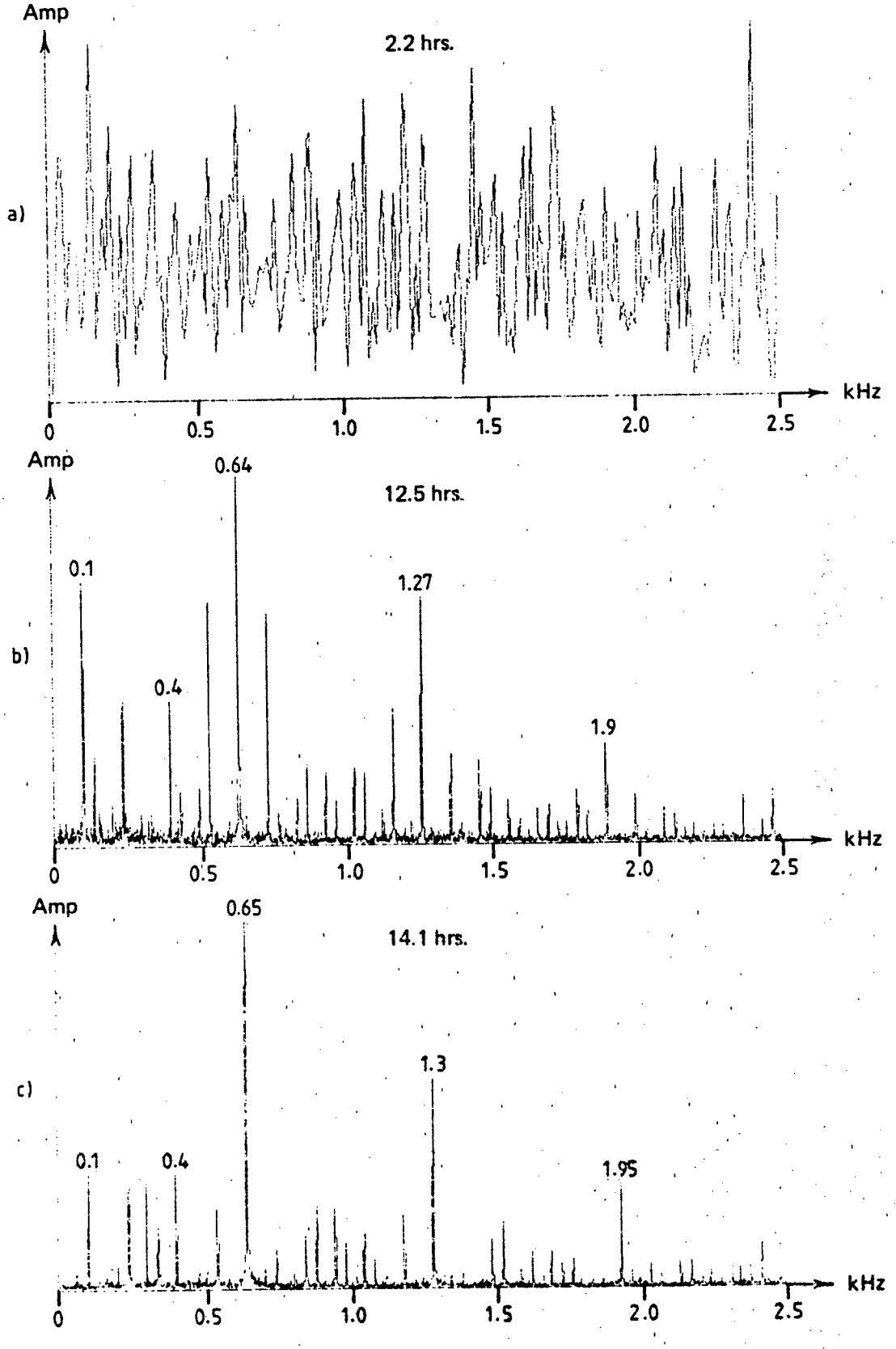

FIG E.2
Bearing C
K - meter: 0-10 kHz band

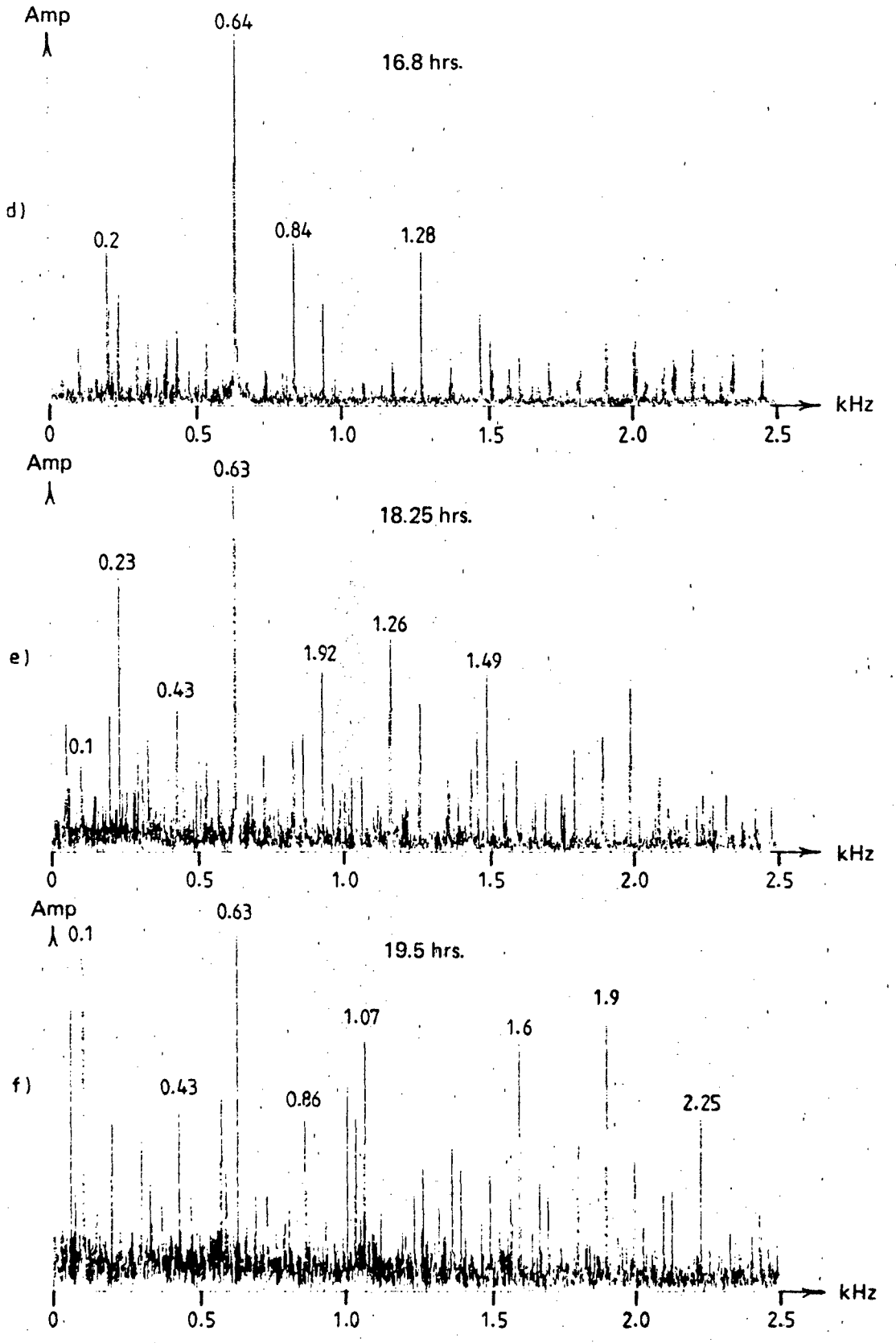

FIG E.2 cont'd.
Bearing C
K - meter: 0-10 kHz band

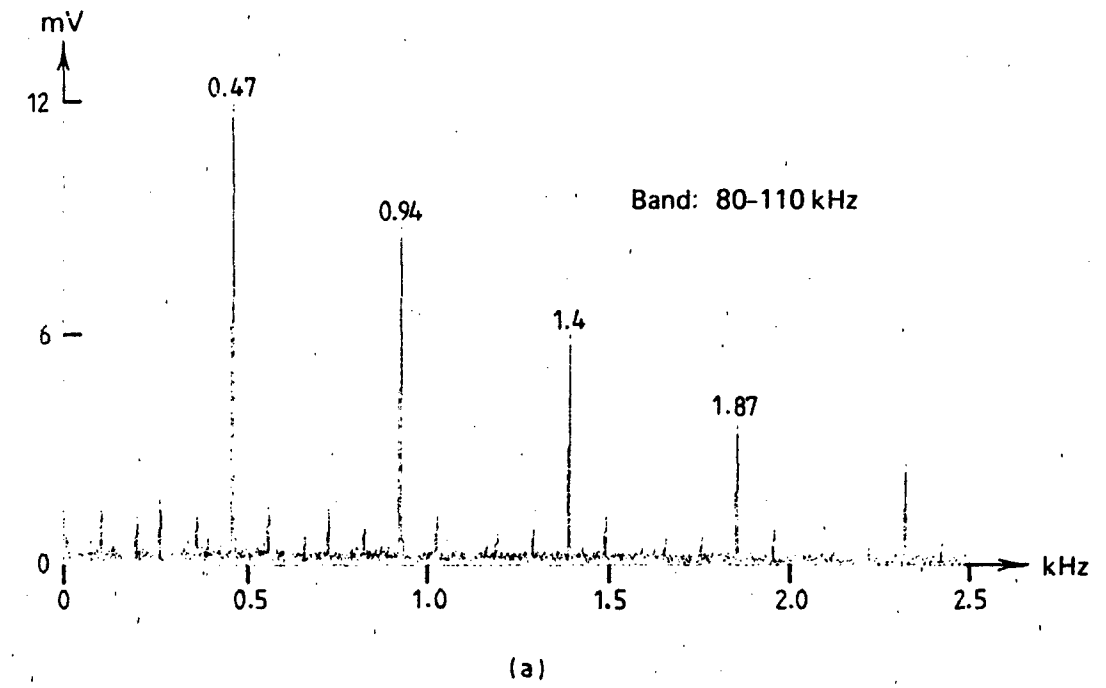

(a)

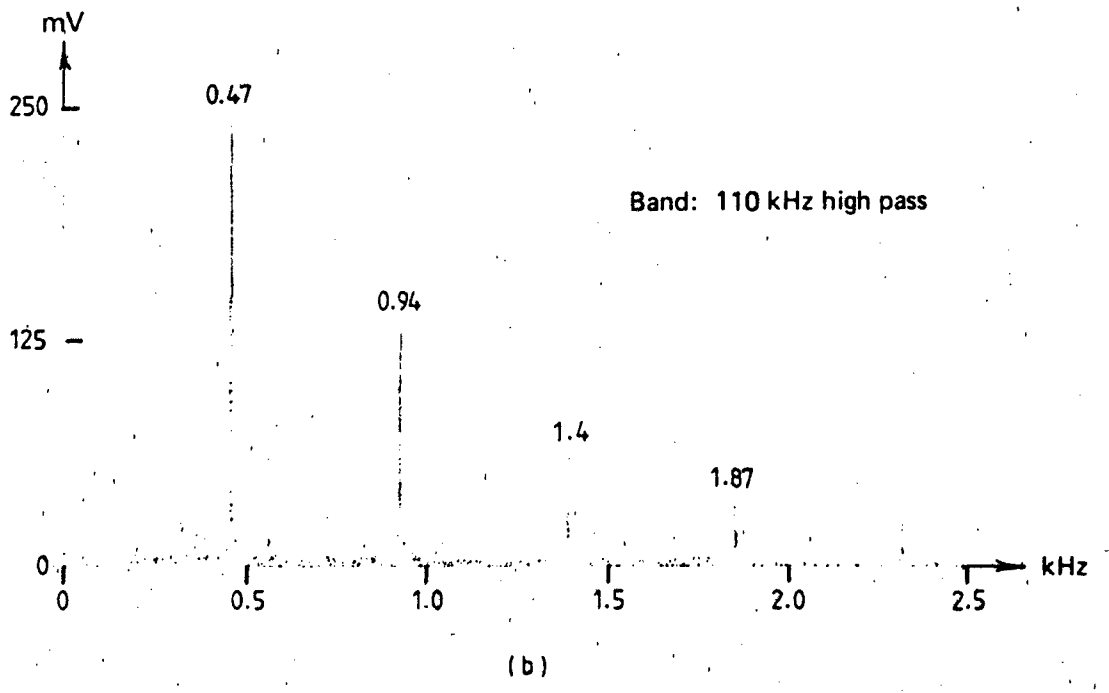

(b)

FIG E.3
Bearing D – 1 hr runtime
– Acoustic emission transducer,
– Amplitude in millivolts (mV)

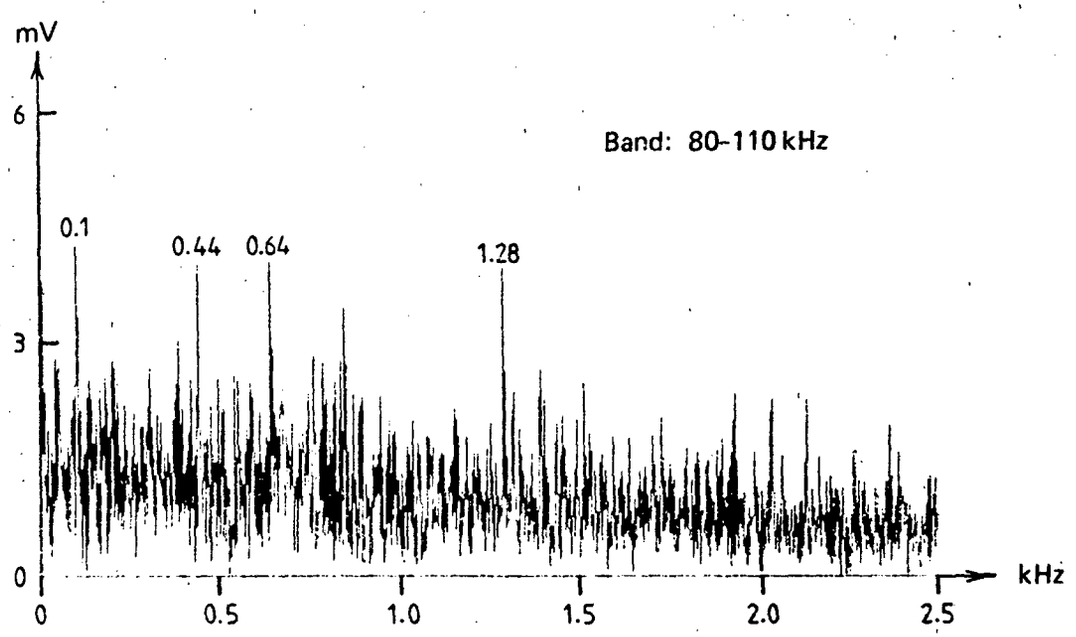

(a)

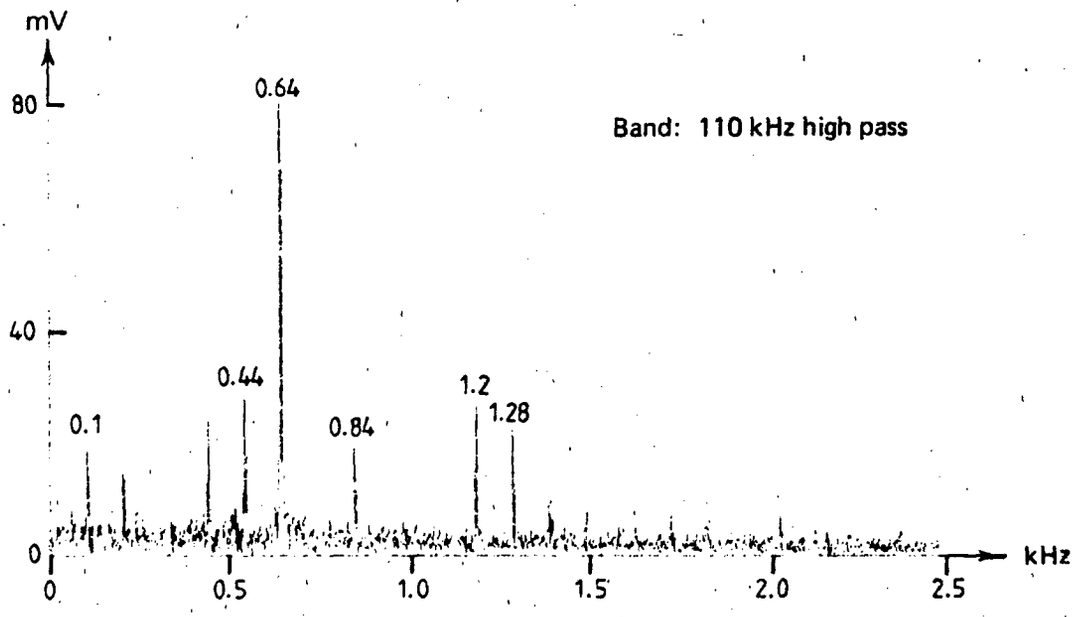

(b)

FIG E.4
Bearing D – 2 hrs runtime
Acoustic emission transducer –
– Amplitude in millivolts (mV)

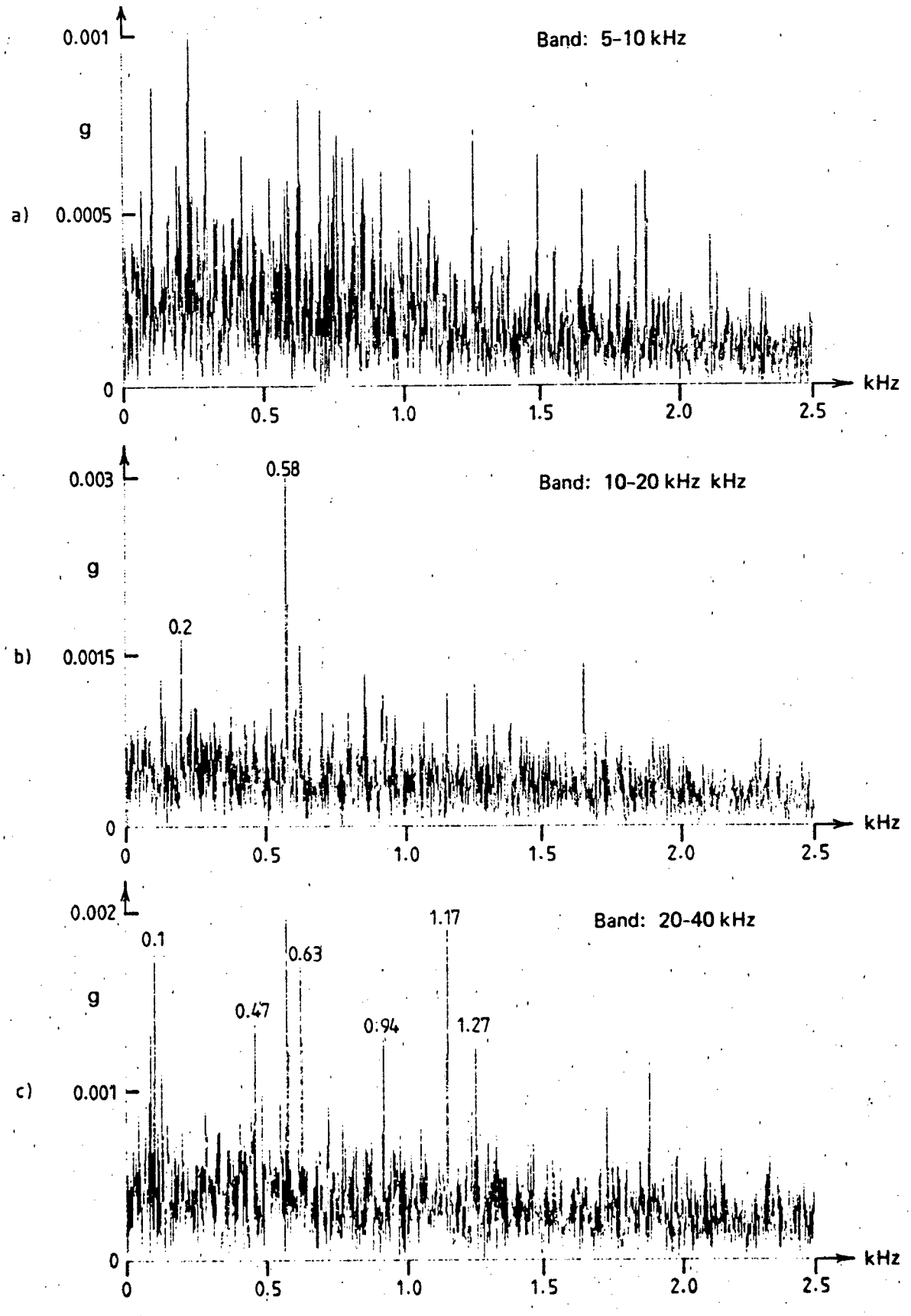

FIG E.5
Bearing D — 0.5 hrs runtime
PCB Accelerometer

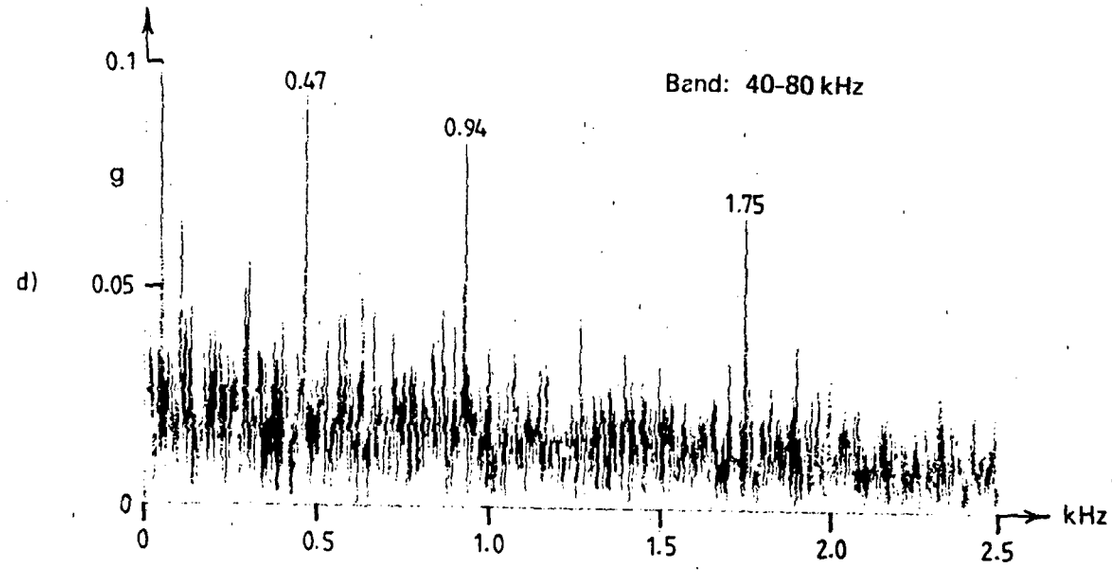
d)
0.1
g
0.05
0
0.47
0.94
1.75
Band: 40-80 kHz
0
0.5
1.0
1.5
2.0
2.5
kHz

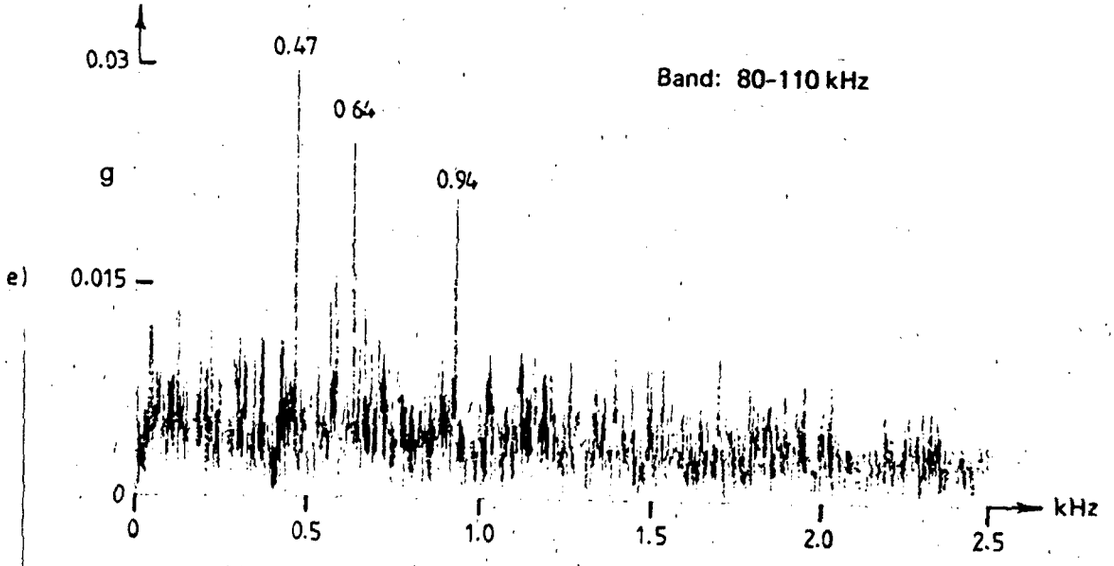
e)
0.03
g
0.015
0
0.47
0 64
0.94
Band: 80-110 kHz
0
0.5
1.0
1.5
2.0
2.5
kHz

FIG E.5 cont'd

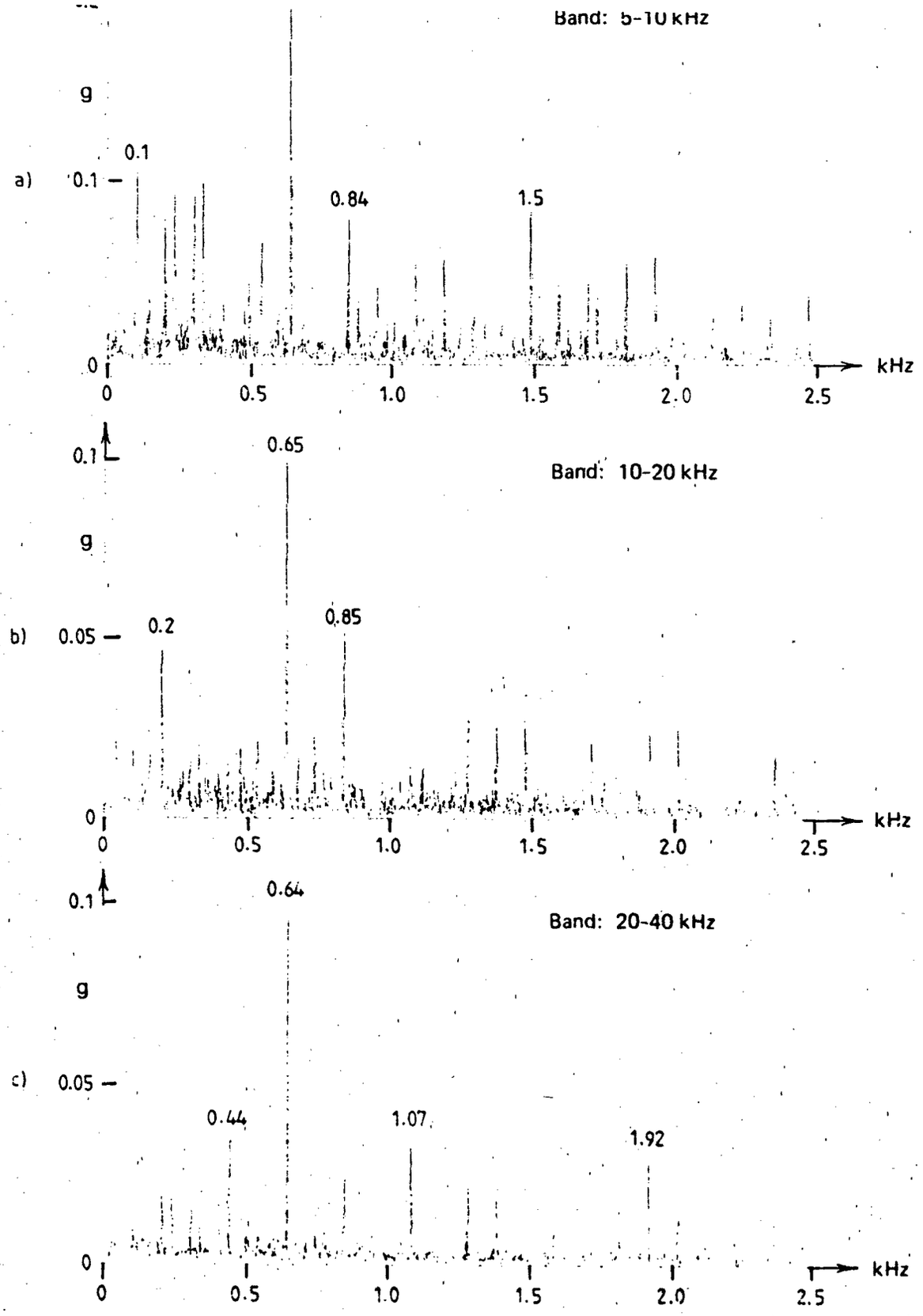

FIG E.6
Bearing D — 2 hrs. runtime
PCB Accelerometer

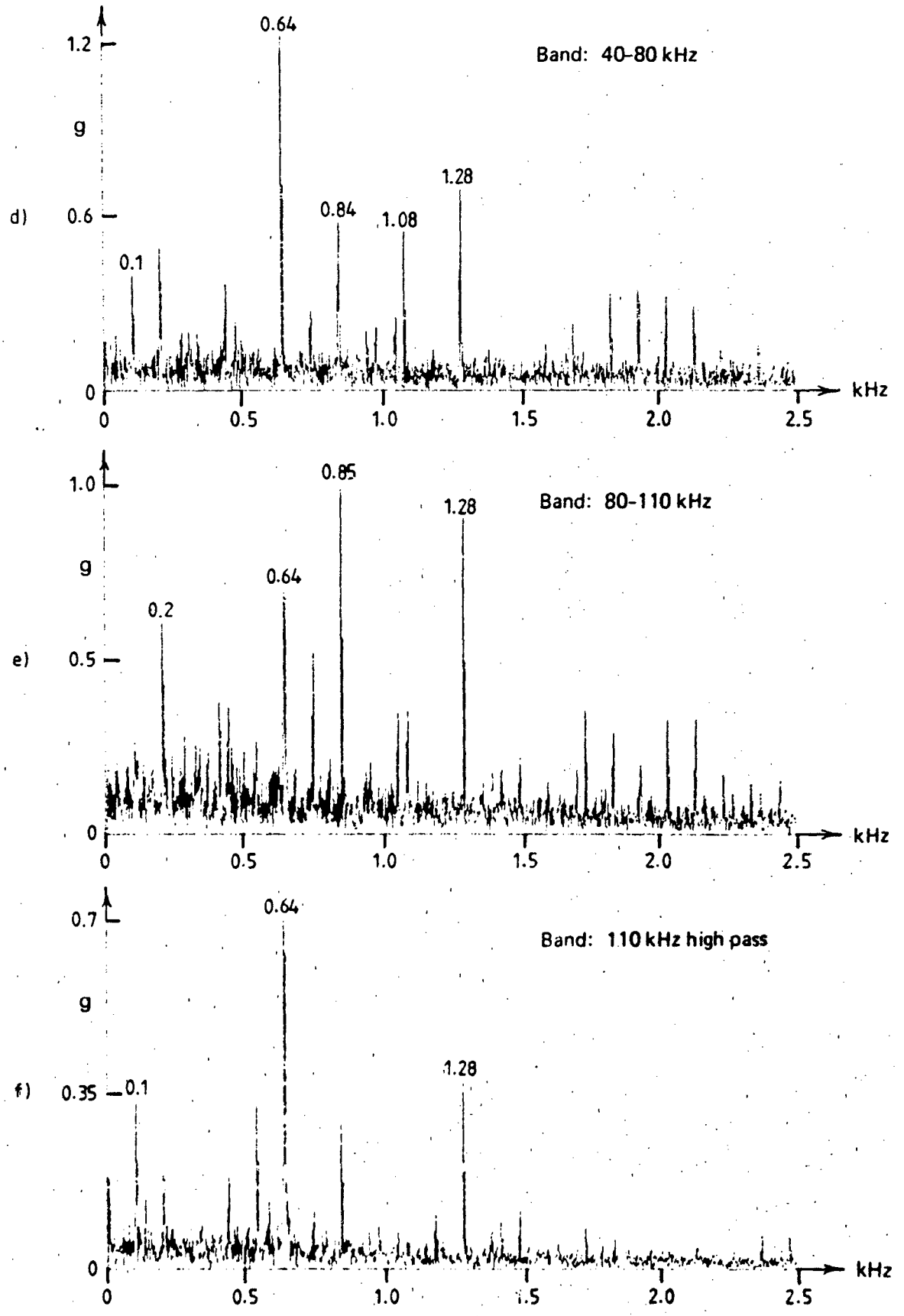
d)
Band: 40-80 kHz
1.2
0.6
0
g
0.64
0.84
1.08
1.28
0.1
0
0.5
1.0
1.5
2.0
2.5
kHz
e)
Band: 80-110 kHz
1.0
0.5
0
g
0.85
1.28
0.64
0.2
0
0.5
1.0
1.5
2.0
2.5
kHz
f)
Band: 110 kHz high pass
0.7
0.35
0
g
0.64
1.28
0.1
0
0.5
1.0
1.5
2.0
2.5
kHz

FIG E.6 cont'd

APPENDIX F

Time Domain Signals

Time Domain signals of undamaged and damaged (single spall) bearings using Kistler accelerometer.

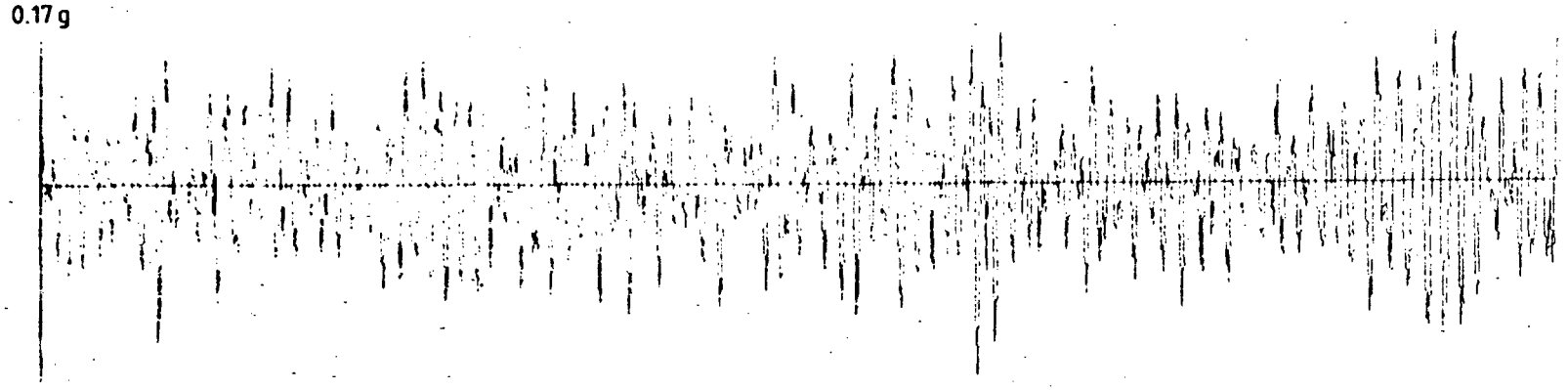

(a) Runtime = 1 hr.
K = 2.9

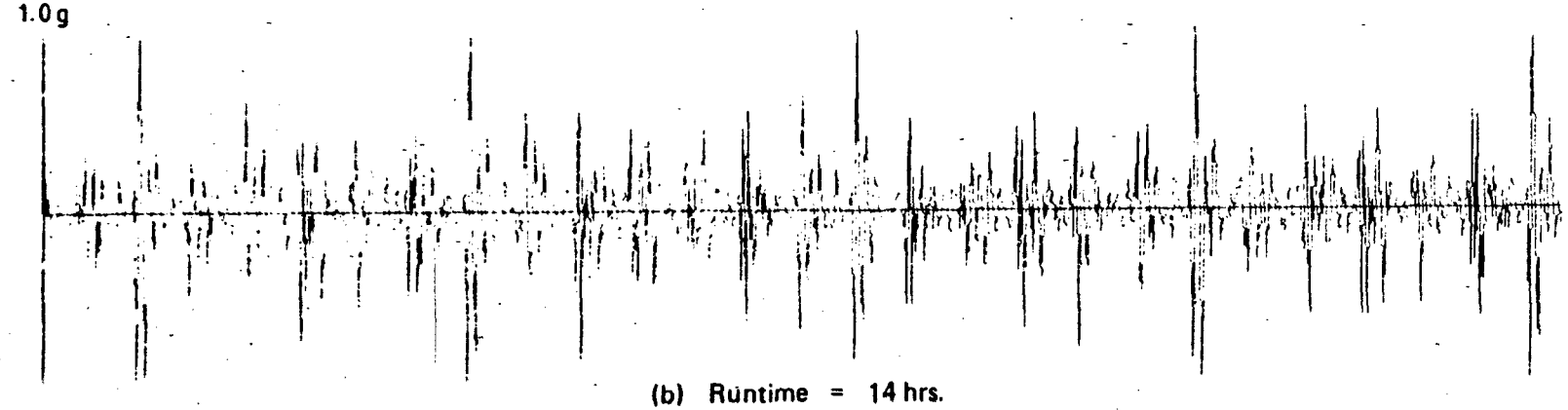

(b) Runtime = 14 hrs.
K = 7.0

FIG F.1 BEARING C
Frequency band: 2-5 kHz
Time scale: 1" = 5msec.

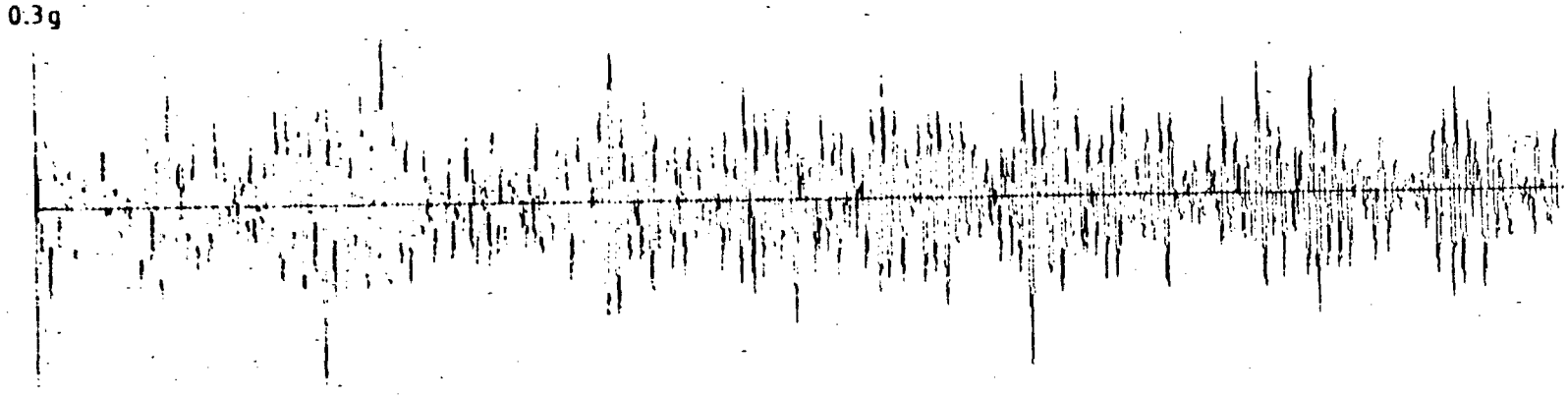

(a) Runtime = 1 hr.
K = 3.2

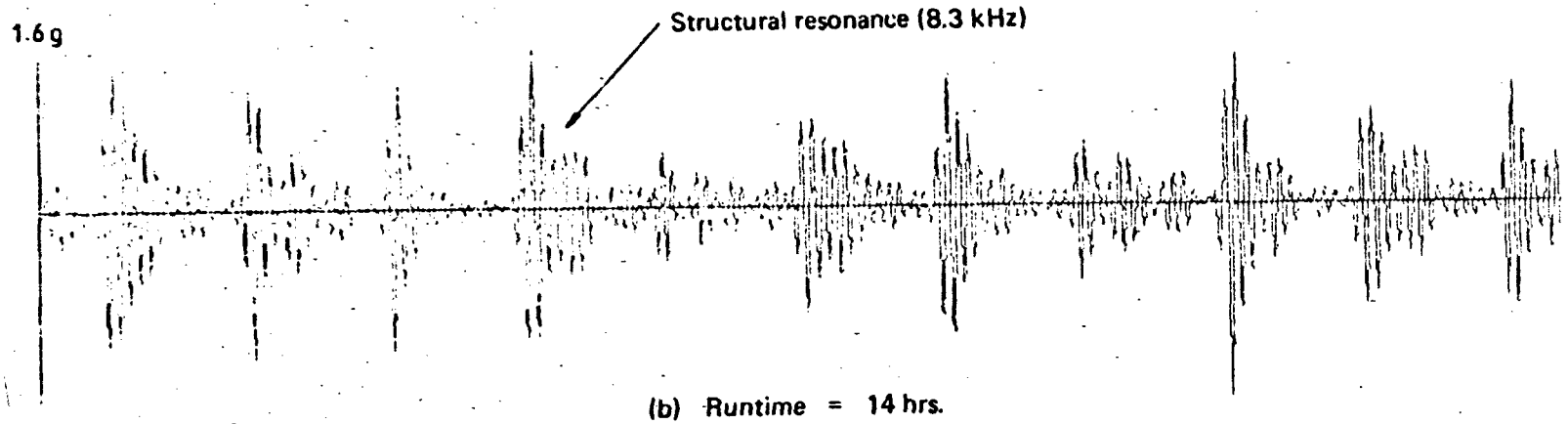

(b) Runtime = 14 hrs.
K = 6.5

FIG F.2 BEARING C
Frequency band: 5-10 kHz
Time scale: 1" = 2msec.

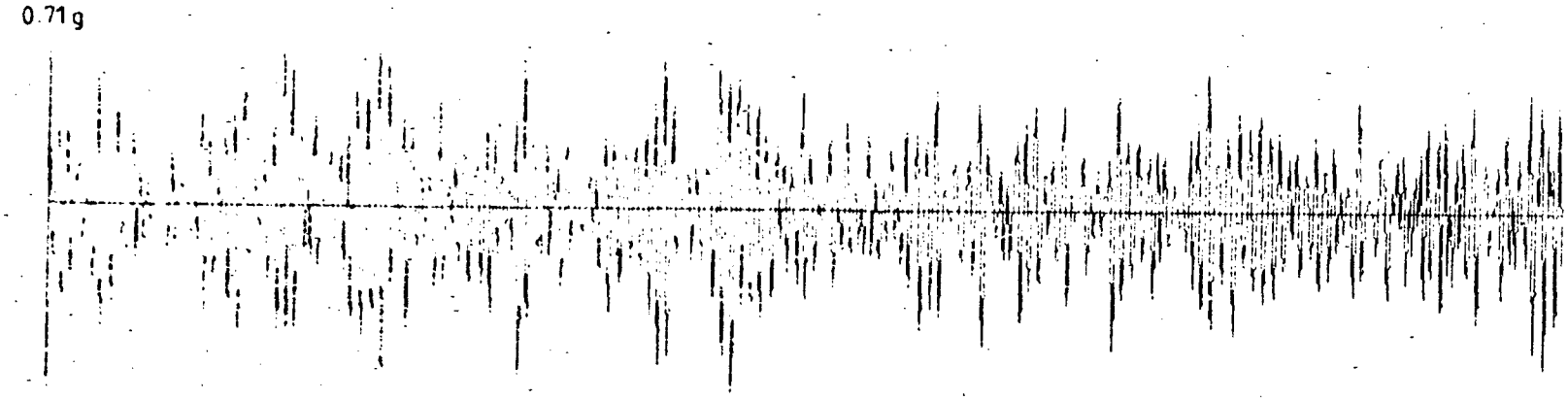

(a) Runtime = 1 hr.
K = 3.1

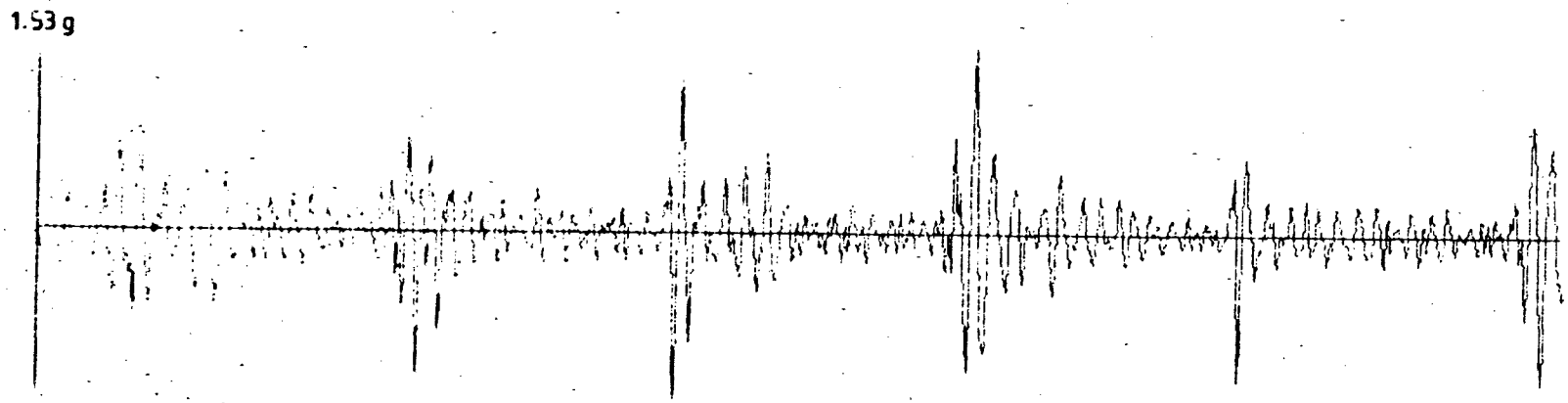

(b) Runtime = 14 hrs.
K = 6.5

FIG F.3 BEARING C
Frequency band: 10-20 kHz
Time scale: 1" = 1 msec.

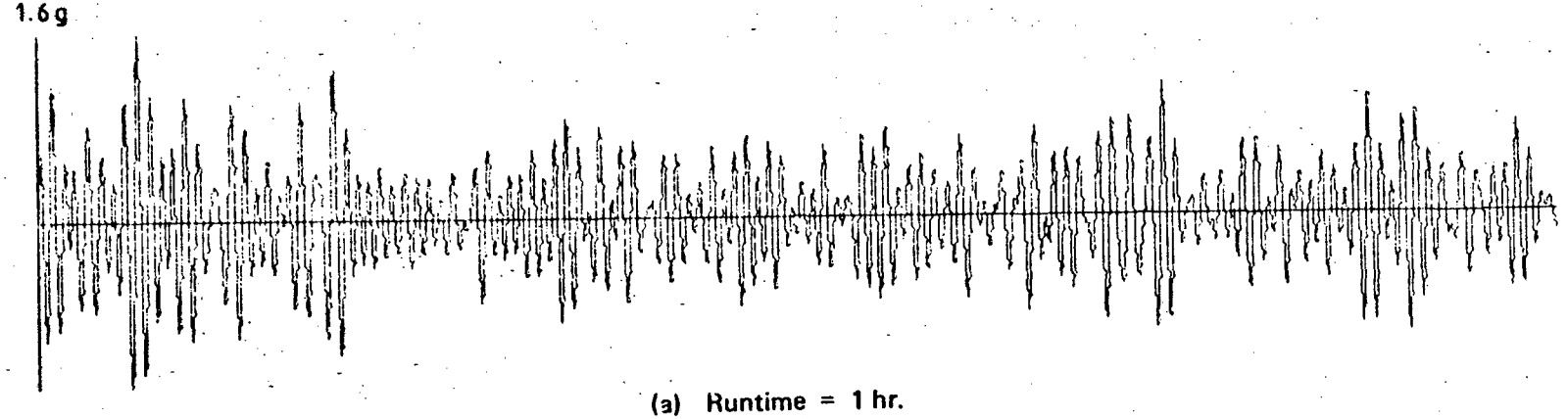

(a) Runtime = 1 hr.
K = 3.0

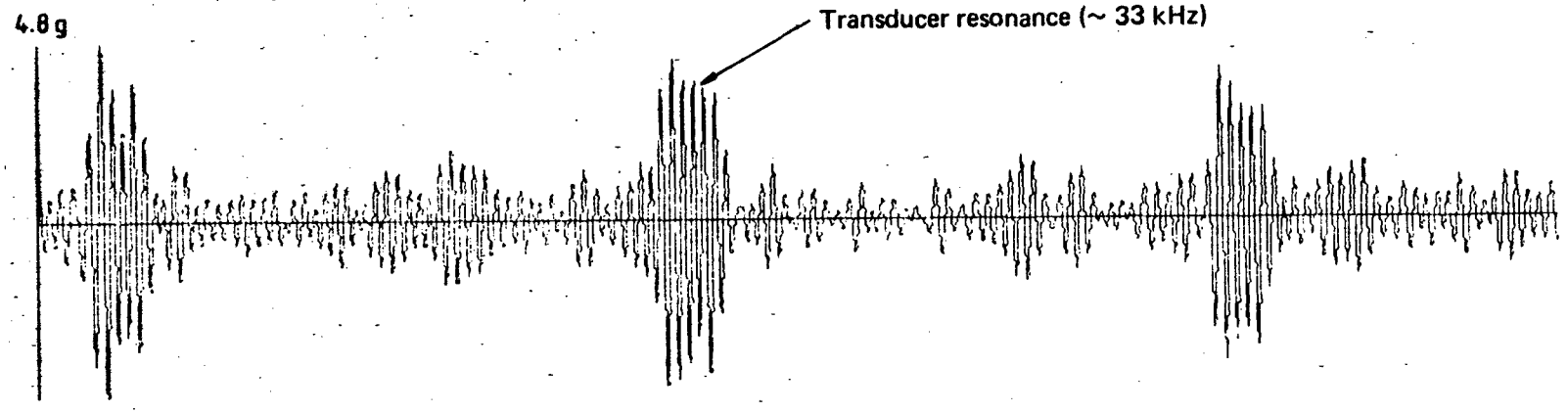

(b) Runtime = 14 hrs.
K = 7.0

FIG F.4 BEARING C
Frequency band: 20-40 kHz
Time scale: 1" = .05 msec.

APPENDIX G

Progressive Damage Details

Progressive damage details and photographs of deep groove ball bearings.

Runtime (hrs)	Progressive Damage Details	Photographs (Figures) (Divisions = cm)
	Bearing A	
151	Inner Race: spall, 1 × 3 mm	
	Outer Race: slight pitting and reentrainment.	
152·25	*End Test*	
	Inner Race: 80°–90° failure	Fig. G.1
	Outer Race: 360° reentrainment/pitting	
	Bearing B	
102	Inner Race: slight bruising	
	Outer Race: spall, 2 × 2 mm	—
105	*End Test*	
	Inner Race: 120° failure	Fig. G.3
	spall, 4 × 3 mm	Fig. G.4
	2 spalls, 10 × 3 mm	
	Outer Race: spall, 4 × 3 mm	Fig. G.2
	reentrainment, 360°	
	Bearing C	
11	Inner Race: spall, 1 × 3 mm	—
	Outer Race: slight bruising	—
15	Inner Race: spall, 2 × 3·5 mm	—
	slight bruising	—
	Outer Race: bruising/reentrainment 360°	—
18·5	Inner Race: spall, 8 × 3 mm	
	spall, 11 × 3 mm (separated by 2 mm)	
	severe bruising over remainder	—
	Outer Race: severe bruising, 360°	
20	*End Test*	
	Inner Race: 180° failure	Figs G.5, G.6, G.7
	initiation of 2 spalls	Fig. G.8
	severe bruising overall	
	Outer Race: initiation of one spall	
	bruising/pitting worsened	
	Balls: each ball is damaged with spalls and pitting	Fig. G.9
	Bearing D	
1·5	Inner Race: spall, 2 × 1 mm	
	slight bruising	
2·5	*End Test*	
	Inner Race: spall, 15 × 3 mm	Fig. G.10
	spall, 5 × 3 mm (5 mm separation)	
	Outer Race: bruising 360°	

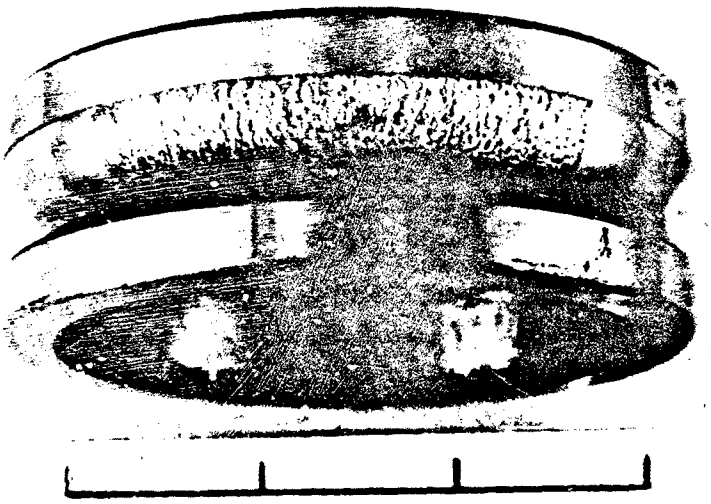

A

FIG G.1

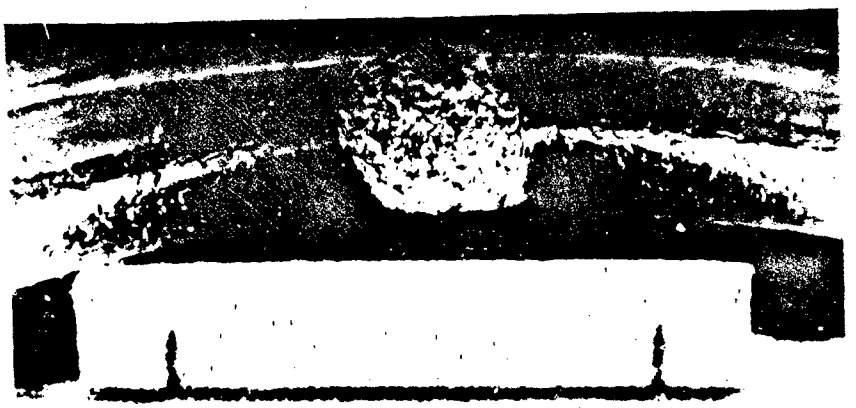

B

FIG G.2

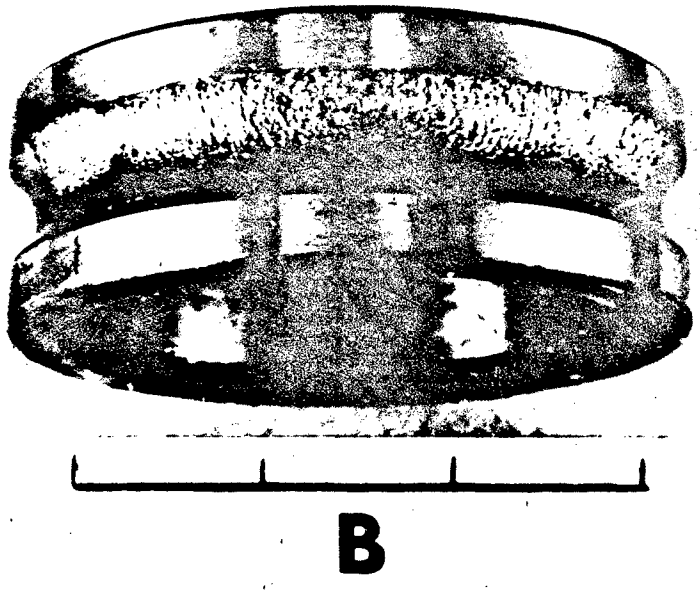

FIG G.3

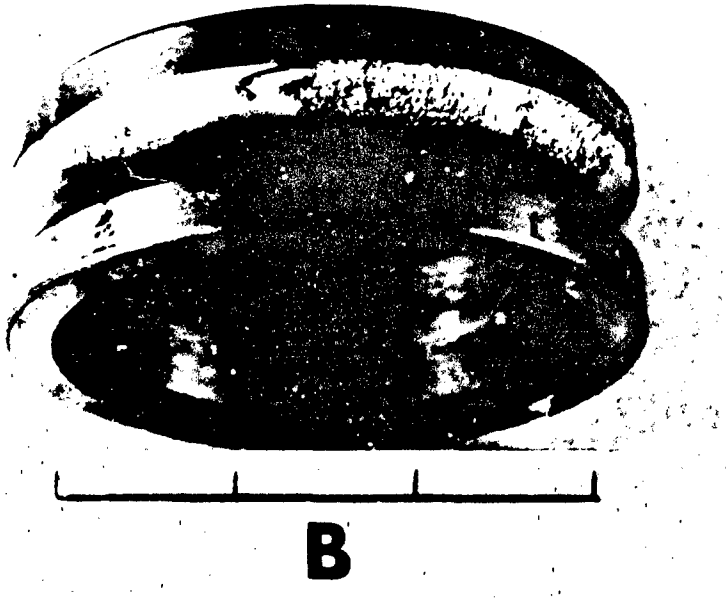

FIG G.4

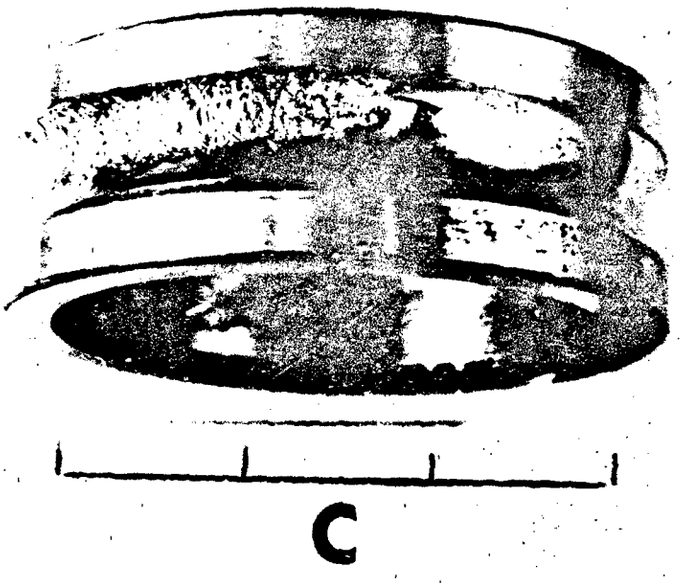

FIG G.5

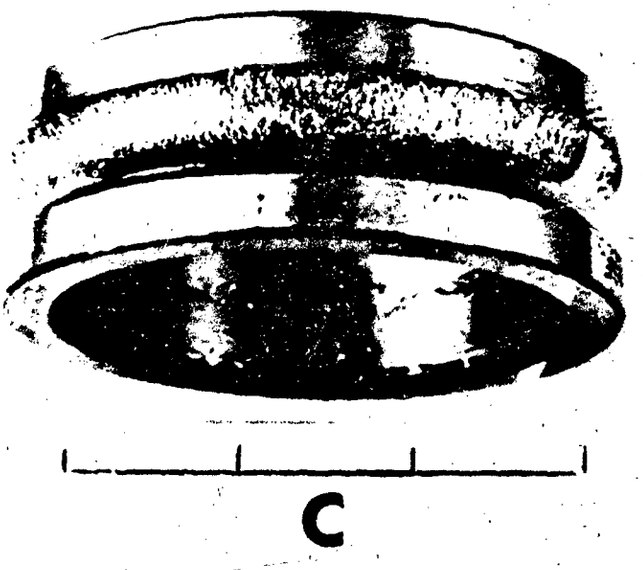

FIG G.6

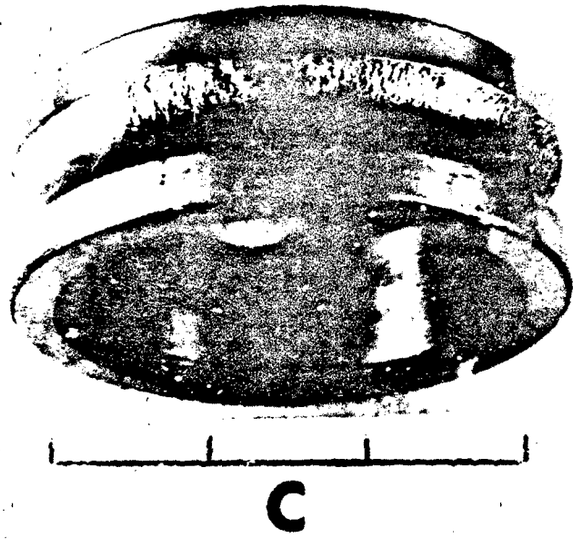

FIG G.7

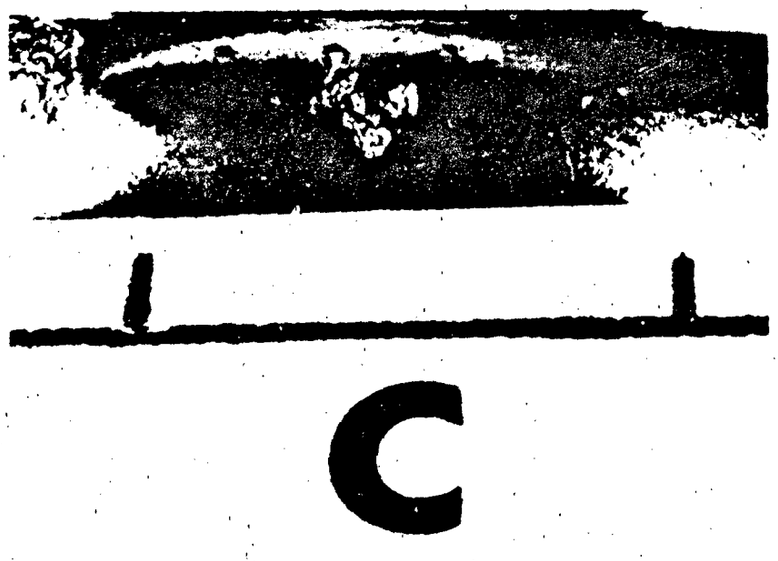

FIG G.8

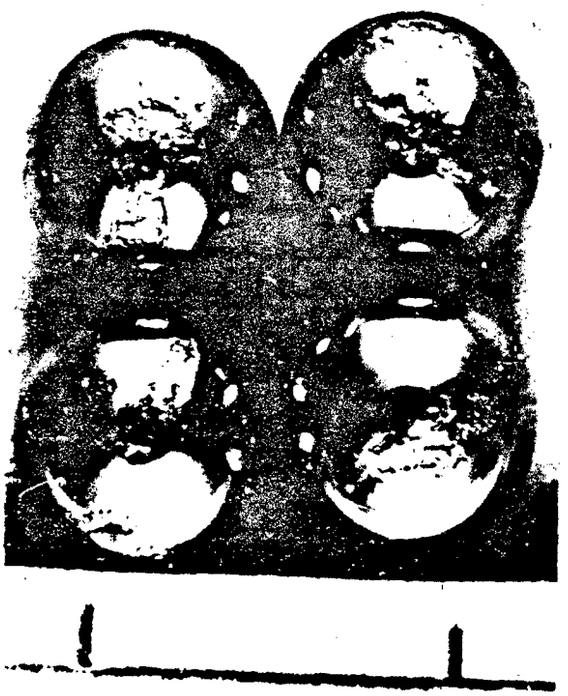

C

FIG G.9

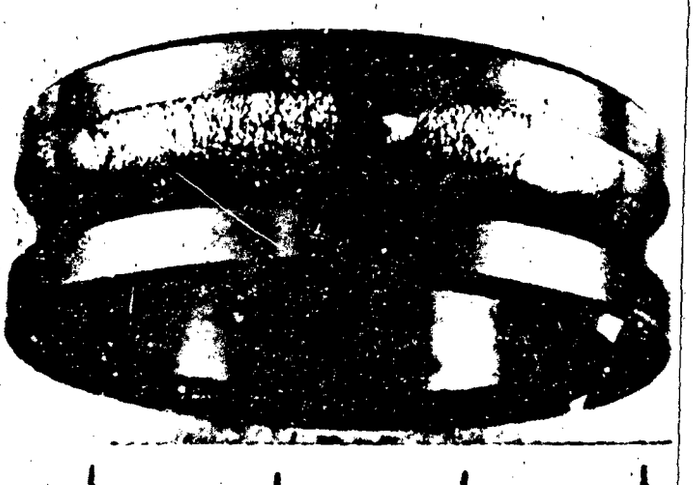

D

FIG G.10

DISTRIBUTION

AUSTRALIA

DEPARTMENT OF DEFENCE

Central Office

Chief Defence Scientist
Deputy Chief Defence Scientist
Superintendent, Science and Technology Programmes } (1 copy)
Controller, Projects and Analytical Studies
Defence Science Representative (U.K.) (Doc. Data sheet only)
Counsellor, Defence Science (U.S.A.) (Doc. Data sheet only)
Defence Central Library
Document Exchange Centre, D.I.S.B. (18 copies)
Joint Intelligence Organisation
Librarian H Block, Victoria Barracks, Melbourne
Director General—Army Development (NSO) (4 copies)
Defence Industry and Material Policy, FAS

Aeronautical Research Laboratories

Director
Library
Superintendent—Aero Propulsion
Divisional File—Aero Propulsion
Authors: N. S. Swansson
S. C. Favaloro
C. N. King
M. L. Atkin
B. Rebechi

Materials Research Laboratories

Director/Library

Defence Research Centre

Library

Navy Office

Navy Scientific Adviser
RAN Aircraft Maintenance and Flight Trials Unit
RAN Tactical School, Library
Directorate of Naval Aircraft Engineering
Directorate of Naval Aviation Policy
Superintendent, Aircraft Maintenance and Repair
Directorate of Naval Ship Design

Army Office

Army Scientific Adviser
Engineering Development Establishment, Library
Royal Military College Library
US Army Research, Development and Standardisation Group

Air Force Office

Air Force Scientific Adviser
Aircraft Research and Development Unit
Scientific Flight Group
Library
Technical Division Library
Director General Aircraft Engineering—Air Force
Director General Operational Requirements—Air Force
HQ Operational Command (SMAINTSO)
HQ Support Command (SLENGO)
RAAF Academy, Point Cook

Central Studies Establishment

Information Centre

DEPARTMENT OF DEFENCE SUPPORT

Government Aircraft Factories

Manager
Library

DEPARTMENT OF AVIATION

Library
Flying Operations and Airworthiness Division

STATUTORY AND STATE AUTHORITIES AND INDUSTRY

Australian Atomic Energy Commission, Director
Trans-Australia Airlines, Library
Qantas Airways Limited
Gas and Fuel Corporation of Victoria, Manager Scientific Services
SEC of Vic., Herman Research Laboratory, Library
Ansett Airlines of Australia, Library
Australian Coal Industry Research Labs Ltd, Director
B.H.P., Melbourne Research Laboratories
B.P. Australia Ltd, Library
Commonwealth Aircraft Corporation, Library
Hawker de Havilland Aust. Pty Ltd, Bankstown, Library
Institute of Fuel, Australian Branch, Secretary
Australian Institute of Petroleum Ltd
Rolls Royce of Australia Pty Ltd, Mr C. G. A. Bailey

UNIVERSITIES AND COLLEGES

Adelaide	Barr Smith Library
	Professor of Mechanical Engineering
Flinders	Library
Latrobe	Library
Melbourne	Engineering Library
Monash	Hargrave Library
	Dr R. Alfredson, Mechanical Engineering Department
Newcastle	Library
Sydney	Engineering Library
	Head, School of Civil Engineering
N.S.W.	Physical Sciences Library
	Professor R. A. A. Bryant, Mechanical Engineering
	Professor G. D. Sergeant, Fuel Technology
	Assoc. Professor R. W. Traill-Nash, Civil Engineering
Queensland	Library
Tasmania	Engineering Library
Western Australia	Library
	Associate Professor J. A. Cole, Mechanical Engineering
R.M.I.T.	Library
	Dr H. Kowalski, Mech. & Production Engineering
Chisholm I.T.	Library
	The Tribology Group

CANADA

International Civil Aviation Organization, Library
NRC
Aeronautical & Mechanical Engineering Library
Division of Mechanical Engineering, Director

FRANCE

ONERA, Library

GERMANY

Fachinformationszentrum: Energie, Physic, Mathematik GMBH

INDIA

Defence Ministry, Aero Development Establishment, Library
Gas Turbine Research Establishment, Director
Hindustan Aeronautics Ltd, Library
National Aeronautical Laboratory, Information Centre

ISRAEL

Technion-Israel Institute of Technology
Professor J. Singer

ITALY

Professor Ing. Guiseppe Gabrielli

JAPAN

National Research Institute for Metals, Fatigue Testing Division

Universities

Kagawa University Professor H. Ishikawa

NETHERLANDS

National Aerospace Laboratory (NLR), Library

NEW ZEALAND

Defence Scientific Establishment, Library
Transport Ministry, Airworthiness Branch Library
RNZAF, Vice Consul (Defence Liaison)

Universities

Canterbury Library
Professor D. Stevenson, Mechanical Engineering

SWEDEN

Aeronautical Research Institute, Library
Swedish National Defense Research Institute (FOA)

SWITZERLAND

Armament Technology and Procurement Group
F+W (Swiss Federal Aircraft Factory)

UNITED KINGDOM

CAARC, Secretary (NPL)
Royal Aircraft Establishment
Bedford, Library
Commonwealth Air Transport Council Secretariat
Admiralty Marine Technology Establishment
Holton Heath, Dr N. J. Wadsworth
St Leonard's Hill, Superintendent
National Gas Turbine Establishment
Director, Pyestock North
National Engineering Laboratory, Library
British Library, Lending Division
CAARC Co-ordinator, Structures
Aircraft Research Association, Library
British Ship Research Association
National Maritime Institute, Library
Electrical Power Engineering Co. Ltd
GEC Gas Turbines Ltd, Managing Director
Fulmer Research Institute Ltd, Research Director
Motor Industry Research Association, Director
Ricardo & Co. Engineers (1927) Ltd, Manager

Rolls-Royce Ltd
Aero Division Bristol, Library
British Aerospace
Hatfield-Chester Division, Library
British Hovercraft Corporation Ltd, Library
Short Brothers Ltd, Technical Library
Stewart-Hughes Ltd, Manager
Westland Helicopters Ltd, Manager
Naval Air Materials Laboratory, Director

Universities and Colleges

Bristol	Engineering Library
Cambridge	Whittle Library
Manchester	Professor N. Johannesen, Fluid Mechanics
Nottingham	Science Library
Southampton	Library
Strathclyde	Library
Cranfield Institute of Technology	Library
University College of Swansea	Professor B. L. Clarkson

UNITED STATES OF AMERICA

NASA Scientific and Technical Information Facility
Applied Mechanics Reviews
Metals Information
The John Crerar Library
Allis Chalmers Corporation, Library
Boeing Co.
Mr J. C. McMillan
Kentex Research Library
United Technologies Corporation, Library
Lockheed-California Company
Lockheed Missiles and Space Company
Lockheed Georgia
McDonnell Aircraft Company, Library
Nondestructive Testing Information Analysis Center

Universities and Colleges

Johns Hopkins	Professor S. Corrsin, Engineering
Iowa State	Dr G. K. Serovy, Mechanical Engineering
Massachusetts Inst. of Technology	M.I.T. Libraries

SPARES (20 copies)

TOTAL (190 copies)

Department of Defence

DOCUMENT CONTROL DATA

1. a. AR No.	1. b. Establishment No.	2. Document Date	3. Task No.
AR-003-010	ARL-AERO-PROP-R-163	January 1984	DST 82/051

4. Title	5. Security	6. No. Pages
APPLICATIONS OF VIBRATION ANALYSIS TO THE CONDITION MONITORING OF ROLLING ELEMENT BEARINGS	a. document: Unclassified b. title: U c. abstract: U	28 7. No. Refs: 7

8. Author(s)	9. Downgrading Instructions
N. S. Swansson S. C. Favaloro	—

10. Corporate Author and Address	11. Authority (*as appropriate*)
Aeronautical Research Laboratories P.O. Box 4331, MELBOURNE, VIC., 3001	a. Sponsor b. Security c. Downgrading d. Approval —

12. Secondary Distribution (*of this document*)
Approved for public release

Overseas enquirers outside stated limitations should be referred through ASDIS, Defence Information Services Branch, Department of Defence, Campbell Park, CANBERRA, ACT, 2601.

13. a. This document may be ANNOUNCED in catalogues and awareness services available to . . .
No limitations

13. b. Citation for other purposes (i.e. *casual announcement*) may be (select) unrestricted (or) as for 13 a.

14. Descriptors		15. COSATI Group
Bearings	Engine components	13090
Monitors	Antifriction bearings	14040
Vibration meters	Condition monitoring	21100
Acoustic emissions		
Wear		

16. Abstract

Condition monitoring methods for rolling element bearings, which utilise the high frequency vibrations generated by bearing damage, have been investigated and compared experimentally. Kurtosis values, spectra of vibration signal envelopes and pulse measurement methods provided effective detection of early damage, but kurtosis in particular was not effective in evaluating extensive damage, where a combination of methods is required.

Comparison of different accelerometer types used as vibration sensors gave very similar results, but an acoustic emission transducer provided indications of incipient damage significantly earlier than the accelerometers.

Tests were conducted under reasonably favourable conditions of measurement so further testing under less favourable conditions is proposed, and the effect of such conditions is briefly considered.

This page is to be used to record information which is required by the Establishment for its own use but which will not be added to the DISTIS data base unless specifically requested.

16. Abstract (Contd)

17. Imprint

Aeronautical Research Laboratories, Melbourne

18. Document Series and Number	19. Cost Code	20. Type of Report and Period Covered
Aero Propulsion Report 163	417430	—

21. Computer Programs Used

—

22. Establishment File Ref(s)

—

END

FILMED

9-85

DTIC